Generation of Recyclable Liquid Crystalline Polymer Reinforced Composites for Use in Conventional and Additive Manufacturing Processes

Tianran Chen

Dissertation submitted to the faculty of the Virginia Polytechnic Institute and State University in partial fulfillment of the requirements for the degree of

Doctor of Philosophy

In

Macromolecular Science and Engineering

Donald G. Baird, Chair

Justin R. Barone

Michael J. Bortner

Scott W. Case

Stephen M. Martin

May 6, 2021

Blacksburg, VA

Keywords: recycling, thermotropic liquid crystalline polymer, glass fibers, hybrid composite, additive manufacturing, polymer composite

Generation of Recyclable Liquid Crystalline Polymer Reinforced Composites for Use in Conventional and Additive Manufacturing Processes

Tianran Chen

ABSTRACT (academic)

The application of glass fiber reinforced composites has grown rapidly due to their high strength-to-weight ratio, low cost, and chemical resistance. However, the increasing demand for fiber reinforced composites results in the generation of more composite wastes. Mechanical recycling is a cost-effective and environmentally-friendly recycling method, but the loss in the quality of recycled glass or carbon fiber composite hinders the wide-spread use of this recycling method. It is important to develop novel composite materials with higher recyclability. Thermotropic liquid crystalline polymers (TLCPs) are high-performance engineering thermoplastics, which have comparable mechanical performance to that of glass fiber. The TLCP reinforced composites, called *in situ* composites, can form the reinforcing TLCP fibrils during processing avoiding the fiber breakage problem.

The first part of this dissertation is to study the influence of mechanical recycling on the properties of injection molded TLCP and glass fiber (GF) reinforced polypropylene (PP). The processing temperature of the injection molding process was optimized using a differential scanning calorimeter (DSC) and a rheometer to minimize the thermal degradation of PP. The TLCP and GF reinforced PP materials were mechanically recycled up to three times by repeated injection molding and grinding. The mechanical recycling had almost no influence on the mechanical, thermal, and thermo-

mechanical properties of TLCP/PP because of the regeneration of TLCP fibrils during the mold filling process. On the other hand, glass fiber/PP composites decreased 30% in tensile strength and 5% in tensile modulus after three reprocessing cycles. The micro-mechanical modeling demonstrated the deterioration in mechanical properties of GF/PP was mainly attributed to the fiber breakage that occurred during compounding and grinding.

The second part of this dissertation is concerned with the development of recyclable and light weight hybrid composites through the use of TLCP and glass fiber. Rheological tests were used to determine the optimal processing temperature of the injection molding process. At this processing temperature, the thermal degradation of matrix material was mitigated and the processability of the hybrid composite was improved. The best formulation of TLCP and glass fiber in the composite was determined giving rise to the generation of a recyclable hybrid composite with low melt viscosity, low mechanical anisotropy, and improved mechanical properties.

Finally, TLCP reinforced polyamide composites were utilized in an additive manufacturing application. The method of selecting the processing temperature to blend TLCP and polyamide in the dual extrusion process was devised using rheological analyses to take advantage of the supercooling behavior of TLCP and minimize the thermal degradation of the matrix polymer. The composite filament prepared by dual extrusion was printed and the printing temperature of the composite filament that led to the highest mechanical properties was determined. Although the tensile strength of the TLCP composite was lower than the glass fiber or carbon fiber composites, the tensile

modulus of 3D printed 60 wt% TLCP reinforced polyamide was comparable to traditional glass or carbon fiber reinforced composites in 3D printing.

Generation of Recyclable Liquid Crystalline Polymer Reinforced Composites for Use in Conventional and Additive Manufacturing Processes

ABSTRACT (public)

The large demand for high performance and light weight composite materials in various industries (e.g., automotive, aerospace, and construction) has resulted in accumulation of composite wastes in the environment. Reuse and recycling of fiber reinforced composites are beneficial from the environmental and economical point of view. However, mechanical recycling deteriorates the quality of traditional fiber reinforced composite (e.g., glass fiber and carbon fiber). There is a need to develop novel composites with greater recyclability and high-performance.

Thermotropic liquid crystalline polymers (TLCP) are attractive high performance materials because of their excellent mechanical properties and light weight. The goal of this work is to generate recyclable thermotropic liquid crystalline polymer (TLCP) reinforced composites for use in injection molding and 3D printing. In the first part of this work, a novel recyclable TLCP reinforced composite was generated using the grinding and injection molding. Recycled TLCP composites were as strong as the virgin TLCP composites, and the mechanical properties of TLCP composites were found to be competitive with the glass fiber reinforced counterparts. In the second part, a hybrid TLCP and glass fiber reinforced composite with great recyclability and excellent processability was developed. The processing conditions of injection molding were optimized by rheological tests to mitigate fiber breakage and improve the processability. Finally, a high performance and light weight TLCP reinforced composite filament was generated using the dual extrusion process which allowed the processing of two polymers

with different processing temperatures. This composite filament could be directly 3D printed using a benchtop 3D printer. The mechanical properties of 3D printed TLCP composites could rival 3D printed traditional fiber composites but with the potential to have a wider range of processing shapes.

Original Contribution

1. The method of optimization of processing conditions of dual extrusion has been extended to combine TLCP and polyamide (PA) materials. The PA and TLCP materials were purposely selected due to the stronger molecular interactions, which led to stiffer and stronger 3D printed composite parts. Previously, only acrylonitrile butadiene styrene (ABS), polyphenylene sulfide (PPS) and polypropylene (PP) were utilized as matrix polymers and were reinforced by TLCP to generate composite filaments for use in the 3D printing process [1-3]. The poor interfacial adhesion between the matrix and TLCP led to relative low tensile strength.
2. The influence of mechanical recycling on the properties of TLCP reinforced polypropylene (PP) and glass fiber reinforced polypropylene was studied. This work is the first to systematically compare the mechanical, thermal, morphological, rheological, and thermo-mechanical properties of recycled TLCP/PP with those properties of glass fiber/PP. To the author's knowledge, this is the first time that the recyclability of TLCP/PP has been confirmed to be greater than that of glass fiber reinforced polypropylene.
3. Recyclable and high-performance hybrid composites using TLCP and glass fiber were successfully developed. This is the first time that the optimal formulation of TLCP and glass fiber in the composite was determined which led to the generation of hybrid composites with high recyclability, excellent processability, and low mechanical anisotropy.

Reference

1. Ansari, M. Q.; Redmann, A.; Osswald, T. A.; Bortner, M. J.; Baird, D. G., Application of thermotropic liquid crystalline polymer reinforced acrylonitrile butadiene styrene in fused filament fabrication. *Addit. Manuf.* **2019,** *29*.
2. Ansari, M. Q.; Bortner, M. J.; Baird, D. G., Generation of polyphenylene sulfide reinforced with a thermotropic liquid crystalline polymer for application in fused filament fabrication. *Addit. Manuf.* **2019,** *29*, 100814.
3. Gray IV, R. W.; Baird, D. G.; Helge Bøhn, J., Effects of processing conditions on short TLCP fiber reinforced FDM parts. *Rapid Prototyp. J.* **1998,** *4*, 14-25.

Acknowledgments

The author would like to express his deepest gratitude to his adviser, Dr. Donald G. Baird, for continuous guidance and support in the completion of his PhD degree. This dissertation and all that the author have gained during this process would never been achieved without Dr. Baird. In addition, the author likes to acknowledge his committee members: Dr. Justin R. Barone, Dr. Michael J. Bortner, Dr. Stephen M. Martin, and Dr. Scott W. Case, for their encouragement and insightful suggestions throughout his research project.

The author would like to thank the current and former members of polymer processing and rheology lab: Dr. Greg Lambert, Dr. Juan Pretelt, Dr. Jianger Yu, Dr. Ansari Mubashir, Dr. Hongyu Chen, Dr. Jier Han, Dr. Kennedy Boyce, Craig Mansfield, and Vikas Parakh. It was a great pleasure to working with everyone in the lab.

The author thanks the staff in the Macromolecules Innovation Institute (MII) and Department of Chemical Engineering, especially Kim Felix, Jennifer Galford, Andrew Tie, Reilly Henson, Kevin Holshouser, Michael Vaught, Bradley Reed, Diane Cannaday, Andrea Linkous, Jane Price, and Tina Russell.

The author would like to thank General Motors (GM) for financial support on the project providing financial support, materials and their input to carry out this research. In addition, the author thanks David A. Okonski for his suggestions and contribution to this research project.

The author would especially thank his friends for a cherished time spent together at Blacksburg: Dana Kazerooni, Linjie Gu, Deyang Yu, Rui Zhang, Hongxia Dai, Junkai Zeng, Junyi Chen, Meng Cai, Sha Ding, and more.

The author thanks his parents, Weiguo Chen and Lihua Liang. Without your unconditional support and help, graduate school would have been much harder.

Last, the author would like to thank his fiancée, Lin Ju, whose tremendous love and continuous support made this dissertation possible.

Table of Contents

List of Figure

List of Tables

1 Introduction

Chapter 1. Introduction

Thermotropic liquid crystalline polymers (TLCPs) are wholly aromatic polymers that exhibit excellent mechanical performance, low melt viscosity, potentially great recyclability, chemical resistance, and great thermal stability [1]. Because of these advantages, TLCPs were utilized to blend with thermoplastics as reinforcements through various processing techniques such as injection molding, film extrusion and additive manufacturing [2-6]

This dissertation is concerned with the development of recyclable and high-performance TLCP reinforced composites for use in injection molding and additive manufacturing processes. This chapter provides the background of TLCP materials and the previous research work relating to this dissertation. The last section of this chapter is the objectives of this research.

1.1 Thermotropic Liquid Crystalline Polymer

TLCPs consist of the rigid anisotropic unit called a mesogen which shows liquid crystalline order in the melt state. Because of the mesogenic phase, TLCPs could achieve a high degree of molecular orientation along the flow direction under shear or extensional flow. The high degree of orientation gives rise to high tensile and flexural properties. The tensile moduli of TLCPs strands were reported to be between 50 to 100 GPa, depending on the types of TLCP and processing conditions [7]. The stiffness of TLCPs strands is competitive with the tensile modulus of E-glass fiber (i.e., ~72 GPa). In addition, the viscosities of TLCPs are lower than most thermoplastics [8]. The major benefits of

adding TLCPs (reinforcements) into other thermoplastics (matrices) are the enhancement of mechanical properties and improvement of processability.

1.2 Injection Molding of TLCP Reinforced Composite

Injection molding is one of the most common processing techniques to fabricate plastic materials. Over 30% of thermoplastic materials are produced using this process [9]. Injection molding is most suitable to mass production of plastic parts with complex geometries and high precision. The injection molding machine is composed of two units: injection and clamping, as indicated in Figure 1.1. The injection unit is used to completely melt the material and quickly inject the melt into the mold by a hydraulic system. The function of the clamping unit is to clamp the mold so that the material can be injected into the mold cavity to form a specific geometry. Next, the clamping unit opens the mold to eject the part.

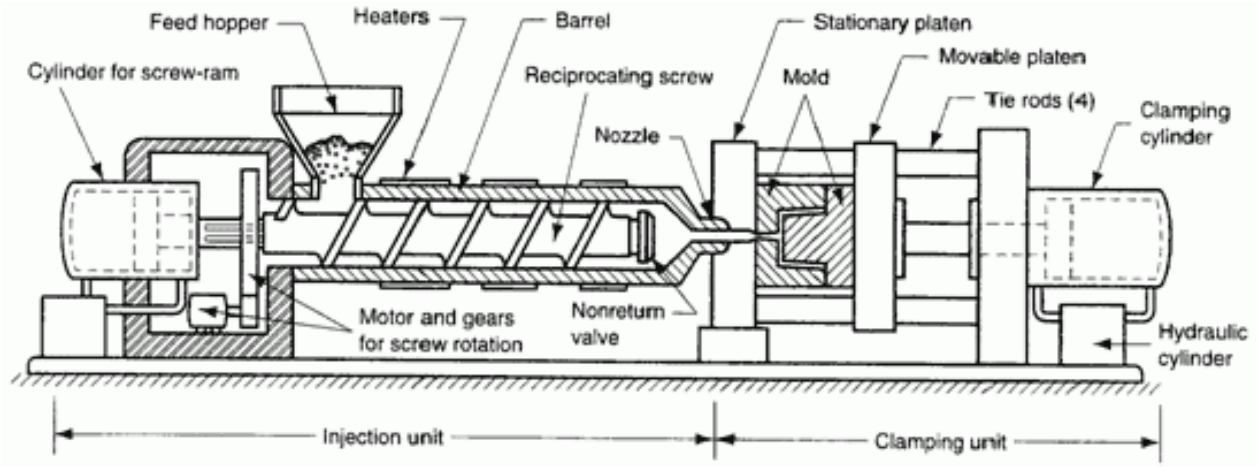

Figure 1. 1 Schematic of the injection molding process [10]

Isayev *et al.* [11] reported the injection molding of the TLCP reinforced thermoplastic composite for the first time in 1987. Significant improvements in Young's modulus and yield strength of TLCP reinforced composites have been observed compared to the polymer matrix. In addition, the apparent shear viscosity of polycarbonate matrix material was decreased with the incorporation of TLCP. Since that time, other researchers have studied processing of the TLCP reinforced composites by using injection molding [12-16]. At the same weight fraction of reinforcement, the stiffness of injection molded TLCP reinforced thermoplastics is similar to that of glass fiber reinforced counterparts [17, 18]. Because the density of TLCP is almost half of the E-glass fiber, the specific tensile modulus of the TLCP composite is much greater than the glass fiber reinforced composite.

1.3 Fused Filament Fabrication (FFF) of TLCP Reinforced Composites

Fused filament fabrication (FFF) is one of the most popular additive manufacturing techniques owing to the reduced printing time, low-cost material, and equipment as compared to other additive manufacturing methods such as stereolithography and selective laser sintering. In this process, the continuous thermoplastic filament is fed by a pinch roller into the hot end where the thermoplastic filament is heated up to above its melting point or glass transition temperature to reach the semi-liquid state and extruded from the nozzle. The extrudate is deposited on the printing bed layer-by-layer to build up a three-dimensional structure. Figure 1.2 presents the schematic of the fused filament fabrication process.

Polylactic acid (PLA) and acrylonitrile butadiene styrene (ABS) are the primary materials for the fused filament fabrication (FFF) process. One of the major challenges for FFF using these pure polymers is achieving excellent mechanical performance. Researchers have begun to tackle this issue by adding fiber reinforcement into the matrix polymer for use in 3D printing process [19, 20]. The reinforcements, such as carbon, glass, and Kevlar fibers, can enhance the mechanical properties of polymer materials [21-24]. The types of fiber reinforcements can be divided into short and continuous fiber categories. Short (discontinuous) fiber reinforced composite filaments are generated by mixing the matrix material and fibers in an extruder shaping the blend into a composite filament by extruding through a die. The extensive fiber attrition during processing limits the composite material from achieving higher reinforcing potential. To overcome the fiber breakage issue and further improve the mechanical properties of the printed parts, the in-nozzle impregnation process has been developed by researchers to 3D print continuous fiber reinforced thermoplastic composites [25-27]. In this in-nozzle impregnation process, the matrix filament and continuous fibers are separately fed to the print head, and then the melted thermoplastic and continuous fiber are combined in the heated nozzle and deposited on the printing platform to construct the specimen [25]. The disadvantages of using the continuous fiber in the 3D printing process are the modification of an existing printer or purchasing high-cost printer, poor wetting of fiber by the matrix, and the requirement of a severing process when the printer head moves from one region to another to continuously print on the printing bed [24, 25, 28].

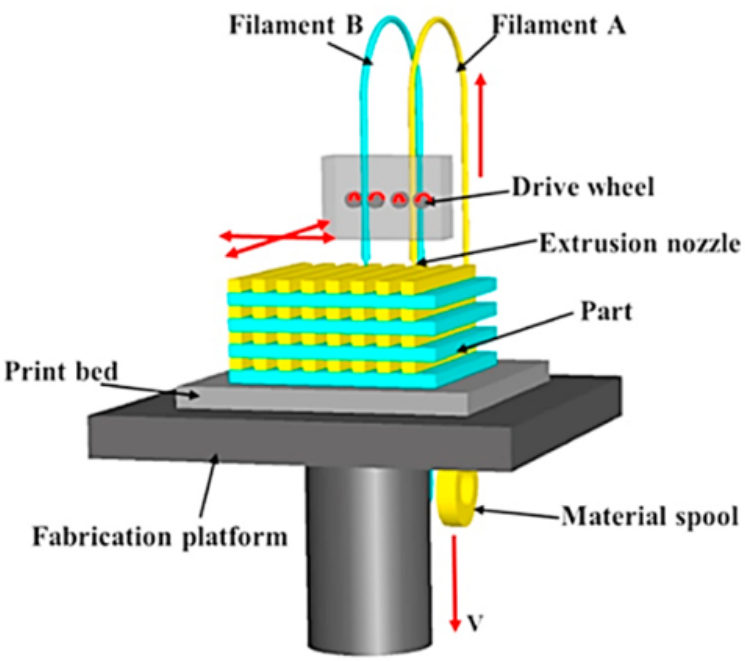

Figure 1. 2 The schematic diagram of the FFF process [29]

Gray *et al.* [5] reported for the first time the generation of the TLCP reinforced polypropylene composite material for the 3D printing process. The continuous TLCP/polypropylene (PP) composite filaments were prepared using the dual extrusion process. The dual extrusion process was patented by Sukhadia and co-workers [30]. In this process, the TLCP and PP were separately plasticated in two single screw extruders. The TLCP and PP melts joined at a T-junction and then the TLCP melt was divided and distributed by static mixers to form a finer TLCP stream. The material exited from the die to form the composite filament. Then, the composite filaments were cut into short strands and molded into rectangular plaques. Finally, the plaques were ground into granules and

the granules were processed by the single screw extruder to fabricate the composite filament with a suitable diameter for fused filament fabrication. The mechanical properties of the 3D-printed composites were found to be higher than that of the matrix material, but the cutting and grinding processes reduced the fiber length of TLCP and restricted the composite material from attaining higher mechanical properties. To retain the longer TLCP fibrils in the composite filament, Ansari *et al*. [28] directly used the composite filament generated from the dual extrusion process for 3D printing. This method enabled the generation of 3D printed composites with superior mechanical properties where the tensile modulus of printed TLCP/ABS was around 16 GPa. In addition, the mechanical properties of TLCP/ABS obtained using 3D printing were found to be higher than that of the injection molded counterpart.

1.4 Recycling of Fiber Reinforced Composites

The rapid growth in manufacturing fiber reinforced composite materials has led to the accumulation of composite waste in landfill sites or natural environments [31, 32]. One of most difficult and complex challenges in the composite field is to recycle these materials. The common recycling methods include mechanical recycling, thermal and chemical processes. During the mechanical recycling process, the composite waste is shredded/ground into smaller composite particulates and then the particulates are remanufactured into recycled parts. The schematic of the mechanical recycling process from grinding composite component waste to manufacturing recycled composites is illustrated in Figure 1.3. In the thermal recycling (also known as pyrolysis) process, the composite material is first subjected to elevated temperature from 300 to 800°C in an oven under an inert environment. The fibers are recovered after the evaporation of matrix

polymer into small molecules. The recovered fibers are recycled to reinforce other matrix materials and the small molecules are converted into energy due to the high calorific value [33]. The chemical process utilizes chemical solvents to depolymerize the matrix polymer into monomers. Both the fiber and degraded matrix can be reclaimed after the chemical recycling. Wide selection of solvents, temperatures, and catalysts allows versatile applications of this method. Among these three recycling methods, mechanical recycling is the most environmentally friendly process because of the low energy consumption and elimination of solvent usage [34].

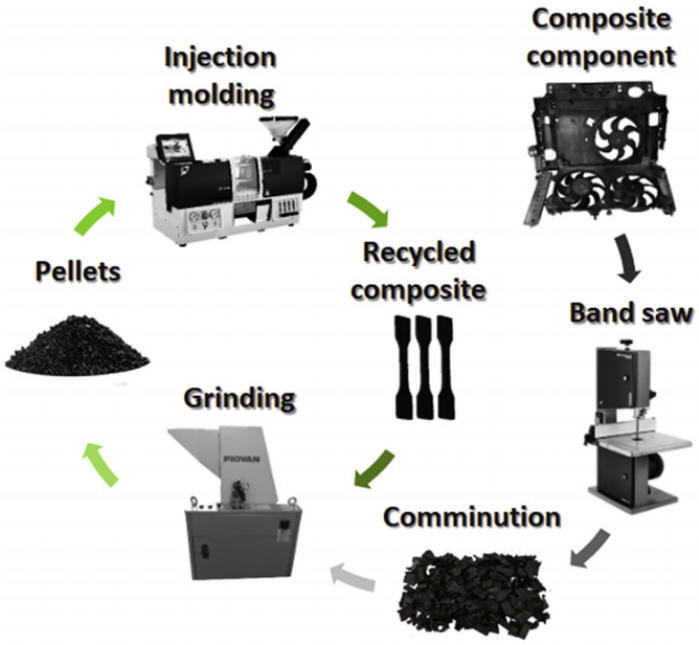

Figure 1. 3 Mechanical recycling of fiber reinforced composites [35]

1.5 Research Objectives

Objective 1: Establish the processing temperature of the dual extrusion process to produce TLCP/nylon composite filaments for use in additive manufacturing process. Additionally, determine the effect of TLCP concentration and printing temperature on the mechanical properties of 3D printed TLCP/nylon composites.

Objective 2: Determine the effect of mechanical reprocessing on the properties (e.g., rheological, mechanical, thermo-mechanical, etc.) of thermotropic liquid crystalline polymer (TLCP) reinforced polypropylene and glass fiber reinforced polypropylene.

Objective 3: Determine the optimal formulation of glass fiber and TLCP to develop a recyclable, *in situ* hybrid TLCP/glass fiber reinforced composite with high mechanical properties and improved processability.

1.6 Reference

1. Sastri, V. R., 8 - high-temperature engineering thermoplastics: Polysulfones, polyimides, polysulfides, polyketones, liquid crystalline polymers, and fluoropolymers. In *Plastics in medical devices (second edition)*, Sastri, V. R., Ed. William Andrew Publishing: Oxford, 2014; pp 173-213.
2. deSouza, J. P.; Baird, D. G., In situ composites based on blends of a poly(ether imide) and thermotropic liquid crystalline polymers under injection moulding conditions. *Polymer* **1996,** *37*, 1985-1997.
3. Kiss, G., Insitu composites - blends of isotropic polymers and thermotropic liquid-crystalline polymers. *Polym. Eng. Sci.* **1987,** *27*, 410-423.
4. Siegmann, A.; Dagan, A.; Kenig, S., Polyblends containing a liquid crystalline polymer. *Polymer* **1985,** *26*, 1325-1330.
5. Gray IV, R. W.; Baird, D. G.; Helge Bøhn, J., Effects of processing conditions on short tlcp fiber reinforced fdm parts. *Rapid Prototyp. J.* **1998,** *4*, 14-25.
6. Gray, R. W.; Baird, D. G.; Bohn, J. H., Thermoplastic composites reinforced with long fiber thermotropic liquid crystalline polymers for fused deposition modeling. *Polym. Compos.* **1998,** *19*, 383-394.
7. Kalfon-Cohen, E.; Marom, G.; Wachtel, E.; Pegoretti, A., Characterization of drawn monofilaments of liquid crystalline polymer/carbon nanoparticle composites correlated to nematic order. *Polymer* **2009,** *50*, 1797-1804.
8. Gotsis, A. D.; Baird, D. G., Rheological properties of liquid crystalline copolyester melts. Ii. Comparison of capillary and rotary rheometer results. *Journal of Rheology* **1985,** *29*, 539-556.
9. Osswald, T. A., *Understanding polymer processing: Processes and governing equations*. Carl Hanser Verlag GmbH Co KG: 2017.
10. Injection unit. https://www.plasticmold.net/injection-unit/ (accessed 1/5/2021).
11. Isayev, A. I.; Modic, M., Self-reinforced melt processible polymer composites - extrusion, compression, and injection-molding. *Polym. Compos.* **1987,** *8*, 158-175.
12. Mehta, A.; Isayev, A. I., Rheology, morphology, and mechanical characteristics of poly(etherether ketone)-liquid crystal polymer blends. *Polym. Eng. Sci.* **1991,** *31*, 971-980.
13. Wang, Y.; Yue, C.; Tam, K.; Hu, X. J. J. o. a. p. s., Relationship between processing, microstructure, and mechanical properties of injection molded thermotropic lcp. **2003,** *88*, 1713-1718.
14. Handlos, A. A. The processing of microcomposites based on polypropylene and two thermotropic liquid crystalline polymers in injection molding, sheet extrusion, and extrusion blow molding. Virginia Tech, 1994.
15. Huang, J.; Baird, D. G., Injection molding of polypropylene reinforced with thermotropic liquid crystalline polymer microfibrils. Part iii: Combination of glass and tlcp. *J. Inj. Mold. Tech.* **2002,** *6*, 187.
16. McLeod, M. A.; Baird, D. G. J. C. P. B. E., The influence of processing variables on the mechanical properties of injection molded pregenerated microcomposites. **1999,** *30*, 297-308.
17. O'Donnell, H. J.; Baird, D. G. J. P., In situ reinforcement of polypropylene with liquid-crystalline polymers: Effect of maleic anhydride-grafted polypropylene. **1995,** *36*, 3113-3126.
18. Sukhadia, A. M. The in situ generation of liquid crystalline polymer reinforcements in thermoplastics. Doctoral Dissertations, Virginia Tech, 1992.
19. Tian, X. Y.; Liu, T. F.; Yang, C. C.; Wang, Q. R.; Li, D. C., Interface and performance of 3d printed continuous carbon fiber reinforced pla composites. *Compos. Pt. A-Appl. Sci. Manuf.* **2016,** *88*, 198-205.

20. Kaynak, C.; Varsavas, S. D., Performance comparison of the 3d-printed and injection-molded pla and its elastomer blend and fiber composites. *J. Thermoplast. Compos. Mater.* **2019,** *32*, 501-520.
21. Tekinalp, H. L.; Kunc, V.; Velez-Garcia, G. M.; Duty, C. E.; Love, L. J.; Naskar, A. K.; Blue, C. A.; Ozcan, S., Highly oriented carbon fiber-polymer composites via additive manufacturing. *Compos. Sci. Technol.* **2014,** *105*, 144-150.
22. Love, L. J.; Kunc, V.; Rios, O.; Duty, C. E.; Elliott, A. M.; Post, B. K.; Smith, R. J.; Blue, C. A., The importance of carbon fiber to polymer additive manufacturing. *J. Mater. Res.* **2014,** *29*, 1893-1898.
23. Li, N. Y.; Li, Y. G.; Liu, S. T., Rapid prototyping of continuous carbon fiber reinforced polylactic acid composites by 3d printing. *J. Mater. Process. Technol.* **2016,** *238*, 218-225.
24. Dickson, A. N.; Barry, J. N.; McDonnell, K. A.; Dowling, D. P., Fabrication of continuous carbon, glass and kevlar fibre reinforced polymer composites using additive manufacturing. *Addit. Manuf.* **2017,** *16*, 146-152.
25. Matsuzaki, R.; Ueda, M.; Namiki, M.; Jeong, T. K.; Asahara, H.; Horiguchi, K.; Nakamura, T.; Todoroki, A.; Hirano, Y., Three-dimensional printing of continuous-fiber composites by in-nozzle impregnation. *Scientific Reports* **2016,** *6*.
26. Luo, M.; Tian, X.; Shang, J.; Zhu, W.; Li, D.; Qin, Y., Impregnation and interlayer bonding behaviours of 3d-printed continuous carbon-fiber-reinforced poly-ether-ether-ketone composites. *Composites Part A: Applied Science Manufacturing*

2019, *121*, 130-138.
27. Omuro, R.; Ueda, M.; Matsuzaki, R.; Todoroki, A.; Hirano, Y. In *Three-dimensional printing of continuous carbon fiber reinforced thermoplastics by in-nozzle impregnation with compaction roller*, 21st International Conference on Composite Materials, Xian, China, 2017; pp 20-25.
28. Ansari, M. Q.; Redmann, A.; Osswald, T. A.; Bortner, M. J.; Baird, D. G. J. A. M., Application of thermotropic liquid crystalline polymer reinforced acrylonitrile butadiene styrene in fused filament fabrication. **2019,** *29*, 100813.
29. Ngo, T. D.; Kashani, A.; Imbalzano, G.; Nguyen, K. T. Q.; Hui, D., Additive manufacturing (3d printing): A review of materials, methods, applications and challenges. *Compos. Pt. B-Eng.* **2018,** *143*, 172-196.
30. Baird, D. G.; Sukhadia, A. Mixing process for generating in-situ reinforced thermoplastics. US5225488, 1993.
31. Pimenta, S.; Pinho, S. T., Recycling carbon fibre reinforced polymers for structural applications: Technology review and market outlook. *Waste Management* **2011,** *31*, 378-392.
32. Rajendran, S.; Scelsi, L.; Hodzic, A.; Soutis, C.; Al-Maadeed, M. A., Environmental impact assessment of composites containing recycled plastics. *Resources Conservation and Recycling* **2012,** *60*, 131-139.
33. Liu, Y.; Farnsworth, M.; Tiwari, A., A review of optimisation techniques used in the composite recycling area: State-of-the-art and steps towards a research agenda. *Journal of Cleaner Production* **2017,** *140*, 1775-1781.
34. Zhang, J.; Chevali, V. S.; Wang, H.; Wang, C. H., Current status of carbon fibre and carbon fibre composites recycling. *Compos. Pt. B-Eng.* **2020,** *193*.
35. Pietroluongo, M.; Padovano, E.; Frache, A.; Badini, C., Mechanical recycling of an end-of-life automotive composite component. *Sustainable Materials and Technologies* **2020,** *23*.

2.0 Literature Review

Chapter 2. Literature Review

2.1 Liquid Crystalline Polymer

2.1.1 Liquid Crystalline Polymer Mesophase

Liquid crystalline polymers consist of rigid backbone structures and exhibit an intermediate phase between highly ordered solid crystalline and isotropic liquid. This intermediate phase is referred to as a mesophase. Friedel [1] defined three different mesophases for certain organic materials: nematic, smectic and cholesteric. Figure 2.1 illustrates the three mesophase structures with orientation director **n**. Nematic liquid crystals can form long-range orientational order, as indicated with orientation director **n**, and there is no short-range positional order. If positional order is added to the nematic phase, the liquid crystals will have both long range orientational order and a layered structure known as the smectic phase. The cholesteric phase contains a set of helical nematic layers in which the layer director rotates from its adjacent layer at a constant angle.

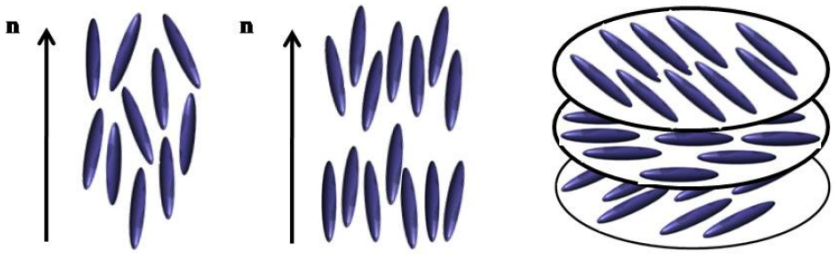

Figure 2. 1: Nematic, smectic, and cholesteric phases (left to right) [2].

2.1.2 Thermotropic Liquid Crystalline Polymers

Liquid crystalline polymers can be categorized into two general types: lyotropic and thermotropic. The formation of mesophase in lyotropic liquid crystalline polymers is governed by the polymer concentration in the solution. For the thermotropic liquid crystalline polymers (TLCPs), the liquid crystalline phase transition is controlled by temperature. The liquid crystalline polymer used in this work is a TLCP, and a review of lyotropic liquid crystalline polymers is beyond the scope of this dissertation.

Due to the rigid monomer unit along the polymer backbone, the melting points of some liquid crystalline polymers (i.e., poly(p-phenylene terephthalamide)) are higher than their thermal degradation temperatures. Enormous efforts have been made to lower the melting point of the thermotropic liquid crystalline polymer, and the techniques are divided into three categories: 1) flexible spacer, 2) addition of linking units 3) disruptive chain packing [2-8]. An example of utilizing the disruptive chain packing method is to replace the benzene unit along the main chain TLCP with naphthalene or a biphenyl unit which leads to the disruption of crystallinity and reduction of the melting temperature. This approach has led to the invention of commercial TLCP products with the trade name Vectra which are currently manufactured by Celanese. Vectra A950 is composed of 73 mol% 4-hydroxy benzoic acid and 27 mol% 2,6-hydroxynaphthoic acid. As a type of aromatic copolyesteramide, Vectra B950 contains 60 mol% 2-hydro-6-xynaphthoic acid, 20 mol% aminophenol and 20 mol% terephthalic acid. The relatively low melting points of Vectra B950 and Vectra A950 (~280°C) enable the melt processing of these TLCPs with commodity and engineering thermoplastics [9-12]. Currently, the only commercially available TLCP material consisting of amide linkages in the polymer backbone is Vectra

B950. The formation of hydrogen bonding among the polymer chains leads to the higher glass transition temperature of Vectra B950 and makes it more suitable for application in an environment with elevated temperature. The physical properties of injection molded Vectra A950 and Vectra B950 are illustrated in Table 2.1.

The highest mechanical properties of TLCPs are usually obtained through strand extrusion or melt fiber spinning. The strong elongation flow during the drawing step aligns the rod-like TLCP molecule in the flow direction, giving the fiber/strand extraordinary mechanical properties. Crevecoeur *et al.* [13] reported modulus of highly drawn TLCP material prepared by fiber spinning were around 75 GPa. The tensile modulus of highly drawn TLCP is comparable to the stiffness of glass fiber.

Table 2. 1: The various properties of injection molded Vectra B950 and Vectra A950 [14]

Properties	Vectra B950	Vectra A950
Tensile Strength (MPa)	188	159
Tensile Elongation (%)	1.3	4.8
Tensile Modulus (GPa)	18.6	10.3
Melting Point (°C)	280	280
Notch Impact Strength (J/m)	415	520
Heat Deflection Temperature (°C)	200	182

2.2 *In Situ* TLCP Reinforced Thermoplastic Composite

Kiss [15] defined the TLCP reinforced thermoplastic as an *in situ* composite due to the formation of reinforcing fibrils during the processing as compared to glass fiber reinforced composites where the reinforcing species are present before the processing of the material. The TLCP fibrils can significantly enhance the mechanical properties of the thermoplastic matrix. Morphology and molecular orientation of TLCP play an important role in the level of reinforcement obtained in the *in situ* composite.

2.2.1 TLCP Fibrillation

Several factors influence the formation of TLCP fibrils during blending with thermoplastics, such as the composition of the polymer blends, the viscosity ratio of TLCP to matrix, external stress (shear or extensional), and interfacial tension. The critical Weber number required to deform the dispersed droplet into fibrils at a viscosity ratio ($\frac{\eta_{dispersed}}{\eta_{continous}}$) for extensional and shear flow is illustrated in Figure 2.2. The Weber number is the ratio of flow stress to the interfacial tension, where the flow stress promotes droplet deformation and breakup and the interfacial tension prevents the deformation of the dispersed phase. The critical Weber number is more dependent on the viscosity ratio in simple shear flow than extensional flow (Figure 2.2). When the viscosity ratio is above 4.0, the drop deformation cannot be observed under shear flow. TLCP fibrillation is significantly influenced by the viscosity ratio. Petrovic and Farris [16] observed that the fibrillation of TLCP occurred at a viscosity ratio between 0.01 to 0.001 for polycarbonate/TLCP blends.

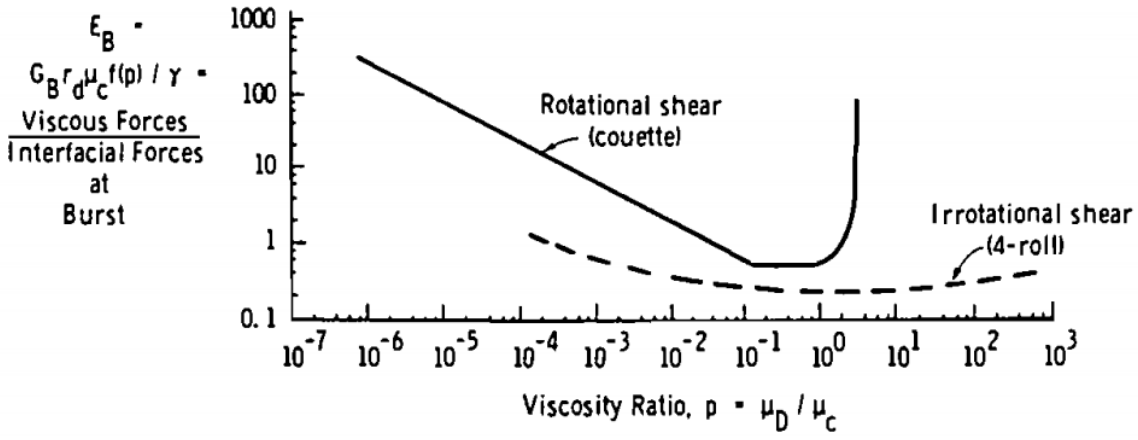

Figure 2. 2: Critical Weber numbers as a function of viscosity ratio [17].

The process of the development of fibrillar structure in the converging flow section of a capillary is shown in Figure 2.3 [18]. First, deformation and coalescence of droplets take place at the entrance region (Zone A). Second, the convergent flow happens when polymer melt flows from a wide to narrow cross-section (Zone B). Third, due to the shear and retardation of the stream, the fibrils lose their parallelism and increase the diameter (Zone C). Last, the shear flow results in the formation of parallel fibrils again. Several researchers have studied *in situ* TLCP composite systems and observed the formation of fibrils in capillary die [19-22].

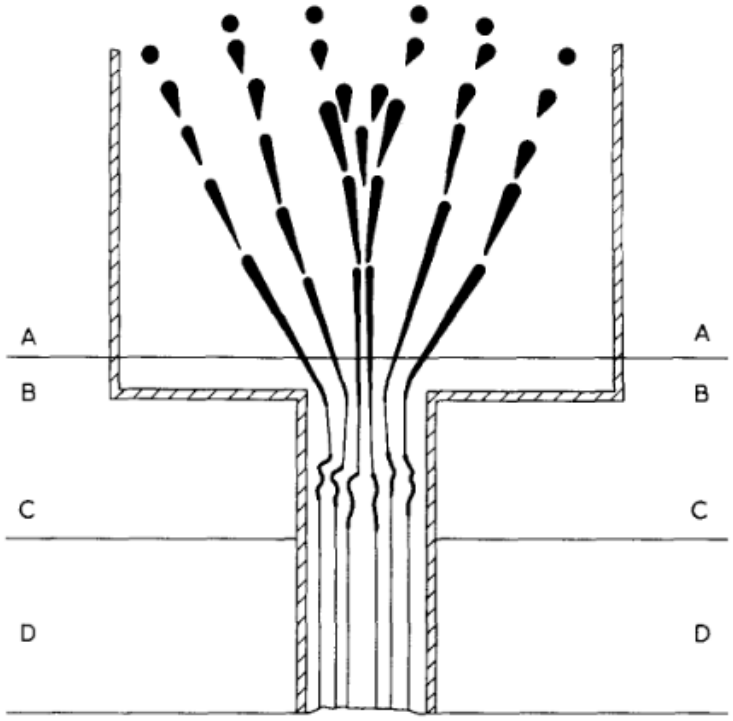

Figure 2. 3: The schematic of fibril formation process in a capillary die. Zone A-tension and fibrillation; Zone B-flow narrowing; Zone C-shear and retardation of stream; Zone D-shear flow [18].

Blizard and Baird [23] investigated the conditions for the development of TLCP fibrillar morphologies in blends of polycarbonate and nylon 6,6 material. The TLCP morphologies of 10 to 70 wt% *in situ* TLCP/polycarbonate (PC) and TCLP/nylon 6,6 have been examined after the polymer blends were subjected to steady shear flow, single screw extrusion, or flow in a capillary die. The specimens were processed in a single screw extruder and the extrudate was immediately quenched in an ice water bath to lock in the TLCP structure. At 10 wt% of TLCP, the reinforcing phase presented as the dispersed droplet morphology because the very low concentration of TLCP prevented the droplet coalescence and formation of fibril. At 30 wt% of TLCP, the polymer blends

exhibited fibrillar morphology and the diameter of the fibrils was less than 10 μm. At 50 wt%, the TLCP showed a continuous phase with large variation in diameter, and phase inversion began at this concentration. To examine the influence of shear flow on the morphological properties of the *in situ* TLCP/PC and TLCP/nylon, the polymer blends were sheared in a rheometer and the morphologies were examined by a scanning electron microscopy. No TLCP fibril was observed under the simple steady shear flow for shear rates up to 100 s^{-1}. The TLCP droplets reduced their size and no preferential alignment was seen. The results from this research work indicated that elongation flow was required to generate the TLCP fibrils in these blends.

2.2.2 The Tsai-Halpin Equation in TLCP Reinforced Composites

The Tsai-Halpin equation provides an expression to predict the tensile modulus of fiber reinforced composites based on their composition and aspect ratio [24]. This equation is often used to predict the moduli of in situ TLCP reinforced composite. The Tsai-Halpin equation estimates the modulus of uniaxially aligned fiber reinforced composite with the following equations:

$$E_c = E_m\left(\frac{1+\eta\xi V_f}{1-\eta\xi V_f}\right) \tag{2. 1}$$

$$\eta = \frac{\frac{E_f}{E_m}-1}{\frac{E_f}{E_m}+\xi} \tag{2. 2}$$

$$\xi = 2\left(\frac{L}{D}\right) \tag{2. 3}$$

where E_c, E_f, E_m, L, V_f, and D are the modulus of composite, modulus of the reinforcing fiber, modulus of the matrix, fiber length of the reinforcement, volume fraction of the reinforcement, and fiber diameter, respectively. Figure 2.4 shows the prediction of the Tsai-Halpin equation for the fiber reinforced composite, where $E_m = 75$ GPa and $E_m = 2$ GPa. The aspect ratio of the fiber significantly influences the tensile modulus of the composite. The 30 vol% fiber reinforced composite with an aspect ratio of 25 has the approximately the same tensile modulus as the one with 40 vol% fiber and an aspect ratio of 10. When the L/D is greater than 100, the Tsai-Halpin equation is approximately reduced to the rule of mixtures:

$$E_c = V_f E_f + (1 - V_f)E_m \quad (2.4)$$

where E_f, E_c, E_m and V_f are modulus of the reinforcement, modulus of the composite, Em, modulus of the matrix and volume fraction of the fiber, respectively.

The modulus values of the *in situ* injection molded TLCP composites obtained from the literature are compared with the moduli predicted using the rule of mixtures as can be seen in Table 2.2 [25, 26]. The moduli of the TLCP composites are lower than those of the predicted values. This may result from the following reason. First, the aspect ratio of the TLCP fibrils is lower than 100. For the injection molded TLCP composite, the core region consists of TLCP droplets or platelets instead of TLCP fibrils. Second, the model assumes all the fibers are uniaxially aligned but the injection molded TLCP composite has a low degree of molecular orientation especially at the core layer because of insufficient extensional flow. Last, the model assumes a perfect interfacial adhesion

between the fiber and matrix. The incompatibility between the TLCP and the matrix gives rise to poor interfacial adhesion.

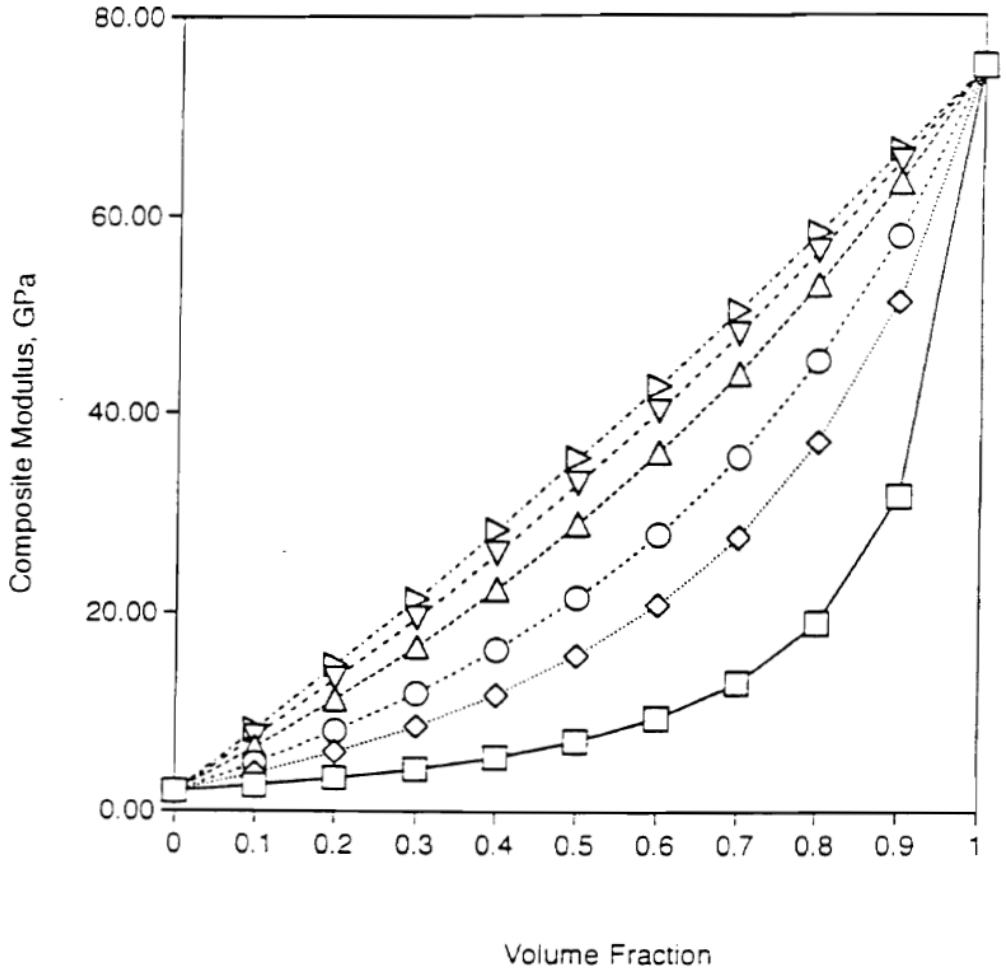

Figure 2. 4: Tsai-Halpin equation for predication of tensile modulus of fiber reinforced composites with different volume fraction and fiber aspect ratio for uniaxially aligned fiber. Fiber modulus = 75 GPa, matrix modulus = 2 GPa. Aspect ratio: □-1; ◊-5; ○-10; △-25; ▽-50; ▷-100.

Table 2. 2: Experimental and predicted tensile moduli of injection molded TLCP reinforced composite

Composite Material	Tensile modulus (GPa)-experimental	Tensile Modulus (GPa)-prediction using rule of mixtures	Reference
30 wt% Vectra A/PP	2.7	4.24	[25]
30 wt% Vectra B/PP	5.3	7.55	[26]
20 wt% Vectra A/PET	3.42	3.68	[27]

2.2.3 Mechanical Properties of *In Situ* TLCP Composite vs Glass Fiber Composite

Besides comparing the tensile modulus of TLCP reinforced composites to the modulus predicted by theoretical calculation, moduli of TLCP composites can be compared with moduli of fiber reinforced composite materials. Due to the outstanding mechanical properties, TLCP composites may have competitive mechanical performance to that of traditional fiber reinforced composites and have the potential to replace them. Therefore, the mechanical properties of the injection molded TLCP composites will be compared against the glass fiber reinforced thermoplastics with the same reinforcement concentration. Table 2. 3 illustrates the tensile properties of TLCP/PP, TLCP/PET, and

glass fiber reinforced composites. The injection molded TLCP composites show a similar level of reinforcement of tensile modulus compared to glass fiber reinforced composites. However, the tensile strengths of the injection molded TLCP composites are usually less than glass fiber reinforced composites. In addition, it has to be noted that the tensile modulus and strength reported here are measured in the flow direction, and mechanical properties of TLCP reinforced composite are typically lower or equal to that of the matrix polymer in the transverse direction.

Table 2. 3: Tensile properties of *in situ* injection molded TLCP reinforced composites and glass fiber reinforced thermoplastics obtained from tensile bar

Composite Materials	Tensile Modulus (GPa)	Tensile Strength (MPa)	Reference
20 wt% TLCP/PP	3.3	36.85	[28]
20 wt% glass fiber/PP	3.66	49.05	[28]
PP	1.37	31.34	[28]
20 wt% TLCP/PET	8.87	96.6	[29]
20 wt% glass fiber/PP	7.02	107.8	[29]
PET	2.69	58.3	[29]

2.3 Injection Molding of TLCP Reinforced Composite

TLCPs are the ideal materials for the injection molding process because of their low melt viscosity, low shrinkage, and great dimensional stability. Several studies of the mechanical properties, morphology, and orientation distribution of injection molded TLCPs have been performed [13, 20, 30-32]. Skin-core morphologies have been consistently observed in the literature where TLCP shows a higher degree of orientation in the skin layer and a much lower molecular orientation in the core layer. The complex flow pattern during the mold filling process gives rise to the skin-core morphology of injection molded TLCP.

Figure 2.5 illustrates the flow kinematics during the mold filling processing. The material at the advancing front is extended towards the mold wall by strong elongational flow. As the material reaches the cold wall, the solidification of the material quickly happens leading to the formation of a highly oriented molecular structure along the flow direction near the surface. Behind the advancing front, the material primarily experiences shear stress and the shear stress is not able to effectively align the molecules along the flow direction as compared to the extensional stress. Therefore, the TLCP molecules orient in the flow direction at the skin layer and the core region consists of more randomly oriented TLCP. In addition, the anisotropy in physical properties arises from the greater extension rate in the flow direction than the direction transverse to the flow.

The morphology of injection molded TLCP blends has been characterized by Silverstein *et al*. [33]. Various compositions of TLCP/PET blends (5 to 95 wt%) were prepared through compounding the TLCP and PET in a single screw extruder. The TLCP/PET pellets were injection molded into a 15 x 15 x 0.3 cm plaque at an injection

temperature of 290°C and a mold temperature of 27°C. To prepare the specimen for scanning electron microscopy, the PET material was chemically etched from the blends. The hierarchal structure of 50 wt% TLCP/PET blends is shown in Figure 2.6. About a 20 μm thick top microlayer contained highly oriented TLCP fibrils with diameter around 2 μm. TLCP fibrils with diameter from 2 to 5 μm were observed in the skin microlayer. The formation of TLCP fibrils in these two layers resulted from the elongational flow at the advancing front. At the central microlayer, the large platelike TLCP phase arranged in a parabolic flow pattern because of the shear flow. The multilayer morphologies of TLCP/thermoplastic blends have also been observed by other researchers [34-36]. The complex flow field during the injection molding process leads to the hierarchical structure of *in situ* TLCP composite.

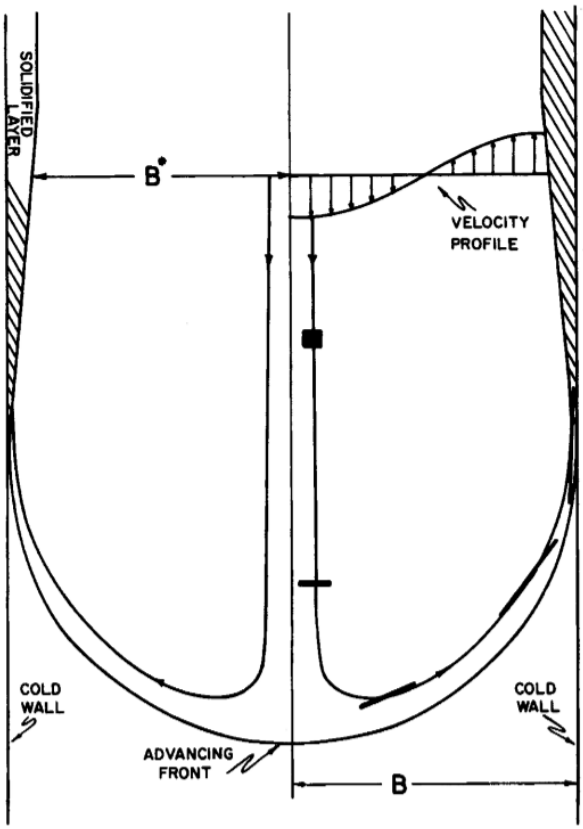

Figure 2. 5 : The schematic of the injection molding flow. The shaded areas indicate the orientation of a fluid particle [37].

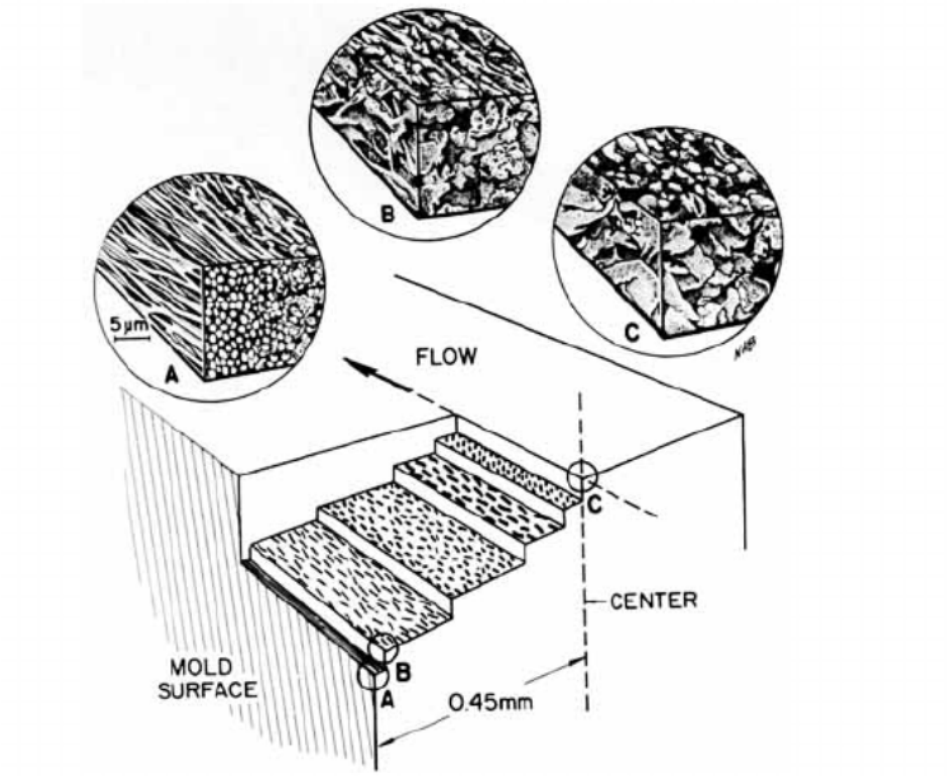

Figure 2. 6: Schematic of the hierarchical structure of 50 wt% TLCP/PET blend. A-top microlayer, B-skin microlayer, and C-central microlayer [33].

The properties of TLCPs are significantly affected by the injection molding conditions. Heynderickx *et al*. [38] studied the impact of injection speed and the thickness of mold on the mechanical and thermal properties of a TLCP material. In Figure 2. 7, the flexural moduli of TLCP in the flow direction were significantly higher than those of the transverse direction at different mold thicknesses indicating high mechanical anisotropy. The increase of flexural moduli with decreasing mold thickness was observed. The heat

conduction of the TLCP material showed the same trend where the heat conductivity of TLCP in the flow direction was higher than that of the transverse direction for injection speeds of both 1 and 10 cm/s as illustrated in Figure 2. 8. X-ray diffraction confirmed the correlation between the molecular orientation and mechanical and thermal properties. Ophir *et al.* [39] injection molded TLCP into tensile and flex bars with different molding conditions. The mechanical properties of TLCP as a function of melt temperature, mold temperature, and injection speed are presented in Table 2. 4. Lower mold temperature and slow injection speed generally resulted in the injection molded TLCP with higher tensile and flexural properties. Lower mold temperature provided less time for the TLCP to relax into random orientation leading to favorable mechanical properties.

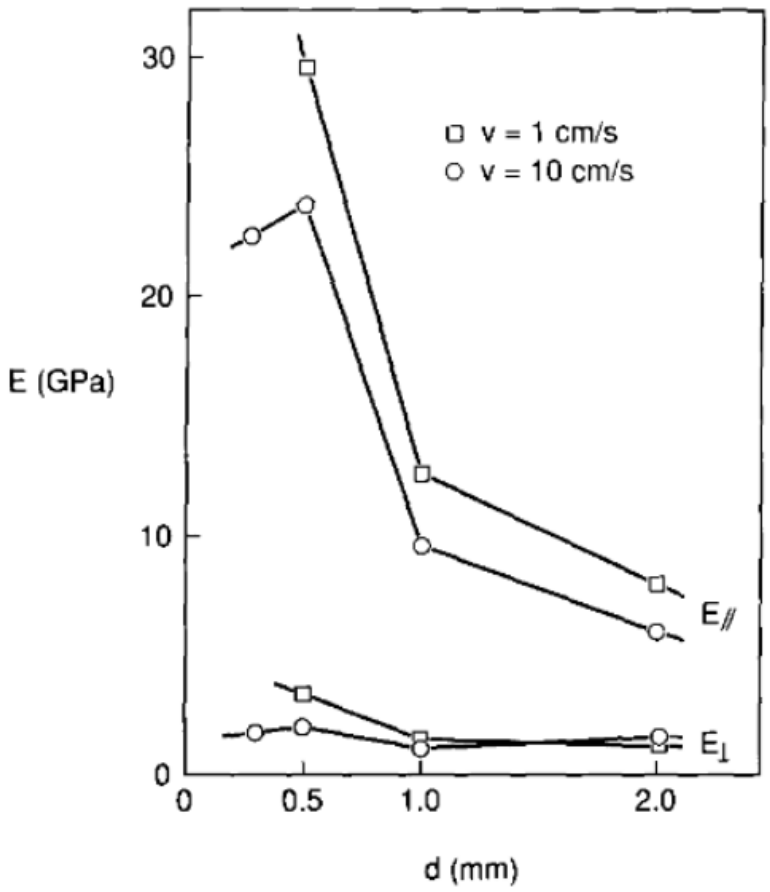

Figure 2. 7: Flexural modulus of TLCP material under different mold thicknesses and injection molded speeds. $E_{\perp}$, modulus perpendicular to the flow direction; $E_{//}$, modulus parallel to the flow direction.

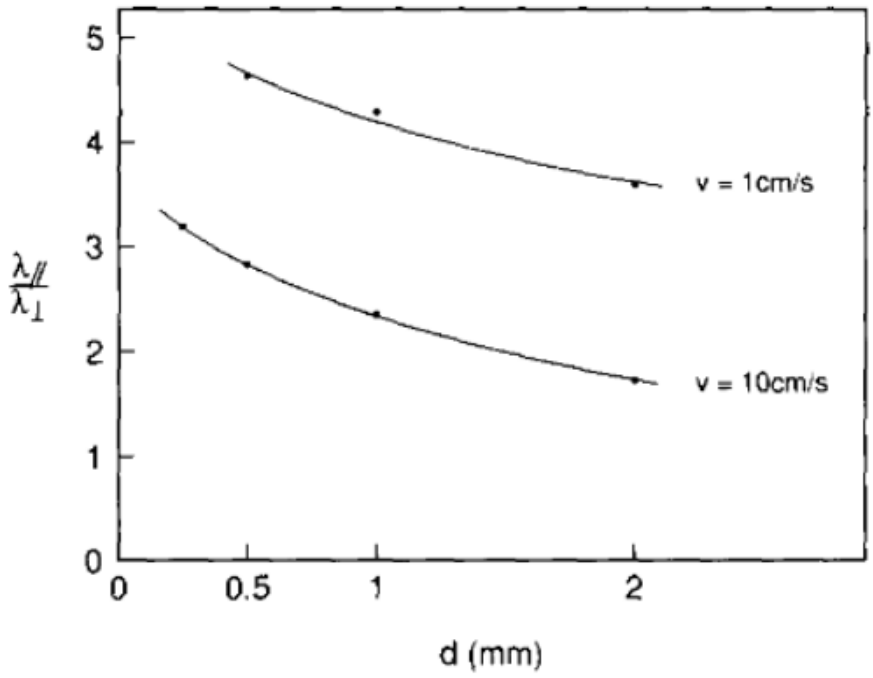

Figure 2. 8: Heat conduction of TLCP material under different mold thicknesses and injection molded speeds. $\lambda_{//} / \lambda_{\perp}$: heat conduction in the flow direction divided by the property in the direction perpendicular to the flow.

Table 2. 4: Mechanical properties of injection molded thermotropic liquid crystalline polymer. The TLCP was synthetized from 60 mol% p-acetoxy-benzoic acid, 20 mol% naphthalene diacetate, and 20 mol% terephthalic acid [39].

Mold temperature (°C)	40	40	40	100	100	100
Barrel temperature (°C)	320	340	340	340	340	340
Injection speed	Fast	Fast	Slow	Slow	Fast	Fast
Flexural modulus (GPa)	15.2	15.2	15.2	14.5	13.1	13.1

Tensile modulus (GPa)	17.2	20.0	19.3	18.6	15.2	16.5
Flexural strength (MPa)	178	174	175	175	170	176
Tensile strength (MPa)	192	173	189	208	176	153
Impact strength (J/m)	395	427	230	283	283	347

2.4 Dual Extrusion Process

Besides the injection molding and extrusion process, there is an unique process to blend TLCP with other thermoplastics, known as the dual extrusion process, which has been developed and patented by Baird and Sukhadia [40]. This mixing technique has several advantages over other processing methods. First, the dual extrusion process can be used to blend TLCPs and matrix polymers which have mismatched processing temperatures, such as processing TLCP (T_m=280°C) and polypropylene (T_m=160°C) [41]. Second, the dual extrusion technique does not depend on the droplet breakup and deformation to form TLCP fibrils, so the continuous TLCP fibrils reinforced composite material can be produced. Third, a higher melt strength of the polymer blend is achieved by utilizing the TLCP supercooling behavior, which makes the drawing process much easier [34].

Figure 2. 9 demonstrates the schematic of the dual extrusion process. The TLCP and matrix materials are separately plasticated in two single screw extruders at their optimal processing temperatures. The TLCP is usually processed at a temperature higher than the matrix material. The two polymer melts meet at the “T” junction and then pass through a

series of static mixers (Kenics or Koch mixers) to distribute and striate the TLCP melt stream. Different dies can be attached to the system to produce either a composite strand or sheet.

Sukhadia *et al.* [42] compared the mechanical properties and morphologies of extruded TLCP composite strands from dual extrusion process and single screw extrusion. The tensile moduli of Vectra A/PET composite prepared by those two mixing methods are shown in Table 2. 5. At all different draw ratios from around 4 to 49, the moduli of 30 wt% Vectra A/PET composite filament from the single screw extrusion were lower than the same material generated by the dual extrusion process. The significant difference in mechanical properties of Vectra A/PET from single screw extrusion and dual extrusion process was mainly due to the different morphology. The skin-core structure was observed for all the composite filaments prepared by the single screw extrusion process where the TLCP fibrils presented in the skin region and the core region consisted of TLCP droplets. In contrast, the morphology of the dual extrusion filaments showed TLCP fibrils throughout the entire cross-section region. The PET phase in the composite filaments was selectively dissolved by the n-propylamine. The continuous TLCP fibrils were observed in the dual extrusion filament while the blend from single screw extrusion process showed discontinuous TLCP fibrils as shown in Figure 2. 10. The length of continuous TLCP fibrils was about 50 mm and the diameters of the TLCL fibrils were from 0.5 to 2 μm which indicated the aspect ratio of the TLCP fibrils could be treated as infinite. The continuous form of TLCP fibrils along with the absent skin-core structure for dual extrusion filament led to the much higher mechanical properties than those of composite filament produced by single screw process.

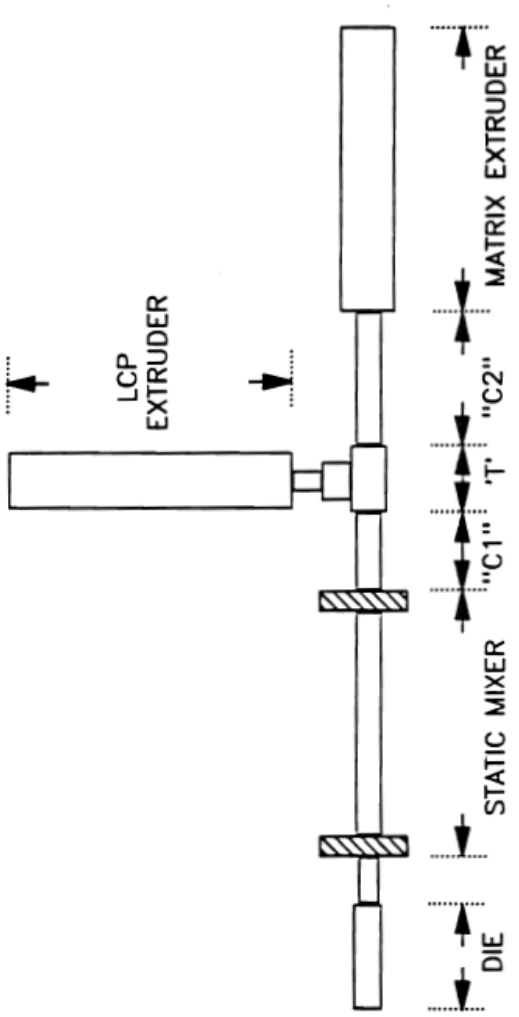

Figure 2. 9: Schematic of the dual extrusion mixing technique [27].

Table 2. 5. Tensile modulus of 30 wt% Vectra A/PET generated by dual extrusion and single screw extrusion

Dual Extrusion	Single Screw Extrusion

Draw Ratio	Tensile Modulus (GPa)	Draw Ratio	Tensile Modulus (GPa)
3.25	5.45	4.55	3.98
3.80	8.93	7.1	7.08
39.0	13.31	20	8.49
49.7	18.99	49.0	13.39

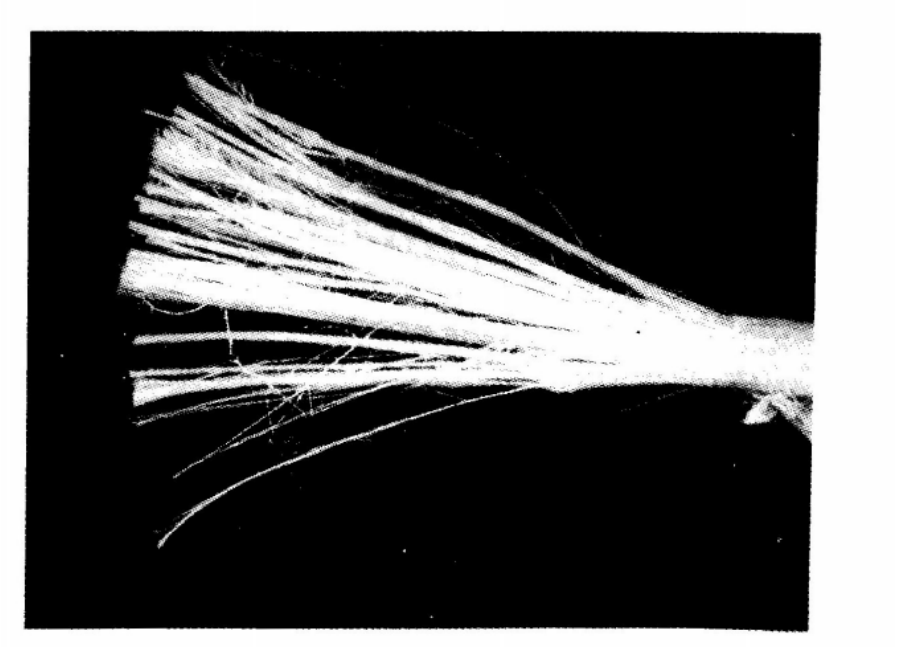

Figure 2. 10: Photograph of 30 wt% TLCP/PET after selectively dissolving the PET phase. The length of the sample is around 5 cm. [27]

2.5 Additive Manufacturing

In contrast to traditional manufacturing, additive manufacturing (AM) utilizes computer-aided design to create a three-dimensional object layer by layer. The first 3D

printing patent was filed by Charles Hull [43] in 1984 and the printing process was named “stereolithography”. 3D printing processes have evolved rapidly over the years and several printing processes have been invented such as fused filament fabrication, powder bed fusion, and inkjet printing [44]. The initial application of the AM process was only on prototyping through rapidly building the 3-D models for visualization. With the improvement of processing technologies and expansion of material selection, end-use products have been manufactured by the AM process. One of the advantages of AM is the mass production of customized products at a low cost. There are increasing market needs for mass customization in industries such as healthcare, automobile, and agriculture [45]. Additive manufacturing has experienced massive growth in the past decade relative to other manufacturing technologies. Wohler’s report stated that the global market of all AM products and services in 2019 reached 11.867 billion dollars with the growth rate at 21.2% [46].

2.5.1 Types of Additive Manufacturing Process

The American Society for Testing and Materials (ASTM) categorized the additive manicuring processes into the following groups: material extrusion, vat photopolymerization, powder bed fusion, directed energy deposition, binder jetting, sheet lamination, and material jetting. The type of 3D printing process relevant to the current work is the material extrusion-based additive manufacturing and will be discussed in detail in section 2.6.

2.5.2 Vat Photopolymerization

Vat photopolymerization, also called stereolithography (SLA), uses UV light (or visible light sometimes) to initiate the chain reaction of photopolymer resin which is then

solidified to form a layer [47]. Acrylic or epoxy based monomer solutions are the most commonly used photopolymer resins for vat photopolymerization [48, 49]. High resolution and smooth surface without layer-by-layer appearance are the main advantages of vat photopolymerization. The unique properties of vat photopolymerization lead to the increasing number of applications in aerospace, automotive and medical fields [50]. Align Technology Inc. is a global medical device company manufacturing customized clear aligners (Invisalign®) for patients using the SLA process [51]. The drawbacks of this printing technique include the low speed, costly equipment, and limited material selection. In addition, the curing kinetics of the photopolymer are complex [44].

2.5.3 Powder Bed Fusion

Powder bed fusion contains layers of closely packed powder, which are fused together with either laser beams or binders. The new layer of powder is spread across the previous layer and they are fused together. Selective laser sintering (SLS) only partially melts the powders while selective laser melting (SLM) completely melts the powders to form a layer. Selective laser sintering has a wider range of material selections such as polymer, metal and alloy. The selective laser melting process usually leads to higher mechanical properties of the printed part [52]. The high resolution and no usage of support materials make powder bed fusion a suitable process for the application in scaffolds for tissue engineering, lattice and electronics [44, 53]. The long printing time is the major disadvantage for utilizing the powder bed fusion process.

2.6 Material Extrusion Additive Manufacturing

The material extrusion additive manufacturing, also called fused filament fabrication (FFF), is the most common and low-cost additive manufacturing method. This is because

of the low cost for equipment and material, fast printing speed, and wide range of material selection [44, 54-57]. The global market size of fused filament fabrication was estimated at around 471.3 million dollars in the year of 2019 and high demand driven by applications in automotive and aerospace industries led to a compound annual growth rate of 18.8% [58].

2.6.1 Fused Filament Fabrication

In the fused filament fabrication process, a continuous filament is pushed into the hot end by the pinch roller mechanism as shown in Figure 2. 11. The continuous filament is softened at the hot end, where the material reaches a semi-liquid state and is pushed out from the nozzle by the pinch roller. After one layer is deposited on the printing bed, the second layer is printed next to it. The movement of the printing head and bed, pinch roller, and temperature of the hot end is controlled by the computer.

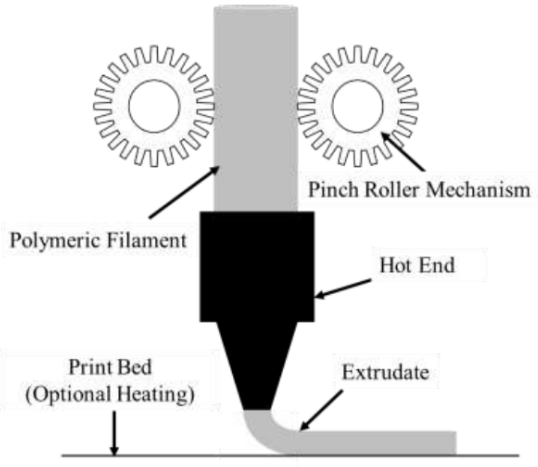

Figure 2. 11: The schematic of fused filament fabrication process [59]

In addition to feeding the material by pinch roller mechanism, a screw feeding mechanism is commonly used in fused filament fabrication. The screw feeding mechanism utilizes a single screw extruder to feed the pellets and the screw drives the pellets down through the heated barrel where the polymer pellets are melted. Finally, the melted polymer is extruded through the deposition nozzle on the print bed [60]. The Big Area Additive Manufacturing (BAAM) utilizes the screw feeding mechanism and a much higher flow rate can be realized as compared to the pinch roller method [61-63]. The material can be deposited at a flow rate of up to several hundred kilograms per hour [64]. Another advantage of using the BAAM to print the polymer material is the elimination of the filament fabrication step. The drawbacks of BAAM are the low printing resolution due to large layer thickness and large defects.

2.6.2 Printing Composite Material using Fused Filament Fabrication

The most commonly used matrices material in FFF are acrylonitrile butadiene styrene (ABS), polylactic acid (PLA), polycarbonate (PC), and nylon. However, the low tensile properties of the pure matrix materials limit the wider adoption of these materials for use as final products [65-68]. The tensile properties of matrix polymers used in fused filament fabrication are shown in Table 2. 6. The tensile properties of 3D printed matrices are lower than those of injection molded counterparts [69]. The voids that are generated during printing and poor interlayer adhesion result in a decrease in the tensile properties of printed parts. Ecker *et al.* [70] compared the mechanical properties of PLA prepared by injection molding with 3D printing. The PLA pellets were injection molded into dog bone specimens at the temperature of 190°C. PLA filaments were printed with a 3D printer at the printing temperature of 205°C. Injection molded PLA samples showed

much higher tensile moduli, tensile strengths, and impact strengths. The porous structure of 3D printed PLA samples has been observed by computer tomography. Figure 2. 12 shows the computer tomography scan of the cross-section of 3D printed and injection molded PLA specimens where printing voids could be seen over the entire 3D printed sample.

Table 2. 6: Tensile properties of common matrices used in FFF

Material	Manufacturer	Tensile Modulus (GPa)	Tensile Strength (MPa)	Reference
PLA	3DXTech	3.4	59.3	[71]
ABS	Stratasys	2.2	26.0	[72]
PC	N/A	1.6	44.3	[73]
Nylon	Markforged	0.5	61.0	[74]

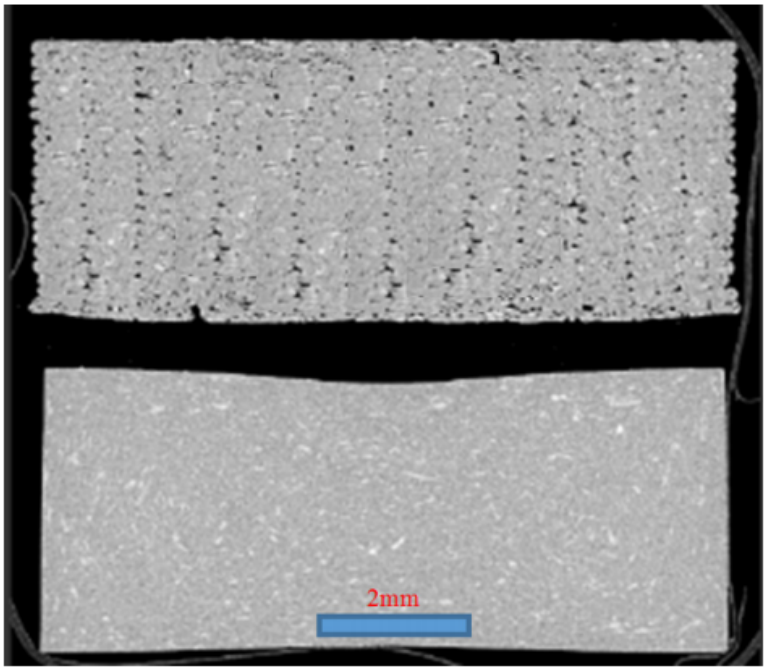

Figure 2. 12: Computer topology of the cross section of 3D printed PLA (top) and injection molded PLA specimen (bottom)

2.6.3 Short Fiber Reinforcement in 3D Printing

To improve the tensile properties of the matrix polymers, reinforcements such as short fiber, nanofiber, and continuous fiber have been used to form the composite material for use in additive manufacturing [63, 74-81]. Short fibers have been the most widely used reinforcement in the 3D printing process. To fabricate a short fiber reinforced composite filament, the matrix and fibers are blended in a single screw extruder and the polymer melt passes through a die to generate the fiber reinforced matrix filament. Then the filament is fed into a 3D printer to print high-performance parts. Short fibers have been utilized to reinforce a wide range of polymeric materials [67, 82-84].

The advantages of using carbon fiber as the reinforcement include low density, high tensile properties and, high thermal conductivity. The tensile modulus and strength of carbon fiber can achieve 4.5 GPa and 200 GPa, respectively, which are higher than the mechanical properties of other reinforcements such as glass fiber and Kevlar fiber [85]. Love *et al*. [63] used carbon fiber to reinforce ABS material for fused filament fabrication. 3.2 mm long carbon fiber was compounded with ABS pellets in a high-shear mixer and then the compounded material was extruded through a 1.75 mm die using a piston-type extrusion unit at the temperature of 220°C. By incorporating 13 wt% of reinforcement, the modulus of ABS in the x-direction was enhanced from 2.05 to 8.91 GPa while the strength was improved from 24.08 to 70.69 MPa. The distortion was reduced because of the increased thermal conductivity of the 3D printed composite. The thermal conductivity of 13 wt% carbon fiber/ABS was 0.397 W/mK in the printing direction in comparison with 0.177 W/mK for pure ABS. A bar with large dimension (a width of 0.05 m, 1.83 m in length, and 0.1 m in thickness) was 3D printed to demonstrate the influence of thermal conductivity on the geometric accuracy. The pure ABS sample bar curled around 25.0 mm on both sides, but the distortion of 3D printed carbon fiber reinforced ABS was negligible. Higher thermal conductivity reduced the thermal gradients during the printing leading to the decrease of distortion (curl and warp) of the printed part.

2.6.4 Continuous Fiber Reinforcement in 3D Printing

The use of short fiber reinforced composites results in the improvement of the tensile properties of 3D printed parts. The major drawback of using short fiber as the

reinforcement is the fiber length attrition during filament fabrication which limits the composites from reaching a higher level of reinforcement.

In the past few years, continuous fiber reinforced composites were developed by industry and academia for use in additive manufacturing [79, 86-88]. There are two processing methods to generate the continuous fiber reinforced composite. The first method, known as nozzle impregnation, involves combining the continuous fiber and matrix filament in the hot end during the printing process, and the other approach is to sandwich the fiber material in between lower and upper of matrix material made from 3D printing. Mori *et al*. [89] used the second method to develop continuous carbon fiber reinforced ABS composite using the fused filament fabrication process. To prepare the carbon fiber reinforced composite using this die-less formation process, the lower plate was first 3D printed and the 70 mm long carbon fibers were deposited on the lower plate, and finally another plate was manufactured on the top to sandwich the carbon fiber. The 3D printed specimen was annealed in the oven for about 15 min to form better bonding between the matrix material and fiber. The strength of the carbon fiber reinforced composite increased almost 100% as compared to that of neat ABS. Significant improvement in fatigue strength of ABS has been observed with the addition of carbon fiber.

In the nozzle impregnation process, matrix filament and continuous fiber tow are supplied into the printer head where continuous fiber is coated with melted matrix polymer as shown in Figure 2. 11. Next, the impregnated composite passes through the nozzle and is deposited on the printing surface to form a layer. No extra feeding equipment is required for the fiber material, because the continuous fiber is pulled into

the hot end through the motion of the matrix material. The matrix material is fed into the nozzle by the pinch roller. Matsuzaki *et al*. [90] modified a commercially available FFF 3D printer to print continuous carbon fiber and jute fiber reinforced polylactic acid (PLA). Around 6 vol% continuous carbon or jute fiber reinforced PLA was printed at a printing and bed temperature of 210°C and 80°C, respectively. The tensile modulus of the PLA composite was around 20 GPa and the tensile strength of this material was around 185 MPa. As compared to the neat PLA resin, the improvements in the tensile modulus and strength were 599% and 435%, respectively. The jute fiber reinforced PLA had a tensile modulus of 5.11 GPa and a tensile strength of 57.1 MPa. The poor interfacial adhesion between the fiber and thermoplastic was confirmed by examining the fracture surface of the specimen after the tensile test. Fiber pullout has been observed at the fracture surface indicating insufficient interfacial adhesion between the PLA and jute fiber, as illustrated in Figure 2. 14.

Tian *et al*. [80] systematically studied the impact of printing conditions on the properties of continuous carbon fiber/PLA. The flexural modulus of 30 GPa and strength of 335 MPa were reached with optimal printing parameters and fiber content of 27 vol%. The flexural modulus and strength increased with increasing printing temperature from 180 until 240°C. The overflow of PLA at 240°C resulted in poor printing accuracy. The influence of hatch spacing on the properties of continuous carbon fiber/PLA was also investigated where decreasing the hatch spacing led to the increasing of flexural modulus and strength from 6.26 to 30 GPa and 130 to 335 MPa, respectively. The increasing of layer thickness from 0.3 to 0.8 mm gave rise to a significant reduction in the mechanical properties due to the decrease in carbon fiber composition.

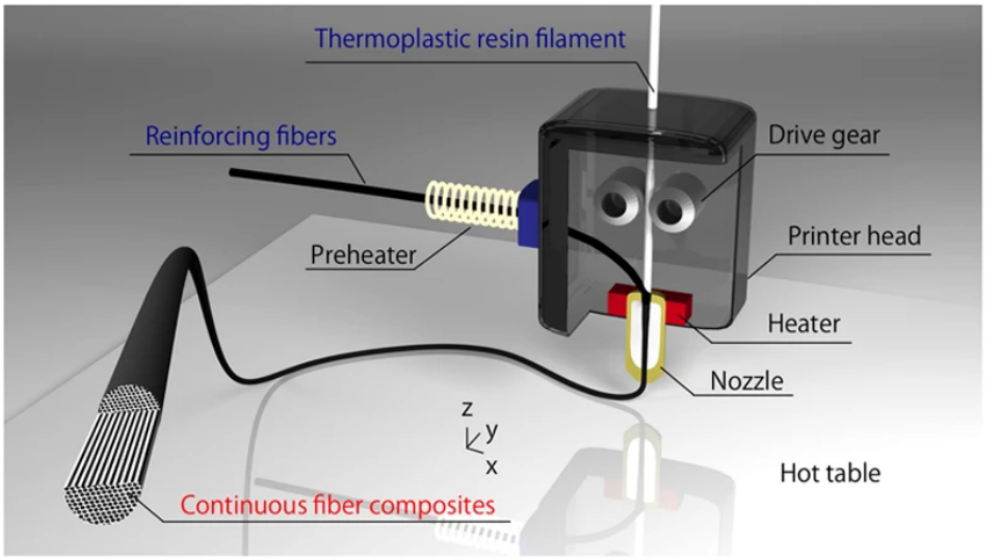

Figure 2. 13: Schematic of in-nozzle impregnation process to produce continuous fiber reinforced composite [90].

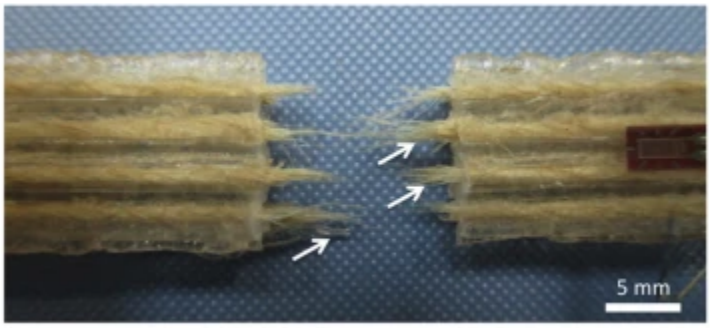

Figure 2. 14: The facture surface of jute fiber reinforced PLA prepared by FFF [90].

2.6.5 3D Printing TLCP Reinforced Composites

The use of TLCP reinforced thermoplastic in conventional manufacturing processes, such as injection molding and extrusion processes, has been discussed in sections 2.3 and 2.4. Researchers have extensively explored the processing of TLCP/thermoplastics using

different conventional manufacturing processes [9, 10, 91, 92]. However, the additive manufacturing of TLCP reinforced thermoplastics has been rarely reported. Gray *et al*. [93] reported for the first time the development of TLCP reinforced PP filament which could be used in additive manufacturing. The dual extrusion technique was utilized to fabricate TLCP composite filament. The composite filament was then pelletized and re-extruded to produce a monofilament with a diameter of 0.07 inches. Finally, this monofilament was printed with different lay-down patterns using a fused deposition modeling (FDM 1600) extrusion system. As compared to neat PP material, the 3D printed composite with 40 wt% TLCP increased the tensile modulus by 150%. The significant improvements in tensile performance have been observed. However, the pelletizing and re-extrusion process resulted in the fiber breakage and prevented composite material from achieving higher mechanical properties.

Ansari *et al*. [94] developed nearly continuous TLCP reinforced ABS composite filaments for fused filament fabrication. The continuous formation of TLCP was achieved by eliminating the pelletizing and re-extrusion, so that the composite filament fabricated by dual extrusion was directly printed using a 3D printer. The specific tensile modulus of continuous TLCP/ABS composite filaments is higher than aluminum. The 3D printed TLCP/ABS had a tensile modulus of 16.5 GPa compared to 2.3 GPa for ABS. The formation of continuous TLCP fibrils along the flow direction in the composite blends was demonstrated by the morphological analysis. The tensile modulus of TLCP/ABS showed significant improvement as compared to pure ABS material. However, the weak interfacial adhesion between TLCP and ABS resulted in a relatively low tensile strength. The large gaps between the TLCP and matrix polymer have been observed by

morphological analysis using scanning electron microscopy, which indicated weak interfacial bonding between TLCP and ABS in Figure 2. 15.

A high performance engineering thermoplastic, polyphenylene sulfide (PPS), was reinforced by TLCP for use in fused filament fabrication [95]. The continuous TLCP reinforced PPS filaments were fabricated by the dual extrusion process. The highest tensile modulus and tensile strength of the 3D printed composite were 25.9 GPa and 108 MPa, respectively, where the optimal printing temperature was determined by a compression molding test. The tensile modulus of TLCP/PPS was higher than conventional continuous fiber reinforced composites. However, the poor interfacial adhesion between TLCP and PPS also led to low tensile strength.

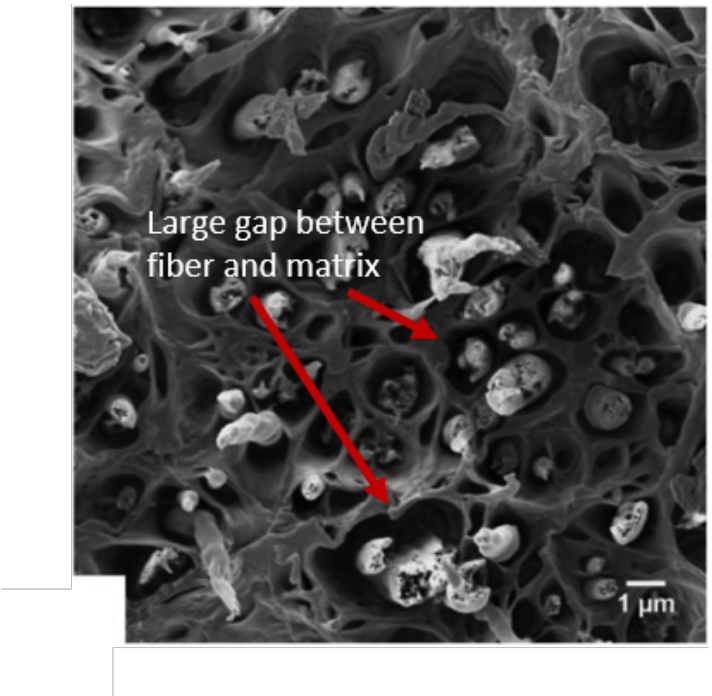

Figure 2. 15: SEM image of TLCP/ABS filament [94].

2.7 Recycling Fiber Reinforced Composite Materials

The application of high strength-to-weight ratio materials has grown rapidly during the last few decades. Fiber-reinforced polymer composites have emerged as one of the materials serving in a variety of fields (e.g., construction, mechanical, automotive, aerospace, etc.) due to their low cost, light weight, high strength and stiffness, and corrosion resistance [96-98]. The global market of fiber-reinforced composites is expected to achieve 131.6 billion dollars with a 7.7% compound annual growth rate at 2024 [99]. The rising demand for these composites is mainly driven by automotive and aerospace industries. However, the enhanced demand of fiber reinforced composites led to a massive accumulation of composite waste in the environment and landfill [100, 101].

Every year about 3000 tons of carbon fiber reinforced composited waste is generated in Europe and United States [102]. Recycling and reuse of composite waste is environmentally and economically beneficial to the society. The price of carbon fiber is relatively expensive compared to other reinforcement at about 9 dollars/lb in 2015 [103]. If the carbon fibers are recycled from composite waste, the much cheaper recycled carbon fibers will be available to the market. In the past twenty years, major attempts have been made to reduce, reuse and recycle composite waste to mitigate the negative environmental effects and transform waste material into useful products [101, 104, 105].

2.7.1 Types of Recycling Processes

The major recycling techniques consist of mechanical recycling, thermal processes, and chemical recycling. Each of these techniques to recycle the composite material has its own advantages and drawbacks. The recycling technique relevant to this research is mechanical recycling which will be discussed in subsections 2.7.2 to 2.7.3.

2.7.2 Mechanical Recycling of Traditional Fiber Reinforced Composite

In the mechanical recycling process, composite waste is ground or shredded into small particulates with a length from 50 μm to 10 mm [106]. The ground materials can be sieved and separated into resin-rich particulates and fiber-rich powders. The resin-rich particulates can be reused as fillers in the process such as sheet molding compound. The recycled fiber is used in manufacturing thermoset composite materials [107]. The different grinding processes impact the quality of recycled composite materials. Schinner *et al*. [108] studied the influence of grinding processes on the fiber length of recycled carbon fiber reinforced polyether-ether-ketone (PEEK) resin. The cutting mills process delivered longer carbon fiber and more homogenous fiber length distribution than the hammer mills method. Up to 50 wt% of recycled composites were compounded with virgin PEEK resin using injection molding or press molding process. The approach to reuse the carbon fiber reinforced composite was reforming process. The author found the thermoplastic laminate can be melted and reformed into another shape or geometry without changing the mechanical properties.

Among all the recycling methods, one of the advantages of mechanical recycling is low energy consumption [109]. Howarth *et al*. [110] developed the model to theoretically calculate the electrical energy requirement of mechanical recycling (milling process). The theoretical estimation was compared and validated with the experimentally measured energy demand of Mikron HSM 400 milling machine. At the recycling rate of 10 kg/hr, the energy used for recycling carbon fiber composite was only 2.03 MJ/kg as compared with the required energy for producing the virgin carbon fiber which was 200 MJ/kg. The form of the recycled fiber (discontinuous or short) was much different from

the virgin fiber (continuous). The recycled fibers have the potential to be reused for the applications where the mechanical performance is less important.

Even though mechanical recycling consumes less energy without solvent usage, the wider application of the mechanical recycling is restricted by lower cost of other fillers and poor quality of the recycled material. The commonly used fillers such as silica and calcium carbonate have a relatively low price as compared to the recycled fiber composite. The fiber breakage and poor bonding between the virgin resin and recycled fiber result in the deterioration of mechanical performance of the final products (e.g., tensile strength, impact strength and surface quality) [111-116]. Kuram *et al*. [117] investigated the effects of mechanical recycling on the performance of glass fiber reinforced poly(butylene terephthalate) (PBT)/polycarbonate (PC) composite. 10 wt% glass fiber reinforced PBT/PC composite with an average fiber length of 4 mm was injection molded into specimens for mechanical testing and remaining composite parts were crushed into small particulates. The ground composites were injection molded into the recycled specimens, and the injection molding and shredding processes were repeated up to five times. The mechanical properties of glass fiber reinforced PBT/PC decreased with increasing number of recycling as shown in Figure 2. 16. The decrease in both tensile modulus and strength was due to the fiber attrition induced by the recycling process. SEM analysis was utilized to study the impact-fractured surface of glass fiber reinforced PBT/PC. The number of voids due to the fiber pull-out increased with increasing number of reprocessing cycles indicating the weaker interfacial bonding. The rheological properties of recycled glass fiber reinforced PBT/PC were measured by melt flow index (MFI) tester. The rheological analysis of glass fiber/PBT/PC showed more

than a 90% decrease in MFI (26 g/10 min^{-1} to 50 g/min^{-1}) after five recycling steps. The crystallinity of recycled glass fiber reinforced PBT/PC increased from 35 to 50% with the increasing number of recycling owing to the chain scission degradation of PBT and PC during the repeated injection molding. Lower molecular weight allowed the polymer chains to fold leading to the increase of crystallinity [118]. The mechanical recycling had a strong influence on the mechanical, rheological and chemical properties of recycled glass fiber reinforced composite.

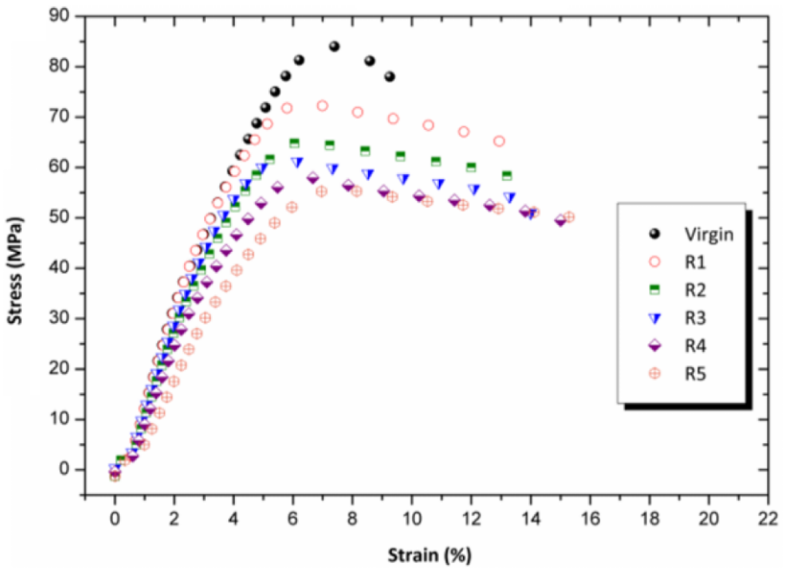

Figure 2. 16: Stress-strain curves of glass fiber reinforced PBT/PC composite. R1 to R5 represent the number of reprocessing cycles (recycle no.1 to recycle no.5) [117].

The influence of injection molding conditions and the number of recycling iterations on the properties of glass fiber reinforced nylon was reported by Kuram *et al.* [114]. The Taguchi method was applied to design the experiments with mixed level design. The control parameters were the number of reprocessing cycles, barrel temperature, injection molding pressure, holding pressure, and mold temperature. The

chemical, thermal and mechanical properties of recycled glass fiber reinforced nylon were characterized. FTIR analysis demonstrated that the chemical structure of nylon 6 was not affected with increasing number of reprocessing cycles. Analysis of variance (ANOVA) results indicated that the influence of recycling number on the tensile strength dominated among all the other parameters (e.g., melt temperature and holding pressure). The recycling number had statistical significance on the tensile, yield strength, impact energy and impact strength of recycled fiber reinforced composites with the percentage contributions of 95.08%, 96.31%, 92.22% and 92.60%, respectively. The relationships between the injection molding conditions and mechanical properties were determined by regression analysis. The predicted values of tensile and impact properties by regression analysis showed a great agreement with the experimental observations. The number of reprocessing cycles imposed the strongest influence on the mechanical properties of composites as compared to impacts from injection molding parameters. The decrease in mechanical properties of recycled glass fiber reinforced nylon was because of the fiber attrition during the re-injection molding and grinding process.

2.7.3 Recycling of TLCP Reinforced Composite

The impact of mechanical recycling on the performance and properties of traditional fiber reinforced composites (e.g., glass fiber or carbon fiber) has been extensively studied [119-122]. However, literature involving the recycling or reusing TLCPs or TLCP reinforced composites are scarce [123-125]. The cost of the TLCP was found to be much higher than that of glass fiber where the cost of TLCP ranges from 8 to 12 dollars/pound and the cost of glass fiber is less than 1 dollar/pound [126]. Due to the high cost associated with the TLCPs, it is desired to recycle and reuse the TLCP to

reduce the overall raw material cost. The influence of mechanical recycling on the properties of TLCPs has been systematically investigated by Bastida *et al.* [127]. Two types of thermotropic liquid crystalline polymers have been studied: Vectra B950 and Rodrun LC-5000. The mechanical recycling consisted of injection molding and grinding the pure TLCPs up to five reprocessing cycles. The rheological properties of recycled TLCP were examined by means of a melt flow index (MFI) tester. The MFI increased with increasing number of recycling as illustrated in Figure 2. 17. The threefold increase in MFI over five recycling numbers was attributed to the decrease in the molecular weight of TLCP. The mechanical and thermal degradation during recycling process led to the reduction of molecular weight. It has to be noted the increase of MFI of Vectra B950 was minimal within the two reprocessing cycles. The tensile modulus of recycled TLCPs as a function of number of recycles is exhibited in Figure 2. 18. The decrease of tensile modulus of Vectra B950 after five recycling steps was less than 15% where the Rodrun LC-5000 showed no change in tensile modulus after recycling. The decrease in the crystallinity and molecular weight may explain the decrease in the tensile modulus of Vecatra B950.

Xu *et al.* [128] studied the influence of mechanical recycling on the mechanical, rheological, and morphological properties of TLCP/polycarbonate (PC) using two recycling methods. One of the recycling routes was to mechanically recycle the TLCP first, and then the virgin PC material was compounded with recycled TLCP using an injection molding machine. The other method was to directly recycle the TLCP/PC blends by repeated injection molding and the grinding process. The composite materials were mechanically recycled up to four times. Recycled TLCP/PC utilizing the former

recycling route decreased in tensile strength only in the first reprocessing cycle as shown in Figure 2. 19. On the other hand, the recycled TLCP/PC using the second method significantly decreased in tensile properties after the first recycling steps as shown in Figure 2. 20. Figure 2. 21 showed the melt flow rate (MFR) of recycled TLCP/virgin PC as a function number of reprocessing cycles. The MFR of recycled TLCP/virgin PC did not change significantly with increasing number of recycling steps especially when the recycling step was greater than one. In comparison, the recycled TLCP/PC increased the MFR from 75 to 380 g/10 min within four recycling numbers. The mechanical and thermal degradations that occurred during the recycling process resulted in a significant decrease in the molecular weight of PC. The authors believed the degradation of PC during the mechanical recycling resulted in the decrease in mechanical properties of composite rather than degradation of TLCP.

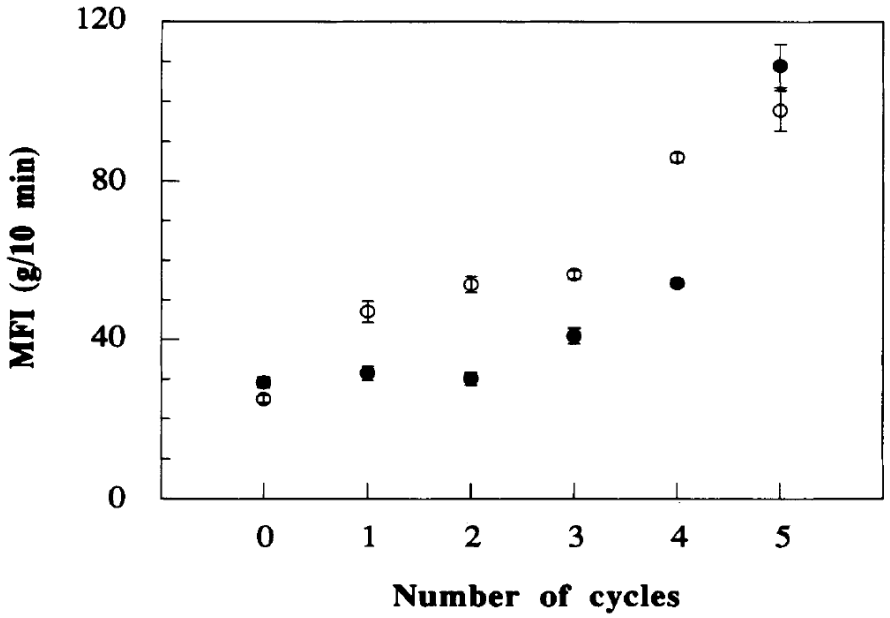

Figure 2. 17: The melt flow index of TLCP as a function of number of recycling. ○-Rodrun LC-5000; ●-Vectra B950 [127].

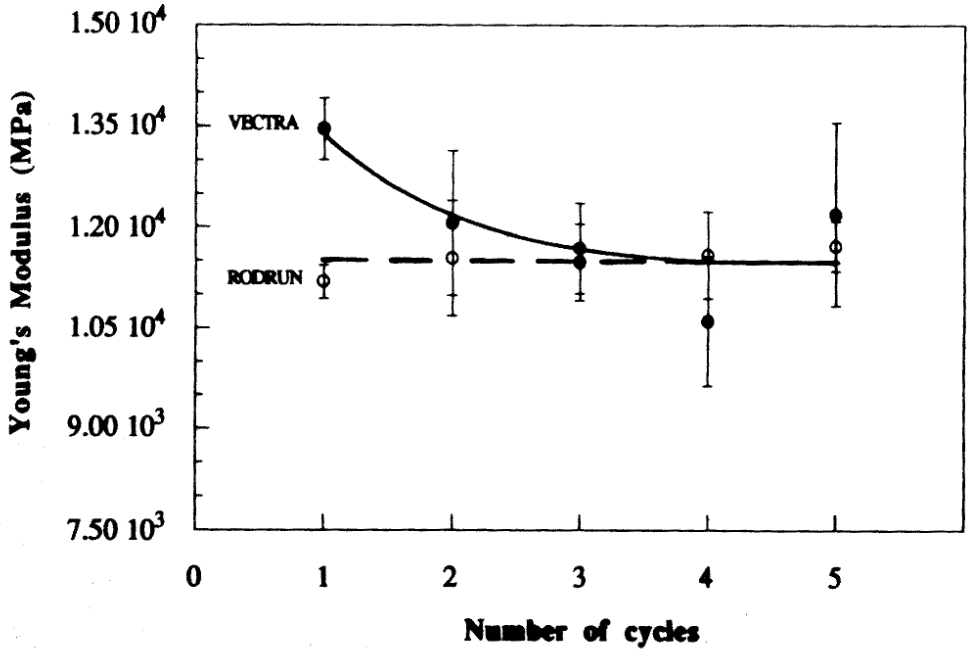

Figure 2. 18: Tensile modulus of recycled TLCPs vs number of recycling. ○-Rodrun LC-5000; ●-Vectra B950 [127].

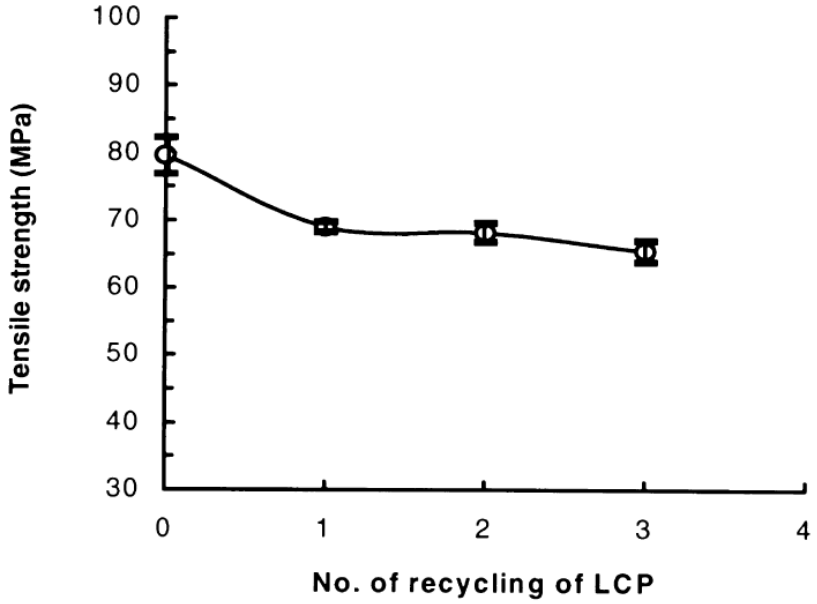

Figure 2. 19: Tensile strength of recycled TLCP/virgin PC versus number of recycling steps [128].

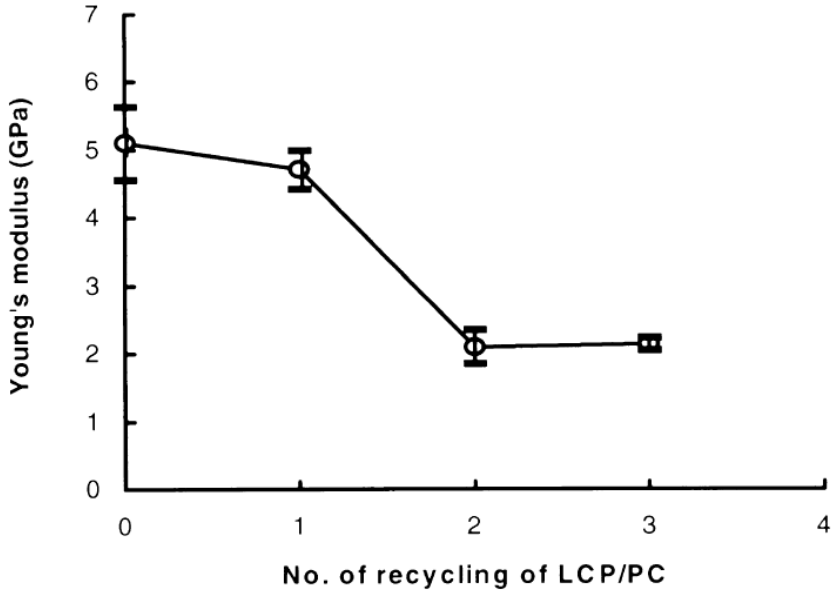

Figure 2. 20: Tensile modulus of recycled TLCP/PC versus number of recycling steps [128].

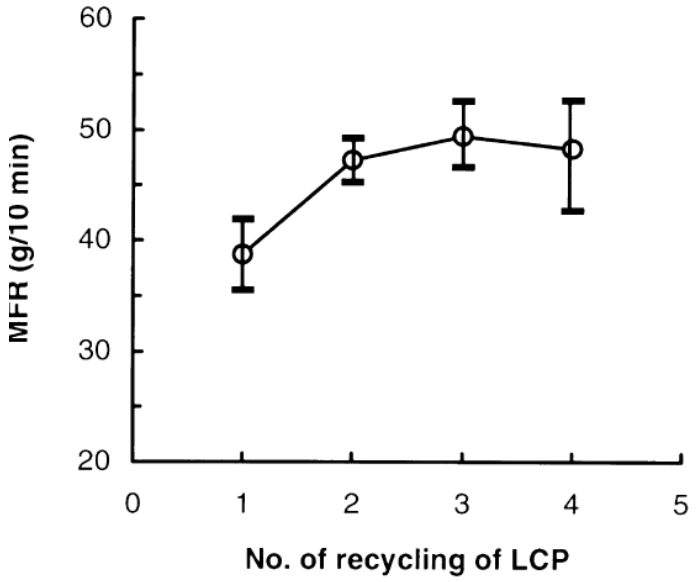

Figure 2. 21. Melt flow rate of recycled TLCP/virgin PC versus number of recycling steps [128].

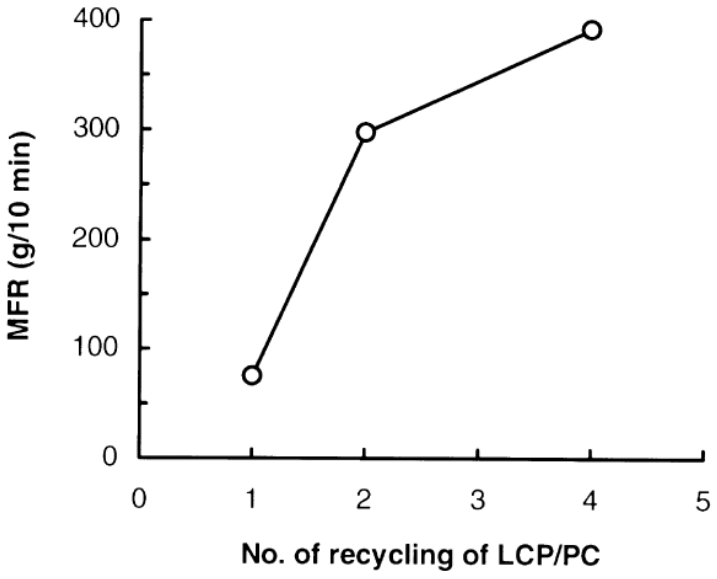

Figure 2. 22: Melt flow rate of recycled TLCP/PC versus number of recycling steps [128].

2.8 Reference

1. Friedel, M. G., *The mesomorphic states of matter*. US Army Engineer Research and Development Laboratories: 1967.
2. Qian, C. Linking the rheological behavior to the processing of thermotropic liquid crystalline polymers in the super-cooled state. Virginia Tech, 2016.
3. Zhou, Q.-F.; LENZ, R. In *Substituent effects on the liquid-crystalline properties of thermotropic polyesters*, ABSTRACTS OF PAPERS OF THE AMERICAN CHEMICAL SOCIETY, AMER CHEMICAL SOC 1155 16TH ST, NW, WASHINGTON, DC 20036: 1983; pp 131-POLY.
4. Antoun, S.; Lenz, R.; Jin, J., Liquid crystal polymers. Iv. Thermotropic polyesters with flexible spacers in the main chain. *Journal of Polymer Science: Polymer Chemistry Edition* **1981,** *19*, 1901-1920.
5. Blumstein, A., *Polymeric liquid crystals*. Springer Science & Business Media: 2013; Vol. 28.
6. Cottis, S.; Economy, J.; Nowak, B., Fabricable infusible para-oxybenzoyl polyester production. Google Patents: 1974.
7. Ward, I. M., *Developments in oriented polymers—2*. Springer Science & Business Media: 2012.

8. Collyer, A. A., *Liquid crystal polymers: From structures to applications*. Springer Science & Business Media: 2012; Vol. 1.
9. Sabol, E. A.; Handlos, A. A.; Baird, D. G., Composites based on drawn strands of thermotropic liquid-crystalline polymer reinforced polypropylene. *Polym. Compos.* **1995,** *16*, 330-345.
10. Datta, A.; Baird, D. G., Compatibilization of thermoplastic composites based on blends of polypropylene with 2 liquid-crystalline polymers. *Polymer* **1995,** *36*, 505-514.
11. Campoy, I.; Gómez, M. A.; Marco, C., Structure and thermal properties of blends of nylon 6 and a liquid crystal copolyester1dedicated to the memory of prof. J.G. Fatou.1. *Polymer* **1998,** *39*, 6279-6288.
12. Gopakumar, T. G.; Ponrathnam, S.; Lele, A.; Rajan, C. R.; Fradet, A., In situ compatibilisation of poly(phenylene sulphide)/wholly aromatic thermotropic liquid crystalline polymer blends by reactive extrusion: Morphology, thermal and mechanical properties. *Polymer* **1999,** *40*, 357-364.
13. Crevecoeur, G.; Groeninckx, G., Morphology and mechanical-properties of thermoplastic composites containing a thermotropic liquid-crystalline polymer. *Polym. Eng. Sci.* **1990,** *30*, 532-542.
14. Tjong, S., Structure, morphology, mechanical and thermal characteristics of the in situ composites based on liquid crystalline polymers and thermoplastics. *Materials Science Engineering: R: Reports*

2003, *41*, 1-60.
15. Kiss, G., Insitu composites - blends of isotropic polymers and thermotropic liquid-crystalline polymers. *Polym. Eng. Sci.* **1987,** *27*, 410-423.
16. Petrović, Z. S.; Farris, R., Structure–property relationship in fibers spun from poly (ethylene terephthalate) and liquid crystalline polymer blends. I. The effect of composition and processing on fiber morphology and properties. *J. Appl. Polym. Sci.* **1995,** *58*, 1077-1085.
17. Grace, H. P., Dispersion phenomena in high viscosity immiscible fluid systems and application of static mixers as dispersion devices in such systems. *Chemical Engineering Communications* **1982,** *14*, 225-277.
18. Tsebrenko, M. V.; Yudin, A. V.; Ablazova, T. I.; Vinogradov, G. V., Mechanism of fibrillation in the flow of molten polymer mixtures. *Polymer* **1976,** *17*, 831-834.
19. Blizard, K. G.; Federici, C.; Federico, O.; Chapoy, L. L., The morphology of extruded blends containing a thermotropic liquid crystalline polymer. *Polymer Engineering & Science* **1990,** *30*, 1442-1453.
20. Isayev, A.; Modic, M., Self‐reinforced melt processible polymer composites: Extrusion, compression, and injection molding. *Polymer composites* **1987,** *8*, 158-175.
21. Kohli, A.; Chung, N.; Weiss, R., The effect of deformation history on the morphology and properties of blends of polycarbonate and a thermotropic liquid crystalline polymer. *Polymer Engineering and Science* **1989,** *29*, 573-580.
22. Siegmann, A.; Dagan, A.; Kenig, S., Polyblends containing a liquid crystalline polymer. *Polymer* **1985,** *26*, 1325-1330.
23. Blizard, K. G.; Baird, D., The morphology and rheology of polymer blends containing a liquid crystalline copolyester. *Polymer Engineering Science*

1987, *27*, 653-662.
24. Affdl, J. H.; Kardos, J., The halpin‐tsai equations: A review. *Polymer Engineering Science*

1976, *16*, 344-352.

25. Datta, A.; Baird, D. G., Compatibilization of thermoplastic composites based on blends of polypropylene with two liquid crystalline polymers. *Polymer* **1995,** *36*, 505-514.
26. O'Donnell, H. J.; Baird, D. G. J. P., In situ reinforcement of polypropylene with liquid-crystalline polymers: Effect of maleic anhydride-grafted polypropylene. **1995,** *36*, 3113-3126.
27. Sukhadia, A. M. The in situ generation of liquid crystalline polymer reinforcements in thermoplastics. Doctoral Dissertations, Virginia Tech, 1992.
28. Datta, A.; Chen, H.; Baird, D. G., The effect of compatibilization on blends of polypropylene with a liquid-crystalline polymer. *Polymer* **1993,** *34*, 759-766.
29. Handlos, A.; Baird, D., Processing and associated properties of in situ composites based on thermotropic liquid crystalline polymers and thermoplastics. *Journal of Macromolecular Science, Part C: Polymer Reviews* **1995,** *35*, 183-238.
30. Xu, Q. W.; Man, H. C.; Lau, W. S., The effect of a third component on the morphology and mechanical properties of liquid-crystalline polymer and polypropylene in situ composites1some of the results in this paper were presented in the conference of apme'97 in april 1997.1. *Compos. Sci. Technol.* **1999,** *59*, 291-296.
31. O'Donnell, H. J.; Baird, D., The effect of injection molding conditions on the mechanical properties of an in situ composite. I: Polypropylene and a liquid crystalline copolyester based on hydroxynaphthoic acid. *Polymer Engineering & Science* **1996,** *36*, 963-978.
32. Tjong, S. C.; Liu, S. L.; Li, R. K. Y., Mechanical properties of injection moulded blends of polypropylene with thermotropic liquid crystalline polymer. *J. Mater. Sci.* **1996,** *31*, 479-484.
33. Silverstein, M.; Hiltner, A.; Baer, E., Hierarchical structure in lcp/pet blends. *J. Appl. Polym. Sci.* **1991,** *43*, 157-173.
34. Handlos, A. A.; Baird, D. G., Processing and associated properties of in-situ composites based on thermotropic liquid-crystalline polymers and thermoplastics. *J. Macromol. Sci.-Rev. Macromol. Chem. Phys.* **1995,** *C35*, 183-238.
35. Sawyer, L. C.; Chen, R. T.; Jamieson, M. G.; Musselman, I. H.; Russell, P. E., The fibrillar hierarchy in liquid crystalline polymers. *J. Mater. Sci.* **1993,** *28*, 225-238.
36. Weng, T.; Hiltner, A.; Baer, E., Hierarchical structure in a thermotropic liquid-crystalline copolyester. *J. Mater. Sci.* **1986,** *21*, 744-750.
37. Tadmor, Z., Molecular-orientation in injection molding. *J. Appl. Polym. Sci.* **1974,** *18*, 1753-1772.
38. Heynderickx, I.; Paridaans, F., Influence of processing conditions on the anisotropy in injection-moulded thermotropic lcps. *Polymer* **1993,** *34*, 4068-4074.
39. Ophir, Z.; Ide, Y., Injection molding of thermotropic liquid crystal polymers. *Polymer Engineering and Science*

1983, *23*, 792-796.
40. Baird, D. G.; Sukhadia, A. Mixing process for generating in-situ reinforced thermoplastics. US5225488, 1993.
41. Sabol, E.; Baird, D., Morphology in blends of a thermotropic liquid crystalline polymer and polypropylene: A comparison of mixing history. *International Polymer Processing* **1995,** *10*, 124-136.
42. Sukhadia, A. M.; Datta, A.; Baird, D. G., Mixing history on the morphology and properties of thermoplastic lcp blends. *Int. Polym. Process.* **1992,** *7*, 218-228.
43. Hull, C. W. J. U. S. P., Appl., No. 638905, Filed, Apparatus for production of three-dimensional objects by stereolithography. **1984**.

44. Ngo, T. D.; Kashani, A.; Imbalzano, G.; Nguyen, K. T. Q.; Hui, D., Additive manufacturing (3d printing): A review of materials, methods, applications and challenges. *Compos. Pt. B-Eng.* **2018,** *143*, 172-196.
45. Shahrubudin, N.; Lee, T. C.; Ramlan, R., An overview on 3d printing technology: Technological, materials, and applications. *Procedia Manufacturing* **2019,** *35*, 1286-1296.
46. Wohlers report 2020 3d printing and additive manufacuring global state of the industry. http://wohlersassociates.com/2020report.htm.
47. Chartrain, N. A.; Williams, C. B.; Whittington, A. R., A review on fabricating tissue scaffolds using vat photopolymerization. *Acta Biomaterialia* **2018,** *74*, 90-111.
48. Esposito Corcione, C.; Greco, A.; Maffezzoli, A., Photopolymerization kinetics of an epoxy‐based resin for stereolithography. *J. Appl. Polym. Sci.* **2004,** *92*, 3484-3491.
49. Gibson, I.; Rosen, D.; Stucker, B., Vat photopolymerization processes. In *Additive manufacturing technologies: 3d printing, rapid prototyping, and direct digital manufacturing*, Springer New York: New York, NY, 2015; pp 63-106.
50. Mukhtarkhanov, M.; Perveen, A.; Talamona, D., Application of stereolithography based 3d printing technology in investment casting. **2020,** *11*, 946.
51. Wong, B. H., Invisalign a to z. *American Journal of Orthodontics and Dentofacial Orthopedics* **2002,** *121*, 540-541.
52. Lee, H.; Lim, C. H. J.; Low, M. J.; Tham, N.; Murukeshan, V. M.; Kim, Y.-J., Lasers in additive manufacturing: A review. *International Journal of Precision Engineering and Manufacturing-Green Technology* **2017,** *4*, 307-322.
53. An, J.; Teoh, J. E. M.; Suntornnond, R.; Chua, C. K., Design and 3d printing of scaffolds and tissues. *Engineering* **2015,** *1*, 261-268.
54. Guo, N.; Leu, M. C., Additive manufacturing: Technology, applications and research needs. *Front. Mech. Eng.* **2013,** *8*, 215-243.
55. Bahnini, I.; Rivette, M.; Rechia, A.; Siadat, A.; Elmesbahi, A., Additive manufacturing technology: The status, applications, and prospects. *Int. J. Adv. Manuf. Technol.* **2018,** *97*, 147-161.
56. Wong, K. V.; Hernandez, A., A review of additive manufacturing. *ISRN Mechanical Engineering* **2012,** *2012*, 208760.
57. Gibson, I.; Rosen, D. W.; Stucker, B., *Additive manufacturing technologies: Rapid prototyping to direct digital manufacturing*. Springer-Verlag Berlin: Berlin, 2010; p 1-459.
58. 3d printing filament market size, share & trends analysis report. https://www.grandviewresearch.com/industry-analysis/3d-printing-filament-market (accessed 3/2/2020).
59. Ansari, M. Q. Generation of thermotropic liquid crystalline polymer (tlcp)-thermoplastic composite filaments and their processing in fused filament fabrication (fff). Virginia Tech, 2019.
60. Chesser, P.; Post, B.; Roschli, A.; Carnal, C.; Lind, R.; Borish, M.; Love, L., Extrusion control for high quality printing on big area additive manufacturing (baam) systems. *Addit. Manuf.* **2019,** *28*, 445-455.
61. Duty Chad, E.; Kunc, V.; Compton, B.; Post, B.; Erdman, D.; Smith, R.; Lind, R.; Lloyd, P.; Love, L., Structure and mechanical behavior of big area additive manufacturing (baam) materials. *Rapid Prototyp. J.* **2017,** *23*, 181-189.
62. Hassen, A. A.; Lindahl, J.; Chen, X.; Post, B.; Love, L.; Kunc, V. In *Additive manufacturing of composite tooling using high temperature thermoplastic materials*, SAMPE Conference Proceedings, Long Beach, CA, May, 2016; pp 23-26.

63. Love, L. J.; Kunc, V.; Rios, O.; Duty, C. E.; Elliott, A. M.; Post, B. K.; Smith, R. J.; Blue, C. A., The importance of carbon fiber to polymer additive manufacturing. *J. Mater. Res.* **2014,** *29*, 1893-1898.
64. Thermwood Lsam - large scale additive manufacturing. http://www.thermwood.com/lsam_home.htm#whatislsam (accessed 7/15/2020).
65. Zhong, W.; Li, F.; Zhang, Z.; Song, L.; Li, Z., Short fiber reinforced composites for fused deposition modeling. *Materials Science and Engineering: A* **2001,** *301*, 125-130.
66. Fu, S. Y.; Lauke, B.; Mäder, E.; Yue, C. Y.; Hu, X., Tensile properties of short-glass-fiber- and short-carbon-fiber-reinforced polypropylene composites. *Compos. Part A-Appl. S. Compos.* **2000,** *31*, 1117-1125.
67. Ferreira, R. T. L.; Amatte, I. C.; Dutra, T. A.; Bürger, D., Experimental characterization and micrography of 3d printed pla and pla reinforced with short carbon fibers. *Composites Part B: Engineering* **2017,** *124*, 88-100.
68. Mueller, B., Additive manufacturing technologies – rapid prototyping to direct digital manufacturing. *Assembly Automation* **2012,** *32*.
69. Dawoud, M.; Taha, I.; Ebeid, S. J., Mechanical behaviour of abs: An experimental study using fdm and injection moulding techniques. *Journal of Manufacturing Processes* **2016,** *21*, 39-45.
70. Ecker Josef, V.; Haider, A.; Burzic, I.; Huber, A.; Eder, G.; Hild, S., Mechanical properties and water absorption behaviour of pla and pla/wood composites prepared by 3d printing and injection moulding. *Rapid Prototyp. J.* **2019,** *25*, 672-678.
71. Ivey, M.; Melenka, G. W.; Carey, J. P.; Ayranci, C. J. A. M. P.; Science, C., Characterizing short-fiber-reinforced composites produced using additive manufacturing. **2017,** *3*, 81-91.
72. Dizon, J. R. C.; Espera, A. H.; Chen, Q.; Advincula, R. C., Mechanical characterization of 3d-printed polymers. *Addit. Manuf.* **2018,** *20*, 44-67.
73. Cantrell, J. T.; Rohde, S.; Damiani, D.; Gurnani, R.; DiSandro, L.; Anton, J.; Young, A.; Jerez, A.; Steinbach, D.; Kroese, C. J. R. P. J., Experimental characterization of the mechanical properties of 3d-printed abs and polycarbonate parts. **2017**.
74. Dickson, A. N.; Barry, J. N.; McDonnell, K. A.; Dowling, D. P., Fabrication of continuous carbon, glass and kevlar fibre reinforced polymer composites using additive manufacturing. *Addit. Manuf.* **2017,** *16*, 146-152.
75. Tekinalp, H. L.; Kunc, V.; Velez-Garcia, G. M.; Duty, C. E.; Love, L. J.; Naskar, A. K.; Blue, C. A.; Ozcan, S., Highly oriented carbon fiber-polymer composites via additive manufacturing. *Compos. Sci. Technol.* **2014,** *105*, 144-150.
76. Gray, R. W.; Baird, D. G.; Bohn, J. H., Thermoplastic composites reinforced with long fiber thermotropic liquid crystalline polymers for fused deposition modeling. *Polym. Compos.* **1998,** *19*, 383-394.
77. Shofner, M. L.; Lozano, K.; Rodriguez-Macias, F. J.; Barrera, E. V., Nanofiber-reinforced polymers prepared by fused deposition modeling. *J. Appl. Polym. Sci.* **2003,** *89*, 3081-3090.
78. Shofner, M. L.; Rodriguez-Macias, F. J.; Vaidyanathan, R.; Barrera, E. V., Single wall nanotube and vapor grown carbon fiber reinforced polymers processed by extrusion freeform fabrication. *Compos. Pt. A-Appl. Sci. Manuf.* **2003,** *34*, 1207-1217.
79. Li, N. Y.; Li, Y. G.; Liu, S. T., Rapid prototyping of continuous carbon fiber reinforced polylactic acid composites by 3d printing. *J. Mater. Process. Technol.* **2016,** *238*, 218-225.
80. Tian, X. Y.; Liu, T. F.; Yang, C. C.; Wang, Q. R.; Li, D. C., Interface and performance of 3d printed continuous carbon fiber reinforced pla composites. *Compos. Pt. A-Appl. Sci. Manuf.* **2016,** *88*, 198-205.

81. Matsuzaki, R.; Ueda, M.; Namiki, M.; Jeong, T.-K.; Asahara, H.; Horiguchi, K.; Nakamura, T.; Todoroki, A.; Hirano, Y., Three-dimensional printing of continuous-fiber composites by in-nozzle impregnation. *Sci. Rep.* **2016,** *6*, 23058.
82. Nikzad, M.; Masood, S. H.; Sbarski, I., Thermo-mechanical properties of a highly filled polymeric composites for fused deposition modeling. *Materials & Design* **2011,** *32*, 3448-3456.
83. Shofner, M.; Lozano, K.; Rodríguez‐Macías, F.; Barrera, E., Nanofiber‐reinforced polymers prepared by fused deposition modeling. *Journal of applied polymer science* **2003,** *89*, 3081-3090.
84. Gupta, A.; Fidan, I.; Hasanov, S.; Nasirov, A., Processing, mechanical characterization, and micrography of 3d-printed short carbon fiber reinforced polycarbonate polymer matrix composite material. *The International Journal of Advanced Manufacturing Technology* **2020,** *107*, 3185-3205.
85. Hyer, M. W.; White, S. R., *Stress analysis of fiber-reinforced composite materials*. DEStech Publications, Inc: 2009.
86. Brenken, B.; Barocio, E.; Favaloro, A.; Kunc, V.; Pipes, R. B., Fused filament fabrication of fiber-reinforced polymers: A review. *Addit. Manuf.* **2018,** *21*, 1-16.
87. Melenka, G. W.; Cheung, B. K. O.; Schofield, J. S.; Dawson, M. R.; Carey, J. P., Evaluation and prediction of the tensile properties of continuous fiber-reinforced 3d printed structures. *Compos. Struct.* **2016,** *153*, 866-875.
88. Yang, C. C.; Tian, X. Y.; Liu, T. F.; Cao, Y.; Li, D. C., 3d printing for continuous fiber reinforced thermoplastic composites: Mechanism and performance. *Rapid Prototyp. J.* **2017,** *23*, 209-215.
89. Mori, K.-i.; Maeno, T.; Nakagawa, Y., Dieless forming of carbon fibre reinforced plastic parts using 3d printer. *Procedia Engineering* **2014,** *81*, 1595-1600.
90. Matsuzaki, R.; Ueda, M.; Namiki, M.; Jeong, T. K.; Asahara, H.; Horiguchi, K.; Nakamura, T.; Todoroki, A.; Hirano, Y., Three-dimensional printing of continuous-fiber composites by in-nozzle impregnation. *Scientific Reports* **2016,** *6*.
91. Chinsirikul, W.; Hsu, T.; Harrison, I.; Science, Liquid crystalline polymer (lcp) reinforced polyethylene blend blown film: Effects of counter‐rotating die on fiber orientation and film properties. *J. Polym. Eng.* **1996,** *36*, 2708-2717.
92. Saengsuwan, S.; Bualek-Limcharoen, S.; Mitchell, G. R.; Olley, R. H., Thermotropic liquid crystalline polymer (rodrun lc5000)/polypropylene in situ composite films: Rheology, morphology, molecular orientation and tensile properties. *Polymer* **2003,** *44*, 3407-3415.
93. Gray IV, R. W.; Baird, D. G.; Helge Bøhn, J., Effects of processing conditions on short tlcp fiber reinforced fdm parts. *Rapid Prototyp. J.* **1998,** *4*, 14-25.
94. Ansari, M. Q.; Redmann, A.; Osswald, T. A.; Bortner, M. J.; Baird, D. G., Application of thermotropic liquid crystalline polymer reinforced acrylonitrile butadiene styrene in fused filament fabrication. *Addit. Manuf.* **2019,** *29*.
95. Ansari, M. Q.; Bortner, M. J.; Baird, D. G., Generation of polyphenylene sulfide reinforced with a thermotropic liquid crystalline polymer for application in fused filament fabrication. *Addit. Manuf.* **2019,** *29*, 100814.
96. Rajak, D. K.; Pagar, D. D.; Menezes, P. L.; Linul, E., Fiber-reinforced polymer composites: Manufacturing, properties, and applications. *Polymers* **2019,** *11*, 1667.
97. Clyne, T.; Hull, D., *An introduction to composite materials*. Cambridge university press: 2019.
98. Selvaraju, S.; Ilaiyavel, S., Applications of composites in marine industry. *Journal of Engineering Research and Studies* **2011,** *2*, 89-91.

99. Markets, R. a. Composites market by fiber type, resin type, manufacturing process, end-use industry and region-global forecast to 2024. https://www.researchandmarkets.com/reports/4876933/composites-market-by-fiber-type-glass-fiber (accessed Deember 2019).
100. Rajendran, S.; Scelsi, L.; Hodzic, A.; Soutis, C.; Al-Maadeed, M. A., Environmental impact assessment of composites containing recycled plastics. *Resources, Conservation and Recycling* **2012,** *60*, 131-139.
101. Pimenta, S.; Pinho, S. T., Recycling carbon fibre reinforced polymers for structural applications: Technology review and market outlook. *Waste Manage. (Oxford)* **2011,** *31*, 378-392.
102. Ye, S. Y.; Bounaceur, A.; Soudais, Y.; Barna, R., Parameter optimization of the steam thermolysis: A process to recover carbon fibers from polymer-matrix composites. *Waste and Biomass Valorization* **2013,** *4*, 73-86.
103. Liu, Y.; Farnsworth, M.; Tiwari, A., A review of optimisation techniques used in the composite recycling area: State-of-the-art and steps towards a research agenda. *Journal of Cleaner Production* **2017,** *140*, 1775-1781.
104. Oliveux, G.; Dandy, L. O.; Leeke, G. A., Current status of recycling of fibre reinforced polymers: Review of technologies, reuse and resulting properties. *Prog. Mater Sci.* **2015,** *72*, 61-99.
105. Tapper, R. J.; Longana, M. L.; Norton, A.; Potter, K. D.; Hamerton, I., An evaluation of life cycle assessment and its application to the closed-loop recycling of carbon fibre reinforced polymers. *Composites Part B: Engineering* **2019,** 107665.
106. Molnar, A., Recycling advanced composites. *Final report for the Clean Washington Center* **1995**.
107. Morin, C.; Loppinet-Serani, A.; Cansell, F.; Aymonier, C., Near- and supercritical solvolysis of carbon fibre reinforced polymers (cfrps) for recycling carbon fibers as a valuable resource: State of the art. *The Journal of Supercritical Fluids* **2012,** *66*, 232-240.
108. Schinner, G.; Brandt, J.; Richter, H., Recycling carbon-fiber-reinforced thermoplastic composites. *J. Thermoplast. Compos. Mater.* **1996,** *9*, 239-245.
109. Zhang, J.; Chevali, V. S.; Wang, H.; Wang, C.-H., Current status of carbon fibre and carbon fibre composites recycling. *Composites Part B: Engineering* **2020,** 108053.
110. Howarth, J.; Mareddy, S. S.; Mativenga, P. T., Energy intensity and environmental analysis of mechanical recycling of carbon fibre composite. *Journal of Cleaner Production* **2014,** *81*, 46-50.
111. Colucci, G.; Ostrovskaya, O.; Frache, A.; Martorana, B.; Badini, C., The effect of mechanical recycling on the microstructure and properties of pa66 composites reinforced with carbon fibers. *J. Appl. Polym. Sci.* **2015,** *132*.
112. Tomioka, M.; Ishikawa, T.; Okuyama, K.; Tanaka, T., Recycling of carbon-fiber-reinforced polypropylene prepreg waste based on pelletization process. *J. Compos. Mater.* **2017,** *51*, 3847-3858.
113. Kuram, E.; Ozcelik, B.; Yilmaz, F., The influence of recycling number on the mechanical, chemical, thermal and rheological properties of poly (butylene terephthalate)/polycarbonate binary blend and glass-fibre-reinforced composite. *J. Thermoplast. Compos. Mater.* **2016,** *29*, 1443-1457.
114. Kuram, E.; Tasci, E.; Altan, A. I.; Medar, M. M.; Yilmaz, F.; Ozcelik, B., Investigating the effects of recycling number and injection parameters on the mechanical properties of glass-fibre reinforced nylon 6 using taguchi method. *Materials & Design* **2013,** *49*, 139-150.

115. Chrysostomou, A.; Hashemi, S., Influence of reprocessing on properties of short fibre-reinforced polycarbonate. *Journal of materials science* **1996,** *31*, 1183-1197.
116. Ayadi, A.; Kraiem, D.; Bradai, C.; Pimbert, S., Recycling effect on mechanical behavior of hdpe/glass fibers at low concentrations. *J. Thermoplast. Compos. Mater.* **2012,** *25*, 523-536.
117. Kuram, E.; Ozcelik, B.; Yilmaz, F., The influence of recycling number on the mechanical, chemical, thermal and rheological properties of poly(butylene terephthalate)/polycarbonate binary blend and glass-fibre-reinforced composite. *J. Thermoplast. Compos. Mater.* **2016,** *29*, 1443-1457.
118. Ayadi, A.; Kraiem, D.; Bradai, C.; Pimbert, S., Recycling effect on mechanical behavior of hdpe/glass fibers at low concentrations. *J. Thermoplast. Compos. Mater.* **2011,** *25*, 523-536.
119. Colucci, G.; Simon, H.; Roncato, D.; Martorana, B.; Badini, C., Effect of recycling on polypropylene composites reinforced with glass fibres. *J. Thermoplast. Compos. Mater.* **2017,** *30*, 707-723.
120. Eriksson, P. A.; Albertsson, A. C.; Boydell, P.; Prautzsch, G.; Månson, J. A., Prediction of mechanical properties of recycled fiberglass reinforced polyamide 66. *Polym. Compos.* **1996,** *17*, 830-839.
121. Eriksson, P.; Albertsson, A. C.; Boydell, P.; Månson, J. A. J. P. E.; Science, Durability of in‐plant recycled glass fiber reinforced polyamide 66. **1998,** *38*, 348-356.
122. Sarasua, J. R.; Pouyet, J., Recycling effects on microstructure and mechanical behaviour of peek short carbon-fibre composites. *J. Mater. Sci.* **1997,** *32*, 533-536.
123. Bastida, S.; Eguiazabal, J.; Nazabal, J., Reprocessing of liquid‐crystal polymers: Effects on structure and mechanical properties. *J. Appl. Polym. Sci.* **1995,** *56*, 1487-1494.
124. Xu, Q.; Man, H., Recycling of the rodrun lc-5000 lcp/polycarbonate in situ composites. *Polymer* **2000,** *41*, 7391-7397.
125. Collier, M. C.; Baird, D. G., Separation of a thermotropic liquid crystalline polymer from polypropylene composites. *Polym. Compos.* **1999,** *20*, 423-435.
126. Collier, M. C. Reclamation and reprocessing of thermotropic liquid crystalline polymer from composites of polypropylene reinforced with liquid crystalline polymer. Virginia Tech, 1998.
127. Bastida, S.; Eguiazabal, J.; Nazabal, Reprocessing of liquid‐crystal polymers: Effects on structure and mechanical properties. *J. Appl. Polym. Sci.* **1995,** *56*, 1487-1494.
128. Xu, Q. W.; Man, H. C., Recycling of the rodrun lc-5000 lcp/polycarbonate in situ composites. *Polymer* **2000,** *41*, 7391-7397.

3 Thermotropic Liquid Crystalline Polymer Reinforced Polyamide Composite for Fused Filament Fabrication

The first research objective is addressed in this chapter and the manuscript was published in: **T. Chen**, J. Han, D. A. Okonski, D. Kazerooni, L. Ju, D. G. Baird "Generation of Thermotropic Liquid Crystalline Polymer Reinforced Polyamide Composites Filaments and Their Processing in Fused Filament Fabrication", Additive Manufacturing **2021**, *40*, 101931 [1]

Chapter 3. Thermotropic Liquid Crystalline Polymer Reinforced Polyamide Composite for Fused Filament Fabrication

Tianran Chen[1], Jier Han[2], David A. Okonski[3], Dana Kazerooni[1], Lin Ju[1], and Donald G. Baird[1,2]

[1]Macromolecules Innovation Institute, Virginia Tech, VA 24061
[2] Department of Chemical Engineering, Virginia Tech, VA 24061
[3]GM Global Research & Development Center, MI, 48092

3.1 Abstract

Varying reinforcement concentrations (20 to 60 wt%) of thermotropic liquid crystalline polymer (TLCP) were successfully incorporated into a polyamide (PA) matrix using a dual extrusion process for the manufacture of filament for use in fused filament fabrication (FFF). Rheological analyses were used to select the processing conditions for the dual extrusion process that utilized the supercooling behavior of TLCP and minimized the degradation of PA. The optimum 3D-printing temperature was determined as the temperature yielding the printed component with the best mechanical properties. By combining the dual extrusion process with additive manufacturing, it enabled us to generate TLCP/PA composites having greater stiffness (tensile modulus 24.7 GPa) than 3D printed conventional fiber reinforced composites.

3.2 Introduction

Among all the additive manufacturing (AM) processing methods, fused filament fabrication (FFF), also known as extrusion-based additive manufacturing, is the most widely used technique. This is largely due to its fast printing speed, affordable equipment,

and a wide variety of material selection [2-6]. FFF operates by softening a continuous material filament through a hot nozzle and then depositing layer upon layer to build up a part. Currently, this process is able to print large scale geometries at a printing rate of several hundred kilograms per hour [7]. However, there are issues when it comes to making a structurally sound 3D printed part. Due to the nature of the FFF deposition process, the mechanical properties of printed parts are usually lower than that of injection molded counterparts. Using FFF with a neat polymer usually results in a very weak part.

In order to produce stronger and stiffer 3D printed parts, researchers have focused on incorporating fiber reinforcements into various polymer matrices [8-10]. Short fiber, nanofiber, and continuous fiber reinforcements have all been utilized in applications of additive manufacturing to increase a printed part's mechanical performances [11-19]. Presently, 3D printable short fiber composite filament is prepared by blending fibers and polymer matrix in an extruder and passing the blend through a die to form a composite filament. Finally, a 3D printer is used to print the short fiber composite filament into a desired part. The use of short fiber reinforcements has been found to improve the tensile properties of printed parts compared to its printed neat material counterpart. Ning *et al*. [20] reported the tensile modulus of pure matrix resin (1.9 GPa) increased to 2.5 GPa with the addition of 7.5 wt% short carbon fiber using FFF. The incorporation of carbon fiber not only enhanced the tensile strength of the printed component but also increased the flexural modulus and toughness as well. Zhong *et al.* [21] utilized short glass fiber to improve the tensile strength of acrylonitrile-butadiene-styrene (ABS) in FFF. The tensile strength of printed ABS was enhanced by approximately 140% with a fiber loading of 18 wt%. However, one of the disadvantages of using short fiber reinforcement in 3D printing is the

extensive fiber attrition that arises during the filament fabrication step. During the fiber and matrix blending in the extruder, severe fiber attrition can occur from fiber-fiber, fiber-polymer and fiber-equipment interactions [22]. Unfortunately, this is an unavoidable issue because of process limitations preventing the printed composite parts from achieving higher levels of reinforcement.

In the past few years, both academia and industry have developed different processing techniques to use continuous fiber composites for either research or commercial products in the additive manufacturing field [8, 16, 23, 24]. One of the perks of using continuous fiber composites is the ability to further enhance the mechanical properties of 3D printed composite parts because fiber breakage is avoided. Such 3D printers utilize a special dual nozzle head that allows for continuous fiber to be embedded into the thermoplastic filament as it prints. Significant improvements in the mechanical properties of the various polymers have been observed when continuous fibers were incorporated into the matrix material. Dickson *et al*. [19] investigated the impact of incorporating continuous carbon, glass and Kevlar fibers as reinforcements in 3D printed material using a Markforged Mark One 3D printer. It was observed that the continuous fiber improved both tensile and flexural strength to 6.3 and 5 folds as compared to the unreinforced matrix material. Yang *et al.* [24] reported that 3D printed acrylonitrile-butadiene-styrene (ABS) exhibited an approximate 100% enhancement in its tensile modulus and a 400% increase in its tensile strength with embedded continuous carbon fiber. The flexural modulus of the 10 wt% carbon fiber/ABS was 7.7 GPa in comparison with 2.0 GPa for pure ABS. Even though continuous fibers show significant improvements in the mechanical properties of printed materials, continuous fiber fed 3D printers have many shortcomings and challenges such

as the requirement of modifying or purchasing a dual nozzle head printer, severing mechanisms to detach the printing head from the printing bed, and poor fiber wet-out leading to a weak fiber-polymer matrix interface [19, 25, 26]. Moreover, the porosity of 3D printed continuous fiber composite tend to higher than its 3D printed short fiber counterpart, which further reduces the mechanical integrity of the printed parts [27].

Thermotropic liquid crystalline polymers (TLCPs) are a type of high-performance engineering thermoplastic with outstanding mechanical properties, low density, great processability, and excellent recyclability [28-33]. TLCPs have been used as reinforcements to improve the mechanical properties of various thermoplastics [34-36]. Extensive research has been conducted on TLCP/thermoplastic blends for traditional processing techniques such as injection molding, compression molding, film blowing, and film extrusion [37-40]. Seppala *et al.* [41] investigated the mechanical properties of blended polyethylene terephthalate (PET) with 30 wt% TLCP from the injection molding process. Incorporation of TLCP reinforcement enhanced the tensile modulus and strength of PET from 2.6 to 4.1 GPa and 61 to 74 MPa, respectively. Chinsirikul *et al*. [38] utilized polyethylene (PE) blends reinforced with TLCP for film blowing. The addition of 10 wt% TLCP in PE showed a 400% enhancement in tensile modulus over that of pure PE matrix polymer. Anisotropy in the blown TLCP/PE composite film was reduced by using a counter-rotating annular die. As a result, blending TLCP reinforcement with other thermoplastics may significantly improve the mechanical performance of commonly used polymer matrix materials.

The utilizations of TLCP/thermoplastic materials in traditional manufacturing processes have been extensively explored. However, only limited research literature is

available on the additive manufacturing of TLCP/thermoplastic blends. Gray *et al*. [42] developed TLCP/polypropylene (PP) composite filaments which were suitable for FFF. The TLCP composite filaments were prepared by means of a dual extrusion process and then chopped-up and re-extruded to generate the TLCP/PP filaments with suitable diameter for printing on a FFF 3D printer [43]. The printed composite that consisted of 40 wt% TLCP/PP exhibited an approximate 150% increase in tensile modulus relative to that of the pure PP. Although short TLCP fibers enabled the improvements in mechanical properties of 3D printed TLCP/PP composites, the effectiveness of the TLCP reinforcement is still restricted due to the fiber length.

With the exclusion of Gray *et al.*'s pelletizing/re-extruding process, the 3D printing process could be directly combined with the concept of the dual extrusion process. This methodology allowed for the development of a nearly continuous TLCP reinforced high-performance composite filament for direct use in a conventional 3D printer [26]. TLCP/ABS material had a tensile modulus approximately 7.5 times greater than that of the neat matrix material. Regarding morphology, it was determined that the 3D printed TLCP composite had formed nearly continuous TLCP fibrils in the flow direction. Although significant improvements in tensile modulus were obtained by combining TLCP with the dual extrusion process, the incompatibility between the TLCP and ABS matrix polymer led to a relatively low tensile strength caused by poor interfacial adhesion. The polymer incompatibility has been seen with SEM imaging in Fig. 3.1, where the formation of large gaps between the fiber and matrix polymer indicated the poor interfacial adhesion.

The main goal of this work is to blend a TLCP of higher melting point with a polymer matrix of lower melting point which will have stronger intermolecular interactions with the

TLCP to yield a stiffer and stronger 3D printed composite part. A dual extrusion process was used to generate the TLCP reinforced nylon composite filaments. The processing temperatures for dual extrusion were optimized based on the supercooling behavior of the TLCP and the minimization of the matrix polymer's thermal degradation. The optimal printing temperature for the composite filament was identified as the temperature used to create the part that achieved the highest mechanical performance. The influence of TLCP concentration on the printed composite part's properties was systematically studied, and the performances of the TLCP composites were compared against traditional fiber reinforced composites.

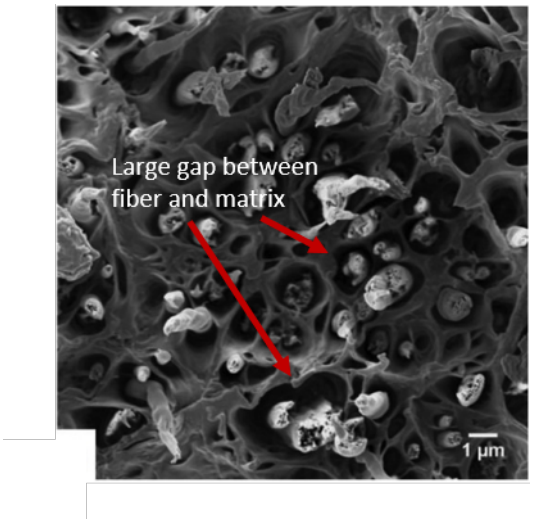

Figure 3. 1 SEM image of TLCP/ABS filament. Reprinted from ref [26], with permission from Elsevier

3.3 Experimental

3.3.1 Materials

The thermotropic liquid crystalline polymer (TLCP) used for this work is an aromatic copolyesteramide, containing 60 mol% 2,6-hydroxynaphthoic acid, 20 mol% terephthalic acid, and 20 mol% aminophenol, purchased from Celanese. The melting point of the TLCP was found to be around 280°C [44]. The polyamide (PA) copolymer matrix material was supplied by Dutch State Mines (DSM).

3.3.2 Dual Extrusion Process

20, 40, and 60 wt% TLCP reinforced PA composite filaments were generated using a dual extrusion process [43]. As shown by the schematic in Fig. 3.2, the process consisted of two single screw extruders (Killion KL-100): one extruder for the TLCP and the other for PA. Therefore, each material was processed independently using appropriate temperature setpoints on the extrusion barrels. The processing temperatures for TLCP and PA extrusion were chosen to be 330 and 250°C, respectively. Both the TLCP and PA polymer streams passed through gear pumps in order to control the flow rate of each material prior to mixing. The processing temperature of the TLCP was subsequently lowered to 270°C before injecting it into the PA matrix through a 28-hole injection nozzle. The polymer blend was subsequently passed through static mixers (Kenics and Koch mixers) where the temperature was maintained at 270°C. The TLCP/PA blend was finally extruded through a 3.0 mm diameter die to form a composite strand. The TLCP/PA extrudate was drawn to a diameter of approximately 1.7 mm and quenched in a water bath to freeze the orientation of the TLCP to form a 3D printable TLCP/PA composite filament. The experimental setup of the dual extrusion process is shown in Fig. 3.3(a).

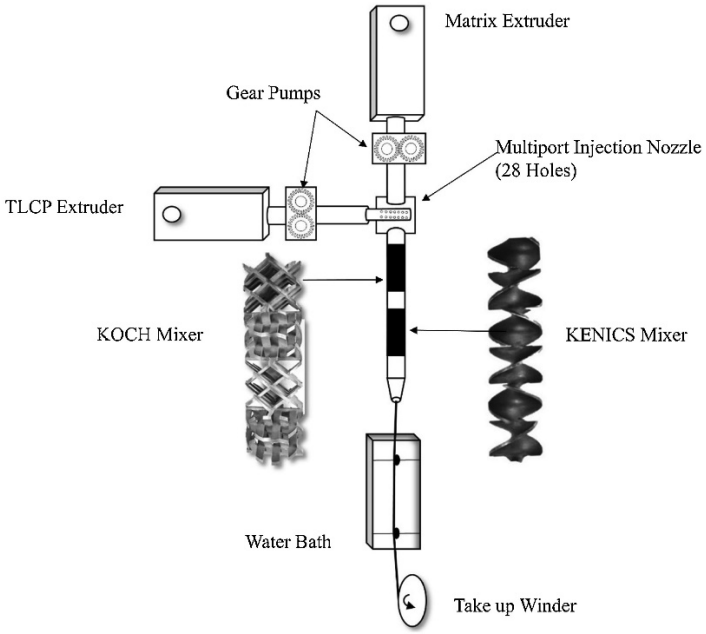

Figure 3. 2: Schematic of the components used in the dual extrusion process. Reprinted from ref [26] ,with permission from Elsevier

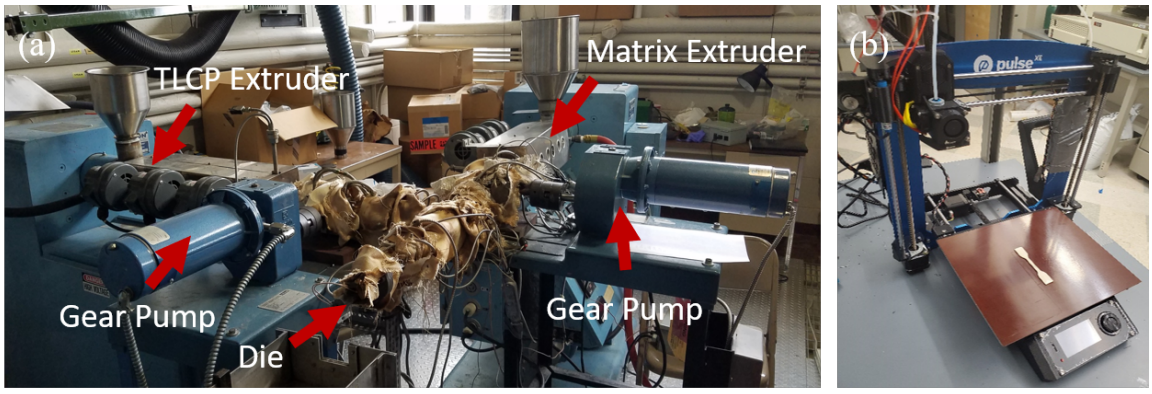

Figure 3. 3:(a) Experimental setup of dual extrusion process (b) 3D printer.

3.3.3 Fused Filament Fabrication

TLCP/PA filaments were printed using a benchtop Pulse 3D printer (MatterHackers) (Fig. 3.3(b)). Different printing temperatures (250 to 290°C) were used with a constant bed

temperature of 80°C to determine the effect of print temperature on the mechanical properties of a 3D printed part. Rectangular tensile bars were printed unidirectionally having a length of 80 mm, a width of 8 mm, and a thickness of 1.5 mm. All TLCP/PA samples were printed using a 0.6 mm diameter nozzle with 20 mm/s printing speed, 0.2 mm layer height, and 100% infill.

3.3.4 Rheological Test

A rheometer (ARES-G2, TA Instrument) with 25.0 mm diameter parallel disk fixtures was utilized to examine the rheological properties of both TLCP and PA. All the tests were administered under a dry nitrogen environment. The first test included investigating the thermal stability of PA at temperatures of 250, 280, 300, and 320ºC to find the maximum operational temperature to prevent severe degradation of PA. The small amplitude oscillatory shear (SAOS) rheology in the time sweep mode was used to measure the complex viscosity of polyamide as a function of time. The second test involved studying the supercooling behavior of the TLCP which correlates to the minimum temperature at which the TLCP will remain molten during processing. The TLCP material was heated up to 300, 310, and 320ºC and then cooled down at a rate of -10ºC/min. Both the storage modulus and loss modulus were tracked as a function of temperature. Thirdly, shear step strain rheology was conducted to investigate the transient flow of the TLCP [45]. After a shear step strain of 0.5%, the relaxation modulus of TLCP was monitored over time at temperatures between 290 and 320ºC. Finally, the stability of TLCP at the supercooled state was analyzed through preheating the TLCP at 320ºC and then cooling it down to either 250 or 260ºC. The storage and loss modulus were tracked carefully as a function of time until the appearance of the crossover point between storage and loss modulus [46].

3.3.5 Mechanical Tests

The mechanical properties of the TLCP/PA filaments and 3D printed composite specimens were examined using an Instron mechanical tester (Model 4204). The cross-head speed was kept at 1.27 mm/min, and a 5kN load cell was used. Tensile strain was measured using an extensometer (MTS 634.12). Elastic modulus and tensile strength were calculated as the average of at least five replicates.

3.3.6 Scanning Electron Microscope (SEM)

The morphologies of 20 wt% TLCP/PA filaments and 3D printed composite specimens were investigated using a scanning electron microscope. The composite filament and 3D printed specimens were cryo-fractured along the direction perpendicular to the flow direction. The composite specimens were subsequently sputter coated with a 10 nm thick gold layer. The cross sections of the composite specimens were examined by a LEO (Zeiss) 1550 SEM.

3.3.7 Differential Scanning Calorimetry (DSC)

The thermal properties of PA and TLCP/PA composite were evaluated by DSC (Q2000 Series TA Instruments). 5-10 mg of each sample were loaded into an aluminum T_{zero} pan and tested by means of the DSC. The sample was first equilibrated at 20°C for 5 minutes and then the temperature was increased to 280°C at 10°C/min. The material was cooled down to 20°C at a rate of -10°C/min, and finally heated up to 280°C at 10°C/min. All the samples were tested under heat/cool/heat cycle under a nitrogen atmosphere.

3.4 Results and Discussion

3.4.1 Rheological Analyses of PA and TLCP

Rheological studies were conducted to obtain the optimal temperature of the dual extrusion process to minimize the PA's thermal degradation and utilize the TLCP's super-cooled state when blending TLCP with PA in the dual extrusion process. Fig. 3.4 illustrates the thermal stability of PA at various testing temperatures. For the temperatures of 250 and 280°C, the complex viscosity of the neat PA increases slightly as a function of time. The constant increase is speculated to be the result of the buildup of molecular weight (MW) [47-49]. Levchik and co-workers [49, 50] proposed that carbodiimide is formed by dimerization of isocyanate groups and which then trimerizes leading to a crosslinking reaction. The average residence time of the material in the dual extruder was measured to be around 900 seconds. In this period of time, the complex viscosity of the PA increases approximately 23% at 280°C, which is very close to the thermal stability range of the polymer melt, as defined by, the 20% change in viscosity [51]. The degradation rate of the PA increases with increasing temperature where the viscosity drops approximately 42% as compared to the measured initial viscosity at 300°C. At a temperature of 320°C, PA maintains the complex viscosity in the first few minutes then decreases as time increases. This phenomenon may be due to the competing factors that cause the increase of MW (increase in complex viscosity) and chain scission (decrease in complex viscosity) degradation of PA [47]. At elevated temperatures, the chain scission mechanism for degradation begins to dominate, leading to the overall decreasing trend in viscosity. As a result, PA should be processed at temperatures lower than 300°C.

Understanding the supercooling behavior of the TLCP is important because it directly impacts the processability of the material during the dual extrusion process. Retaining TLCP's liquid-like behavior at lower temperatures allows mixing to occur at temperatures which will prevent the matrix from degrading. Thus, the supercooling behavior of TLCP was studied using different starting temperatures. The change of storage modulus (G') and loss modulus (G'') as a function of temperature is presented in Fig. 3.5. The storage and loss moduli measure the elastic response and energy dissipation of the material, respectively. The crossover point or the intersection of G' and G'' indicates the temperature where a polymer transitions between its viscous (liquid-like) and elastic (solid-like) states. Since the melting point of the TLCP is around 280°C, this TLCP was heated to a temperature well above the melting point and then cooled until the onset of solidification. From Fig. 3.5, the TLCP material cooled from a temperature of 300°C was found to have a crossover point at approximately 270°C. When the starting temperature was increased by 10°C, the crossover point of G' and G'' dramatically decreases to approximately 235°C (To avoid over torqueing the instrument, the test was stopped before reaching the crossover point). The dramatic change in supercooling behavior is most likely attributed to the presence of residual TLCP crystals at 300°C – the presence of residual TLCP crystals lowers the total energy necessary to crystalize the material causing it to nucleate and crystallize quicker resulting in a higher solidification temperature. The temperature to completely melt all the TLCP crystals was observed to be at or above 305°C [33]. The supercooling behaviors for the TLCP coincides once all of the TLCP crystals are completely melted as shown in Fig. 3.5 with the overlapping curves for 310 and 320°C. Therefore, the ideal starting temperature to liquefy TLCP is above 310°C, and furthermore,

the TLCP will need to remain above a processing temperature of 235°C to retain its liquid state.

To further investigate the rheological behavior of TLCP above its melting temperature, transient rheology was used to examine the TLCP melt properties at elevated temperatures. The state of the TLCP rod-like molecules and domain structures are closely related to its transient rheological behavior [45, 52]. Fig. 3.6 demonstrates the change in the TLCP's relaxation modulus (G) over time following a step strain at varying experimental temperatures. The relaxation modulus of TLCP at 290 and 300℃ is obtained from our previous study [33]. At temperatures below 310℃, the relaxation modulus is found to slowly decay with long relaxation tails as shown in Fig. 3.6. However, when the environmental temperature reaches 310℃, the relaxation modulus drops rapidly without any relaxation tail. As the temperature approached 310℃, all TLCP crystals are liquefied resulting in fast decay in its relaxation modulus. The temperature for TLCP shown by the drastic change in rheological behavior in Fig. 3.6 would be identical to the temperature determined by the TLCP supercooling (310℃) from Fig. 3.5 because the rheological behaviors of TLCP are dependent on the presence of un-melted TLCP crystals. So, it was confirmed that the TLCP has to be heated to at least 310℃ before mixing with PA in the dual extrusion process to successfully utilize the TLCP's supercooling behavior and reduce PA's degradation.

Although the cross-over point for the 310℃ preheated TLCP was measured to be around 235℃, it does not indicate that the TLCP's liquid state is guaranteed to be stable at this temperature. Therefore, the stability of the supercooled TLCP was tested by preheating TLCP above 310℃ to melt all of the TLCP crystals and subsequently cooled to either 250

or 260℃, where the storage modulus and loss modulus were monitored with respect to time as shown in Fig. 3.7. At a temperature of 250℃ the G' and G'' increase rapidly during the first 400 seconds and the storage modulus surpasses the loss modulus indicating the solidification of TLCP. On the other hand, the G' and G'' stay constant over the complete experimental time (longer than the average residence time of dual extrusion process) when the temperature of TLCP is kept at 260℃. Thereby, the temperature to maintain a stable TLCP melt in the super-cooled state is determined to be at least 260℃ to avoid the TLCP's solidification during processing.

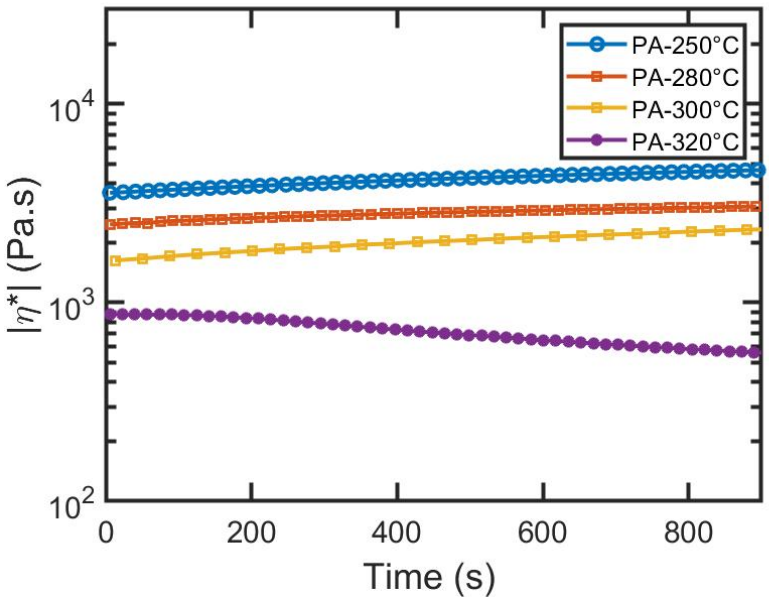

Figure 3. 4: Thermal stability of PA at temperatures of 250, 280, 300, and 320ºC

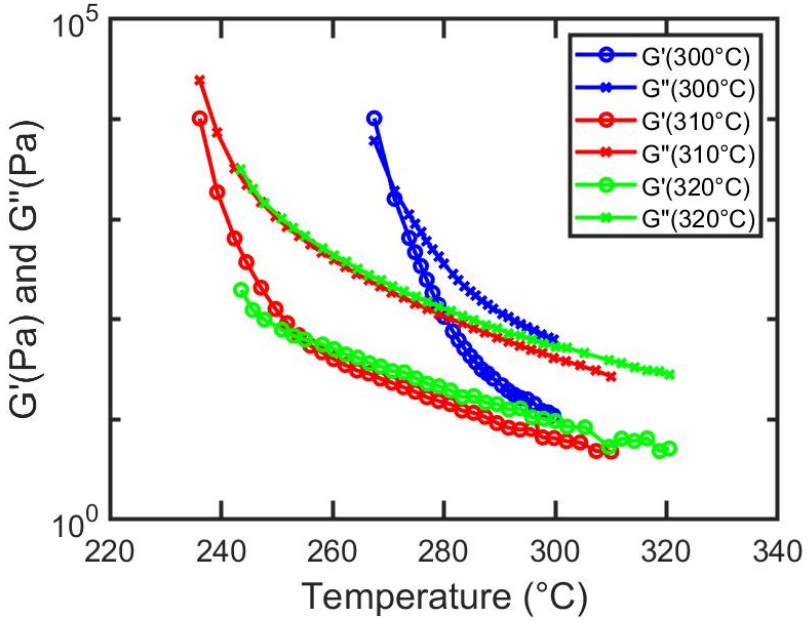

Figure 3. 5: Supercooling behaviors of TLCP at different starting temperatures

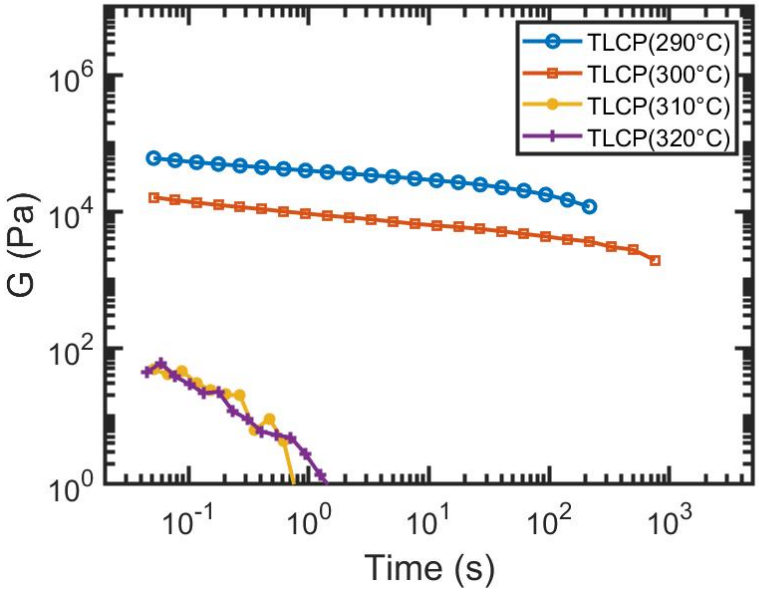

Figure 3. 6: Transient rheology of TLCP followed a step strain at various temperatures

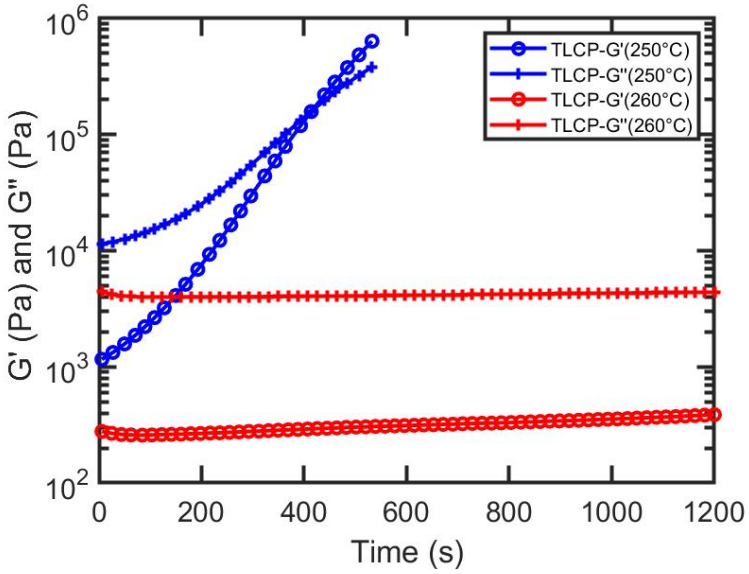

Figure 3. 7: Oscillatory shear rheology measurements in the isothermal time sweep mode for TLCP in super-cooled state.

3.4.2 Processing temperatures of the dual extrusion process

Based on the rheological analyses of TLCP and PA, the temperature profile for generating TLCP/PA composite filament through the dual extrusion process is depicted in Fig. 3.8. The processing temperature of the PA matrix extruder is maintained at 250°C. The molten matrix polymer passes from the extruder to a gear pump at the same temperature. The TLCP reinforcement extruder is maintained at a processing temperature of 330°C to guarantee the TLCP crystals are completely melted. After the TLCP melt stream exits the extruder, the processing temperature continues to decrease towards 270°C. The PA and TLCP melts are then joined in a tee that guides into a set of static mixers which distributes the TLCP within the PA matrix through intensive radial mixing. The temperature of the dual extrusion setup is sustained at 270°C after mixing the TLCP and PA to minimize the degradation of the PA and to avoid the solidification of TLCP. Finally, the TLCP/PA blend is extruded through a die to form the nearly continuous TLCP reinforced PA composite filament for 3D printing.

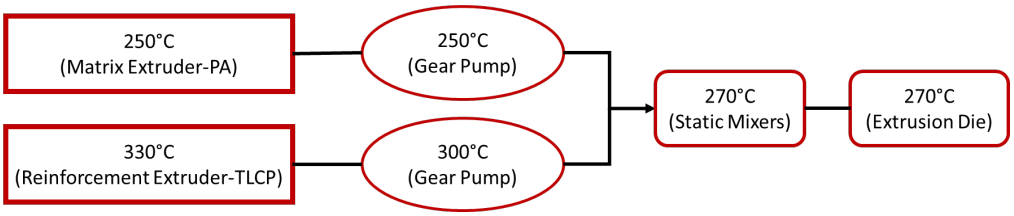

Figure 3. 8: The temperature profile of the dual extrusion process for mixing TLCP and PA

3.4.3 Mechanical performance of printed TLCP/PA composites and TLCP/PA filaments

The composite filaments generated from the dual extrusion process were printed using a conventional benchtop 3D printer. The influence of different printing temperatures on printed parts was investigated. The tensile properties of the unidirectionally printed 20 wt% TLCP/PA composite at various printing temperatures are shown in Fig. 3.9. Both tensile modulus and tensile strength increase with the increase of temperature from 250℃ to 280℃. When the printing temperatures were below 250℃, delamination between printed layers was observed occasionally. The increasing mechanical performance with the increase in temperature is mainly due to the increase in interlayer adhesion. During the fused filament fabrication (FFF) process, the filament is pushed into a heated nozzle where the material is softened and subsequently deposited layer by layer to form a three-dimensional structure. The formation of bonds among adjacent layers can influence the mechanical performance of printed parts. To form the bond, the printing layer contacts with the previously extruded layer. The neck grows between adjacent filaments and molecular diffusion of polymer chains occurs at the interface [53-55]. Molecular diffusion will continue as long as the temperature of printed material is above the glass transition temperature (T_g). If the temperature at the interface stays above the glass transition temperature for a longer time, it is believed that stronger interfacial bonding will form between adjacent layers. Thus, if the part cools too quickly, the interface between the printed layers will not adhere well to its nearest neighbors. By increasing the printing temperature, it may be inferred that the polymer chain at the interface will have a longer time to diffuse into another which would increase the mechanical performance of the

composite part. However at very high temperatures, the mechanical properties of the composite material begin to decrease slightly as demonstrated by the comparison of both the elastic modulus and tensile strength between the specimens printed at 280 and 290℃ in Fig. 3.9. The drop in mechanical performance is believed to be attributed to the relaxation of TLCP's orientation. Because the melting point of this TLCP is around 280℃, the one-dimensional highly oriented TLCP could relax and lose orientation resulting in a more randomly oriented TLCP phase that leads to a decrease in tensile properties of the printed composite. The printing temperature that achieved the highest mechanical properties for the 20 wt% TLCP/PA composite is 280℃.

Furthermore, the tensile modulus and tensile strength of pure PA material 3D printed at temperatures between 250 to 290℃ increase slightly with the increasing of printing temperature, as shown in Fig. 3.9. At a printing temperature of 250℃, the tensile modulus and strength were measured to be 2.1 GPa and 52.0 MPa, respectively. While tensile modulus and strength for pure PA at the printing temperature of 290℃ is around 2.3 GPa and 56.0 MPa, respectively. The increase in the interlayer adhesion of 3D printed PA at higher printing temperature leads to the higher mechanical properties [56, 57].

The 40 and 60 wt% TLCP/PA composite filaments were also prepared using the dual extrusion process. The mechanical properties for the different amounts of reinforcement are presented in Fig. 3.10 and Table 3.1. The printing temperature is selected to be 280℃. Pure nylon was measured to have the tensile modulus and tensile strength of 2.3 GPa and 55.4 MPa, respectively. By incorporating 20 wt% TLCP into the PA, the tensile modulus increases by 240% (Fig. 3.10(a)). The tensile modulus continues to increase with the increasing concentration of TLCP. The tensile modulus for the 60 wt% TLCP/PA is around

25 GPa, which is higher than most traditional glass/carbon fiber reinforced composites used in 3D printing applications according to the literature [8]. The tensile strength of the composite also increases with increasing TLCP content (Fig. 3.10(b)). The tensile strength of 60 wt% TLCP/PA is very close to 100 MPa which is about 1.6 times higher than that of pure polyamide. By combing the dual extrusion process with additive manufacturing, it has enabled the generation of high-performance TLCP/PA composite parts.

To evaluate the influence of FFF on the performance of TLCP/PA composite materials, uniaxial tensile testing was done systematically on the composite specimens before and after 3D printing with various TLCP concentrations. The mechanical properties for the composite filament before 3D printing and 3D printed parts are compared side-by-side in Table 3.2. The 3D printed specimens were printed at 280℃. Both the tensile modulus and tensile strength of the TLCP/PA composite drop after undergoing the FFF printing process. The decrease in the mechanical performance after 3D printing may result from one or a combination of the following reasons: 1) interlayer adhesion 2) orientation of TLCP 3) printed-in defects (Fig. 3.12). First, for the composite filament without any potential negative influence from interlayer bonding, the mechanical properties of the TLCP/PA filament should outperform the 3D printed counterpart. Second, at the elevated printing temperature, the oriented TLCP fibrils in the composite filament could lose their orientation resulting in the decrease of mechanical properties. Lastly, printed-in defects, such as voids, reduces the quality of the final part by decreasing the effective cross-sectional area and the generation of stress concentrations. All these factors will result in a decrease in the mechanical performance of TLCP/PA after the 3D printing process where each concentration of TLCP/PA composite experiences approximately a 30% drop in the

tensile modulus as compared to its composite filament. However, tensile strength decreases significantly more than its tensile modulus at higher loadings of TLCP. The 60 wt% TLCP/PA composite's tensile strength drops more than 50% after printing due to the fact that a highly loaded TLCP composite has a low amount of matrix material meaning there is less matrix material to diffuse between adjacent print layers and form weaker interlayer bonding. For that reason, there is a rapid reduction in the printed part's tensile strength. Furthermore, in Fig. 3.11 the 20 wt% TLCP/PA printed composite demonstrated brittle fracture with a relatively flat fracture surface while at higher TLCP concentrations the tensile failure occurs through the delamination of the printed layers (Fig. 3.11). Consequently, interlayer adhesion is one of the most important factors that decreases the tensile strength of 3D printed parts, and this is especially true for composite filaments with high TLCP concentrations.

Another factor that would influence the material's mechanical properties is the degree of crystallinity. Thus, DSC tests were used to examine the thermal properties of PA and TLCP/PA composite material. Table 3.3 summarizes both the melting and crystallization temperature as well as the heat of fusion for each material. The heat of fusion (ΔH_m) for the composites is calculated from the area under the melting endotherm with respect to the composition of PA. Since the degree of crystallinity is directly proportional to the ΔH_m, changes in the ΔH_m in the TLCP/PA composites would indicate a change in degree of crystallinity in the PA matrix. As shown in Table 3.3, the addition of TLCP has no significant influence on the ΔH_m of PA material. Therefore, the influence of the degree of crystallinity of PA on the mechanical performance of TLCP/PA composites is negligible.

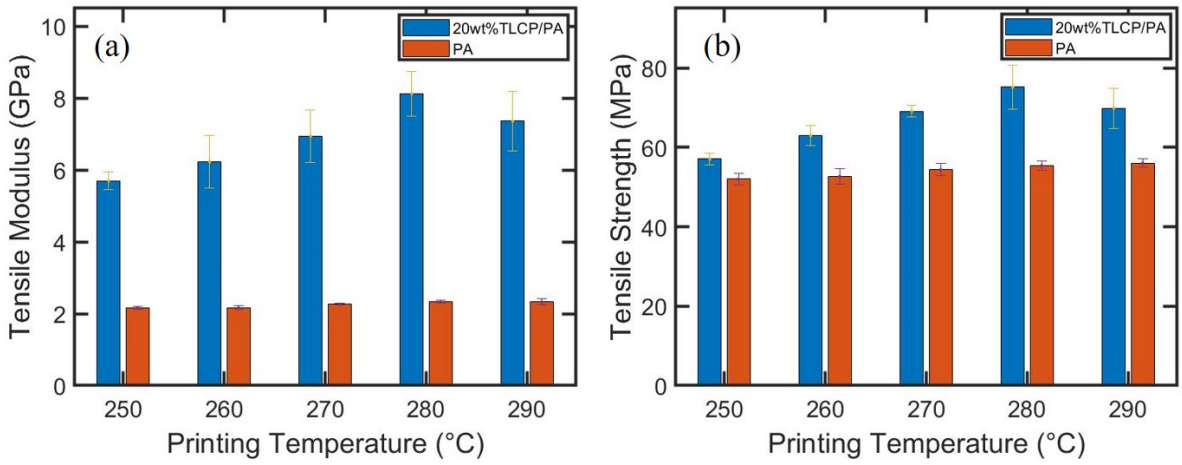

Figure 3. 9: Tensile properties of printed 20 wt% TLCP/PA composite and pure PA in various printing temperatures (a) tensile modulus (b) tensile strength

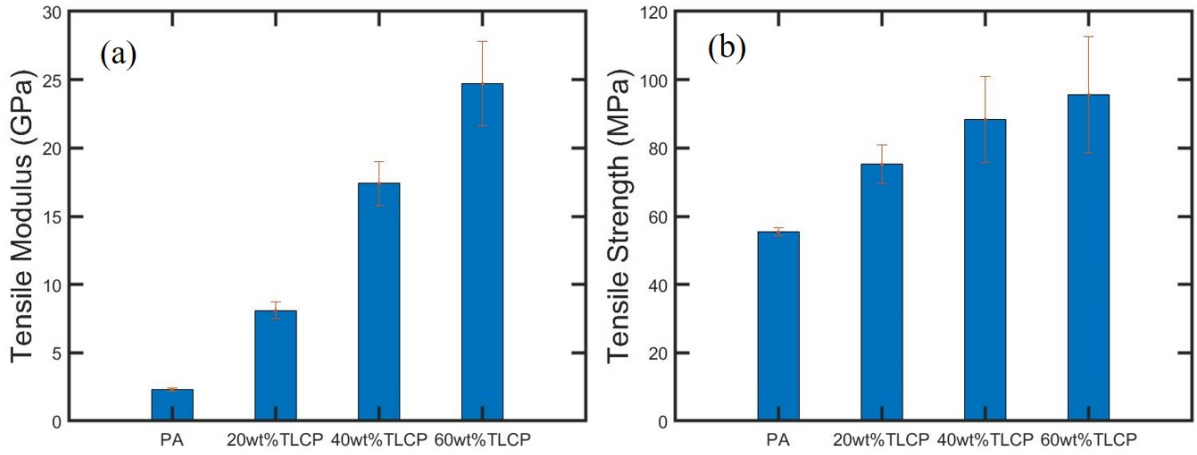

Figure 3. 10: Tensile properties of 3D printed pure PA and TLCP/PA composite with different concentrations of TLCP (20, 40, and 60 wt%) at printing temperature of 280℃ (a) tensile modulus (b) tensile strength

Table 3. 1: Tensile properties of 3D printed materials at printing temperature of 280℃

Properties \ Samples	PA	20 wt% TLCP/PA	40 wt% TLCP/PA	60 wt% TLCP/PA
Tensile Modulus (GPa)	2.3±0.1	8.1±0.6	17.4±1.6	24.7±3.1
Tensile Strength (MPa)	55.4±1.2	75.2±5.6	88.4±12.6	95.6±17.1

Table 3. 2: Tensile properties of composite filament vs 3D printed TLCP/PA materials

Reinforcement Weight Percentage (wt%)	Process	Tensile Modulus (GPa)	Tensile Strength (MPa)
20 wt%	Dual Extrusion	12.5±0.3	84.5±8.3
	Print	8.1±0.6	75.2±5.6
40 wt%	Dual Extrusion	25.9±0.9	152.2±18.8
	Print	17.4±1.6	88.4±12.6
60 wt%	Dual Extrusion	34.0±2.0	206.3±18.5
	Print	24.7±3.1	95.6±17.1

Figure 3. 11: Tensile fractured 20, 40, and 60 wt% 3D printed TLCP/PA composites

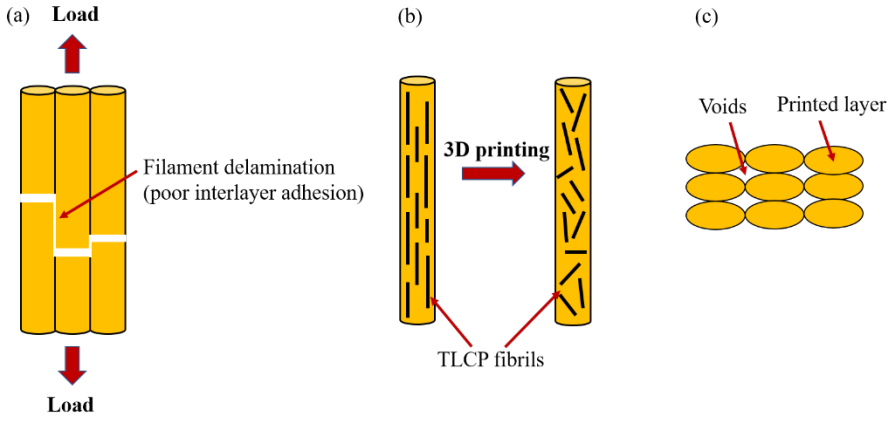

Figure 3. 12: Schematic of factors which may result in the decrease in mechanical performance of TLCP/PA composite after printing (a) poor interlayer adhesion (b) relaxation of TLCP's orientation (c) voids between printed layers

Table 3. 3. DSC result for PA and TLCP/PA composite

Samples	PA	20 wt% TLCP/PA	40 wt% TLCP/PA	60 wt% TLCP/PA
T_m (°C)[a]	193.2	194.0	192.3	191.5
T_c (°C)[b]	163.2	165.2	164.6	163.9
ΔH_m (J/g)[a]	56.5	57.7	54.3	58.6

[a] first heating cycle [b] first cooling cycle

3.4.4 Morphological properties of TLC/PA composite

To examine the morphological properties of TLCP/PA composites, scanning electron microscopy (SEM) was used to look at the cross-section of the composite specimen. The cross-sectional image of a 20 wt% TLCP/PA filament, pictured in Fig. 13(a), shows embedded TLCP fibrils with a measured diameter size of a few microns dispersed in the continuous polyamide matrix phase. The diameter of the TLCP fibrils is usually an order of magnitude smaller than the conventional glass/carbon fiber which tends to be more than 10 μm. The small diameter of a TLCP fibril is due to the fibril generation by the dual extrusion process. Instead of relying on the droplet breakage during mixing like in single screw extrusion, the TLCP streams in the dual extrusion process are divided into much finer streams by the static mixers producing finer TLCP fibrils. The benefit of smaller diameter fibrils/fibers is their high aspect ratio. The higher the aspect ratio (L/D) of the reinforcement in a composite typically leads to higher mechanical properties [58]. TLCP

composites generated through the dual extrusion process have the potential to greatly surpass traditional fiber reinforced composites with regards to mechanical properties.

In the Fig. 13(a), the TLCP fibrils are not uniformly distributed within the nylon matrix. This may be due to the large viscosity differences between the PA matrix and TLCP reinforcement because large viscosity differences between the two components would lower the rate of striation thinning and reduce the mixing performance of static mixers [59, 60]. The viscosities of PA and TLCP were determined using the small amplitude oscillatory shear rheological test to be 2257 and 240 Pa.s, respectively (frequency of 1 rad/s and temperature of 270ºC). Even though the TLCP/PA composite does not have a homogenous distribution of the TLCP, the 20 wt% TLCP/nylon filament still achieves excellent mechanical performance (tensile modulus of 12.5 GPa), which is slightly lower than its theoretical calculation (15 GPa). The Halpin-Tsai equation is used for theoretical calculation where the modulus of nylon and TLCP used in this calculation are 2.3 and 75 GPa, respectively [61]. With better distribution and dispersion, the mechanical properties of TLCP/PA composite are expected to reach their theoretical value.

Even though it is true that any matrix material with TLCP reinforcement will exhibit increased mechanical properties, significantly desirable properties arise when the continuous matrix phase and the reinforcement phase are tailored properly for intimate interaction. The polyamide and the aromatic poly(ester-co-amide) type of TLCP used in this study were purposely selected because of the potential for strong intermolecular interactions. In Fig. 13(a), the SEM image shows small gaps between the nylon matrix and TLCP fibrils indicating relatively good adhesion between the TLCP reinforcement and the polyamide matrix. The ability to form hydrogen bonding between TLCP and nylon chains

results in better compatibility and stronger bonding between the matrix resin and fibrils during the filament generation process [62]. SEM images of TLCP and ABS in a previous study that used the same dual extrusion process showed larger gaps between the TLCP fibrils and the ABS matrix which may be attributed to the absence of strong intermolecular interactions [26]. From that same previous study, the highest tensile strength of 3D printed 40 wt% TLCP/ABS was measured to reach a maximum around 79 MPa which is lower than the printed TLCP/PA composite with the same level of reinforcement [26]. Although, the tensile strength of pure ABS is usually lower than that of pure polyamide. However, the draw ratio of the TLCP/ABS composite in the previous study is higher than this study, in which a higher draw ratio will lead to higher mechanical properties of a TLCP composite. In addition, the pure TLCP used in the previous study had a tensile strength of 825 MPa, while the highly drawn TLCP utilized in this study was only around 500 MPa [61, 63]. The higher mechanical properties of TLCP/PA are believed to be the result of increase in interactive forces between the TLCP reinforcement and matrix material.

The SEM image of printed TLCP/PA composite material was prepared by cryo-fracturing the part in the perpendicular-to-printing direction. Fig. 13(b) shows the thickness of each layer being around 0.2 mm which is consistent with the print parameters. The presence of voids, highlighted in yellow circles in Fig. 13(b), is clearly visible in the SEM image between layers. This is primarily caused by the elliptically shaped extrudate cross-sections. Voids in the 3D printed part reduce the cross-section area of the TLCP composite material and become areas of stress concentration within the part which results in lower mechanical properties in 3D prints as opposed to TLCP/PA composite filament.

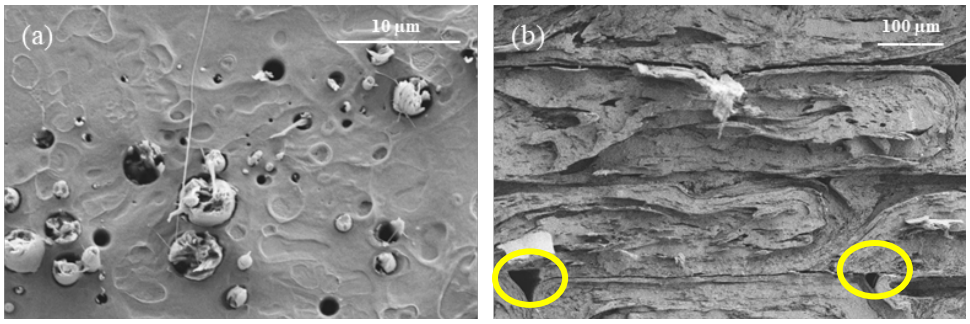

Figure 3. 13: SEM of 20wt% TLCP/PA (a) composite filament (b) 3D printed composite

3.4.5 TLCP/PA vs traditional fiber composite in additive manufacturing

To analyze the performance of the 3D printed TLCP/PA composites, the printed parts were compared against 3D printed traditional fiber (glass fiber and carbon fiber) composite. Currently, additively manufactured fiber composite consists of short or continuous fiber. Short fiber composites can be directly printed with a conventional 3D printer but are unable to achieve high levels of reinforcement compared to continuous fiber composites [8]. On the other hand, continuous fiber composites usually require expensive dual nozzle printers and a severing mechanism for the detachment of the nozzle from the printing bed during the printing process. From Table 3.4, the tensile modulus and strength of a 6 wt% short carbon fiber reinforced composite are measured to be 1.85 GPa and 33.5 MPa, respectively, which are significantly lower than the printed TLCP/PA composite used in this study. Compared to the continuous fiber system, the tensile modulus of 20 wt% TLCP/PA is twice that of 10 vol% glass fiber/nylon (10 vol% glass fiber is approximately equal to 20 wt% glass fiber) and slightly higher than the tensile modulus of 11 vol% continuous carbon fiber/nylon. Even at a very high loading of the fiber system, the stiffness of 60 wt% TLCP reinforced composite is comparable to traditional fiber composites. The tensile strength of

the TLCP/PA is much higher than that of the short fiber composites. However, the tensile strength of the TLCP/PA material is much lower than the continuous glass fiber or carbon fiber/nylon composites. The explanation for this observation includes but not limited to the difference in mechanical properties of the reinforcing material and the degree of the orientation of TLCP. The tensile strength of glass fiber and carbon fiber are reported to be approximately 3.5 GPa and 5.6 GPa, respectively, as compared to the tensile strength of highly drawn TLCP filament at 0.5 GPa [61, 64, 65]. In addition, the draw ratio of this TLCP/PA filament is relatively low (~3) which reduces the degree of orientation of TLCP fibrils in the flow direction which limits mechanical performance [63].

Table 3. 4. Mechanical properties of 3D printed short and continuous glass fiber/carbon fiber reinforced composite and TLCP/PA composite

Material \ **Properties**	**Tensile Modulus (GPa)**	**Tensile Strength (MPa)**
6 wt% carbon fiber/nylon (short)[27]	1.85	33.5
10 vol% glass fiber/nylon (continuous)[19]	3.75	206.0
11 vol% carbon fiber/nylon (continuous)[19]	7.73	216.0

34 vol% carbon fiber/nylon (continuous)[66]	35.7	464.4
20 wt% TLCP/nylon	8.1	75.2
60 wt% TLCP/nylon	24.7	95.6

3.5 Conclusion

The described dual extrusion process allowed for the generation of 3D printable high-performance TLCP reinforced polyamide composite filaments. Rheological tests were used to identify the processing temperature to blend TLCP and PA to minimize the thermal degradation of the PA matrix polymer. The super-cooled state of TLCP was utilized and rheological studies showed that TLCP maintained a stable melt at a temperature of 260°C. The dual extrusion process allowed for the TLCP/PA composite filament to be fabricated by processing PA and TLCP separately at different desired processing temperatures and then mixing them together when the TLCP was in the super-cooled state. The resulting 20 wt% TLCP/PA composite filament was found to achieve a tensile modulus and strength of 8.1 GPa and 75.2 MPa, respectively. The ideal printing temperature of the TLCP/PA filaments which resulted in the maximum retention of the tensile performance of the composite filament was found to be around 280°C. The tensile properties of printed TLCP composite increased with increasing TLCP content. The tensile modulus of 60 wt% TLCP/PA was measured to be above 20 GPa which could rival the current traditional glass or carbon fiber reinforced composite in additive manufacturing processes.

3.6 Acknowledgments

The authors would like to express grateful acknowledgment to General Motors (GM) for financial support.

3.7 Reference

1. Chen, T.; Han, J. Y.; Okonski, D. A.; Kazerooni, D.; Ju, L.; Baird, D. G., Thermotropic liquid crystalline polymer reinforced polyamide composite for fused filament fabrication. *Addit. Manuf.* **2021,** *40*, 101931.
2. Guo, N.; Leu, M. C., Additive manufacturing: Technology, applications and research needs. *Front. Mech. Eng.* **2013,** *8*, 215-243.
3. Bahnini, I.; Rivette, M.; Rechia, A.; Siadat, A.; Elmesbahi, A., Additive manufacturing technology: The status, applications, and prospects. *Int. J. Adv. Manuf. Technol.* **2018,** *97*, 147-161.
4. Wong, K. V.; Hernandez, A., A review of additive manufacturing. *ISRN Mechanical Engineering* **2012,** *2012*, 208760.
5. Gibson, I.; Rosen, D. W.; Stucker, B., *Additive manufacturing technologies: Rapid prototyping to direct digital manufacturing*. Springer-Verlag Berlin: Berlin, 2010; p 1-459.
6. Ngo, T. D.; Kashani, A.; Imbalzano, G.; Nguyen, K. T. Q.; Hui, D., Additive manufacturing (3d printing): A review of materials, methods, applications and challenges. *Compos. Pt. B-Eng.* **2018,** *143*, 172-196.
7. Thermwood Lsam - large scale additive manufacturing. http://www.thermwood.com/lsam_home.htm#whatislsam (accessed 7/15/2020).
8. Brenken, B.; Barocio, E.; Favaloro, A.; Kunc, V.; Pipes, R. B., Fused filament fabrication of fiber-reinforced polymers: A review. *Addit. Manuf.* **2018,** *21*, 1-16.
9. Fallon, J. J.; McKnight, S. H.; Bortner, M. J., Highly loaded fiber filled polymers for material extrusion: A review of current understanding. *Addit. Manuf.* **2019,** *30*, 11.
10. Wang, X.; Jiang, M.; Zhou, Z. W.; Gou, J. H.; Hui, D., 3d printing of polymer matrix composites: A review and prospective. *Compos. Pt. B-Eng.* **2017,** *110*, 442-458.
11. Tekinalp, H. L.; Kunc, V.; Velez-Garcia, G. M.; Duty, C. E.; Love, L. J.; Naskar, A. K.; Blue, C. A.; Ozcan, S., Highly oriented carbon fiber-polymer composites via additive manufacturing. *Compos. Sci. Technol.* **2014,** *105*, 144-150.
12. Love, L. J.; Kunc, V.; Rios, O.; Duty, C. E.; Elliott, A. M.; Post, B. K.; Smith, R. J.; Blue, C. A., The importance of carbon fiber to polymer additive manufacturing. *J. Mater. Res.* **2014,** *29*, 1893-1898.
13. Gray, R. W.; Baird, D. G.; Bohn, J. H., Thermoplastic composites reinforced with long fiber thermotropic liquid crystalline polymers for fused deposition modeling. *Polym. Compos.* **1998,** *19*, 383-394.
14. Shofner, M. L.; Lozano, K.; Rodriguez-Macias, F. J.; Barrera, E. V., Nanofiber-reinforced polymers prepared by fused deposition modeling. *J. Appl. Polym. Sci.* **2003,** *89*, 3081-3090.
15. Shofner, M. L.; Rodriguez-Macias, F. J.; Vaidyanathan, R.; Barrera, E. V., Single wall nanotube and vapor grown carbon fiber reinforced polymers processed by extrusion freeform fabrication. *Compos. Pt. A-Appl. Sci. Manuf.* **2003,** *34*, 1207-1217.
16. Li, N. Y.; Li, Y. G.; Liu, S. T., Rapid prototyping of continuous carbon fiber reinforced polylactic acid composites by 3d printing. *J. Mater. Process. Technol.* **2016,** *238*, 218-225.
17. Tian, X. Y.; Liu, T. F.; Yang, C. C.; Wang, Q. R.; Li, D. C., Interface and performance of 3d printed continuous carbon fiber reinforced pla composites. *Compos. Pt. A-Appl. Sci. Manuf.* **2016,** *88*, 198-205.
18. Matsuzaki, R.; Ueda, M.; Namiki, M.; Jeong, T.-K.; Asahara, H.; Horiguchi, K.; Nakamura, T.; Todoroki, A.; Hirano, Y., Three-dimensional printing of continuous-fiber composites by in-nozzle impregnation. *Sci. Rep.* **2016,** *6*, 23058.

19. Dickson, A. N.; Barry, J. N.; McDonnell, K. A.; Dowling, D. P., Fabrication of continuous carbon, glass and kevlar fibre reinforced polymer composites using additive manufacturing. *Addit. Manuf.* **2017,** *16*, 146-152.
20. Ning, F. D.; Cong, W. L.; Qiu, J. J.; Wei, J. H.; Wang, S. R., Additive manufacturing of carbon fiber reinforced thermoplastic composites using fused deposition modeling. *Compos. Pt. B-Eng.* **2015,** *80*, 369-378.
21. Zhong, W.; Li, F.; Zhang, Z.; Song, L.; Li, Z., Short fiber reinforced composites for fused deposition modeling. *Materials Science Engineering: A* **2001,** *301*, 125-130.
22. Yeole, P.; Hassen, A. A.; Kim, S.; Lindahl, J.; Kunc, V.; Franc, A.; Vaidya, U., Mechanical characterization of high-temperature carbon fiber-polyphenylene sulfide composites for large area extrusion deposition additive manufacturing. *Addit. Manuf.* **2020,** *34*, 101255.
23. Melenka, G. W.; Cheung, B. K. O.; Schofield, J. S.; Dawson, M. R.; Carey, J. P., Evaluation and prediction of the tensile properties of continuous fiber-reinforced 3d printed structures. *Compos. Struct.* **2016,** *153*, 866-875.
24. Yang, C. C.; Tian, X. Y.; Liu, T. F.; Cao, Y.; Li, D. C., 3d printing for continuous fiber reinforced thermoplastic composites: Mechanism and performance. *Rapid Prototyp. J.* **2017,** *23*, 209-215.
25. Matsuzaki, R.; Ueda, M.; Namiki, M.; Jeong, T. K.; Asahara, H.; Horiguchi, K.; Nakamura, T.; Todoroki, A.; Hirano, Y., Three-dimensional printing of continuous-fiber composites by in-nozzle impregnation. *Scientific Reports* **2016,** *6*.
26. Ansari, M. Q.; Redmann, A.; Osswald, T. A.; Bortner, M. J.; Baird, D. G., Application of thermotropic liquid crystalline polymer reinforced acrylonitrile butadiene styrene in fused filament fabrication. *Addit. Manuf.* **2019,** *29*.
27. Blok, L. G.; Longana, M. L.; Yu, H.; Woods, B. K. S., An investigation into 3d printing of fibre reinforced thermoplastic composites. *Addit. Manuf.* **2018,** *22*, 176-186.
28. Donald, A. M.; Windle, A. H.; Hanna, S., *Liquid crystalline polymers*. Cambridge University Press: 2006.
29. Chae, H. G.; Kumar, S., Rigid-rod polymeric fibers. *J. Appl. Polym. Sci.* **2006,** *100*, 791-802.
30. Handlos, A.; Baird, D., Processing and associated properties of in situ composites based on thermotropic liquid crystalline polymers and thermoplastics. *Journal of Macromolecular Science, Part C: Polymer Reviews* **1995,** *35*, 183-238.
31. Crevecoeur, G.; Groeninckx, G., Morphology and mechanical-properties of thermoplastic composites containing a thermotropic liquid-crystalline polymer. *Polym. Eng. Sci.* **1990,** *30*, 532-542.
32. Chen, T.; Mansfield, C. D.; Ju, L.; Baird, D. G., The influence of mechanical recycling on the properties of thermotropic liquid crystalline polymer and long glass fiber reinforced polypropylene. *Compos. Part B Eng.* **2020,** *200*, 108316.
33. Chen, T.; Kazerooni, D.; Ju, L.; Okonski, D. A.; Baird, D. G., Development of recyclable and high-performance in situ hybrid tlcp/glass fiber composites. *J. Compos. Sci.* **2020,** *4*, 125.
34. deSouza, J. P.; Baird, D. G., In situ composites based on blends of a poly(ether imide) and thermotropic liquid crystalline polymers under injection moulding conditions. *Polymer* **1996,** *37*, 1985-1997.
35. Kiss, G., Insitu composites - blends of isotropic polymers and thermotropic liquid-crystalline polymers. *Polym. Eng. Sci.* **1987,** *27*, 410-423.
36. Siegmann, A.; Dagan, A.; Kenig, S., Polyblends containing a liquid-crystalline polymer. *Polymer* **1985,** *26*, 1325-1330.

37. Datta, A.; Baird, D. G., Compatibilization of thermoplastic composites based on blends of polypropylene with 2 liquid-crystalline polymers. *Polymer* **1995,** *36*, 505-514.
38. Chinsirikul, W.; Hsu, T.; Harrison, I.; Science, Liquid crystalline polymer (lcp) reinforced polyethylene blend blown film: Effects of counter‐rotating die on fiber orientation and film properties. *J. Polym. Eng.* **1996,** *36*, 2708-2717.
39. Sabol, E. A.; Handlos, A. A.; Baird, D. G., Composites based on drawn strands of thermotropic liquid-crystalline polymer reinforced polypropylene. *Polym. Compos.* **1995,** *16*, 330-345.
40. Saengsuwan, S.; Bualek-Limcharoen, S.; Mitchell, G. R.; Olley, R. H., Thermotropic liquid crystalline polymer (rodrun lc5000)/polypropylene in situ composite films: Rheology, morphology, molecular orientation and tensile properties. *Polymer* **2003,** *44*, 3407-3415.
41. Seppala, J.; Heino, M.; Kapanen, C., Injection-molded blends of a thermotropic liquid-crystalline polymer with polyethylene terephthalate, polypropylene, and polyphenylene sulfide. *J. Appl. Polym. Sci.* **1992,** *44*, 1051-1060.
42. Gray IV, R. W.; Baird, D. G.; Helge Bøhn, J., Effects of processing conditions on short tlcp fiber reinforced fdm parts. *Rapid Prototyp. J.* **1998,** *4*, 14-25.
43. Baird, D. G.; Sukhadia, A. Mixing process for generating in-situ reinforced thermoplastics. US5225488, 1993.
44. Postema, A. R.; Fennis, P. J., Preparation and properties of self-reinforced polypropylene liquid crystalline polymer blends. *Polymer* **1997,** *38*, 5557-5564.
45. Done, D.; Baird, D. G., Transient flow of thermotropic liquid-crystalline polymers in step strain experiments. *J. Rheol.* **1990,** *34*, 749-762.
46. Qian, C.; Baird, D. G., The transient shear rheology of a thermotropic liquid crystalline polymer in the super-cooled state. *Polymer* **2016,** *102*, 63-72.
47. Holland, B. J.; Hay, J. N., Thermal degradation of nylon polymers. *Polym. Int.* **2000,** *49*, 943-948.
48. He, X. F.; Yang, J.; Zhu, L. C.; Wang, B.; Sun, G. P.; Lv, P. F.; Phang, I. Y.; Liu, T. X., Morphology and melt rheology of nylon 11/clay nanocomposites. *J. Appl. Polym. Sci.* **2006,** *102*, 542-549.
49. Levchik, S. V.; Levchik, G. F.; Balabanovich, A. I.; Camino, G.; Costa, L., Mechanistic study of combustion performance and thermal decomposition behaviour of nylon 6 with added halogen-free fire retardants. *Polym. Degrad. Stabil.* **1996,** *54*, 217-222.
50. Levchik, S. V.; Costa, L.; Camino, G., Effect of the fire-retardant ammonium polyphosphate on the thermal-decomposition of aliphatic polyamides .3. Polyamides 6.6 and 6.10. *Polym. Degrad. Stabil.* **1994,** *43*, 43-54.
51. Qian, C.; Mansfield, C. D.; Baird, D. G., Extrusion blow molding of polymeric blends based on thermotropic liquid crystalline polymer and high density polyethylene. *Int. Polym. Process.* **2017,** *32*, 112-120.
52. Viola, G. G.; Baird, D. G., Studies on the transient shear-flow behavior of liquid-crystalline polymers. *J. Rheol.* **1986,** *30*, 601-628.
53. Sun, Q.; Rizvi, G.; Bellehumeur, C.; Gu, P., Effect of processing conditions on the bonding quality of fdm polymer filaments. *Rapid Prototyp. J.* **2008,** *14*, 72-80.
54. Bellehumeur, C.; Li, L.; Sun, Q.; Gu, P., Modeling of bond formation between polymer filaments in the fused deposition modeling process. *Journal of Manufacturing Processes* **2004,** *6*, 170-178.
55. Gao, X.; Qi, S.; Kuang, X.; Su, Y.; Li, J.; Wang, D., Fused filament fabrication of polymer materials: A review of interlayer bond. *Addit. Manuf.* **2020,** 101658.

56. Wittbrodt, B.; Pearce, J. M., The effects of pla color on material properties of 3-d printed components. *Addit. Manuf.* **2015,** *8*, 110-116.
57. Hwang, S.; Reyes, E. I.; Moon, K.-s.; Rumpf, R. C.; Kim, N. S., Thermo-mechanical characterization of metal/polymer composite filaments and printing parameter study for fused deposition modeling in the 3d printing process. *Journal of Electronic Materials* **2015,** *44*, 771-777.
58. Thomason, J. L., The influence of fibre length and concentration on the properties of glass fibre reinforced polypropylene: 5. Injection moulded long and short fibre pp. *Compos. Pt. A-Appl. Sci. Manuf.* **2002,** *33*, 1641-1652.
59. Regner, M.; Östergren, K.; Trägårdh, C. J. I.; research, e. c., Influence of viscosity ratio on the mixing process in a static mixer: Numerical study. **2008,** *47*, 3030-3036.
60. Thakur, R.; Vial, C.; Nigam, K.; Nauman, E.; Djelveh, G. J. C. e. r.; design, Static mixers in the process industries—a review. **2003,** *81*, 787-826.
61. Baird, D. G.; Robertson, C. G.; De Souza, J. P. Liquid crystalline polymer-reinforced thermoplastic fibers. US5834560, 1998.
62. ZHANG, Z.; ZHANG, W.-x., Crystallization and miscibility of polyamide tlcp/nylon66 molecular composites. *J. Mater. Eng.* **2006,** *7*, 39-42.
63. Krishnaswamy, R. K.; Baird, D. G., Wholly thermoplastic composites from woven preforms based on nylon-11 fibers reinforced in situ with a hydroquinone-based liquid crystalline polyester. *Polym. Compos.* **1997,** *18*, 526-538.
64. Mallick, P. K., *Fiber-reinforced composites: Materials, manufacturing, and design*. CRC press: 2007.
65. Chae, H. G.; Newcomb, B. A.; Gulgunje, P. V.; Liu, Y. D.; Gupta, K. K.; Kamath, M. G.; Lyons, K. M.; Ghoshal, S.; Pramanik, C.; Giannuzzi, L.; Sahin, K.; Chasiotis, I.; Kumar, S., High strength and high modulus carbon fibers. *Carbon* **2015,** *93*, 81-87.
66. Van Der Klift, F.; Koga, Y.; Todoroki, A.; Ueda, M.; Hirano, Y.; Matsuzaki, R., 3d printing of continuous carbon fibre reinforced thermo-plastic (cfrtp) tensile test specimens. *J. Compos. Mater.* **2016,** *6*, 18.

4 The Influence of Mechanical Recycling on the Properties of Thermotropic Liquid Crystalline Polymer and Long Glass Fiber Reinforced Polypropylene

The second research objective is addressed in this chapter and the manuscript was published in: **T. Chen**, C. D. Mansfield, L. Ju, D. G. Baird "The Influence of Mechanical Recycling on the Properties of Thermotropic Liquid Crystalline Polymer and Long Glass Fiber Reinforced Polypropylene", *Composites Part B* **2020**, *200*, 108316 [1]

Chapter 4 The Influence of Mechanical Recycling on the Properties of Thermotropic Liquid Crystalline Polymer and Long Glass Fiber Reinforced Polypropylene

Tianran Chen, Craig D. Mansfield, Lin Ju, and Donald G. Baird

Macromolecules Innovation Institute and Department of Chemical Engineering,

Virginia Tech, Blacksburg, VA 24061

4.1 Abstract

The effect of mechanical recycling on the properties of injection-molded polypropylene (PP) reinforced with thermotropic liquid crystalline polymer (TLCP) or long glass fiber (GF) has been investigated. The 30 and 50 wt*% in situ* TCLP and GF reinforced composites were mechanically recycled for three processing cycles, using an injection molding machine with an end-gated plaque mold. The processing temperatures used in the mechanical recycling were determined using rheological and thermogravimetric analyses to minimize the degradation of polypropylene. Recycled TLCP/PP maintained its mechanical properties, and recycling had no significant influence on its morphological, thermal, rheological, and thermo-mechanical properties. Morphological investigation illustrated the regeneration of TLCP fibrils during the mold filling process of each recycle. By the addition of maleic anhydride-grafted polypropylene (MAPP), significant improvements in the mechanical properties of TLCP/PP without impact on recyclability

were observed. In contrast, the tensile strength of 50 wt% glass fiber reinforced composite decreased 30% while the tensile modulus decreased 5% after the third recycle. Glass fiber filled polypropylene exhibited significant fiber shortening and was not able to regenerate fibers in processing. Fiber length attrition during the recycling process led to the deterioration of the mechanical properties of the recycled glass filled composites.

4.2 Introduction

A continuous increase in the usage of fiber reinforced composites has resulted in a rapid accumulation of composite material ending up in the waste stream, leading to negative environmental impacts [2, 3]. The disposal of composite waste in an environmentally friendly way has become one of the most important challenges in our society. Landfill is one of the most common disposal methods, but yet this approach has become unfavorable due to restrictive environmental legislation, loss of valuable materials, and increasing processing cost [4, 5]. In order to reduce the environmental impacts and to turn composite waste into valuable resources, significant efforts have been made to recycle and reuse the composite waste in the last two decades [3, 6, 7].

The technologies for recycling fiber reinforced composites include thermal process, solvolysis, and mechanical recycling [8-13]. Mechanical recycling consists of grinding materials into small particulates and manufacturing new parts using the ground composites [6]. Among different recycling technologies, the mechanical recycling method is favorable due to lower energy consumption, recovery of both fibers and resin, and no use of any hazardous solvents [14]. Global warming potential (GWP) of mechanical recycling of fiber reinforced composite is on average 700% lower than the solvolysis method [15].

While mechanical recycling is a cost-effective recycling method with low carbon footprint, the wide-spread application of mechanical recycling is limited due to the deterioration of the mechanical properties of recycled composites [16-21]. Because of the lower qualities of recycled composites than virgin materials, recycled materials are usually used as fillers or reinforcements in industries where the incorporation level of the reinforcement/filler is limited to under 10 wt% [6]. Eriksson *et al.* [22] studied the mechanical performance of in-plant recycled glass fiber reinforced polyamide 66. The recycled samples were prepared by a processing method of repeated grinding and injection molding. Mechanical analysis of recycled samples showed more than a 30% decrease in tensile strength and a 40% reduction in impact strength of the composite after eight recycling steps. Applying the Kelly-Tyson model [23] to the fiber length distributions of recycled composites gave good agreement with experimental tensile strength, suggesting that the decrease of mechanical properties was attributed to fiber shortening.

To mitigate the reduction of mechanical properties of recycled composites, Colucci and coworkers [24] produced a partially (50%) recycled glass fiber filled polypropylene composite by blending virgin composite with 100% recycled composite. The 50% recycled glass fiber reinforced composite exhibited 13% and 12% enhancements in tensile and flexural strength, respectively, compared to 100% recycled composite. The mechanical properties of 50% recycled composite, however, were still noticeably lower than those of virgin composite. Thermo-oxidative and thermal-mechanical degradations together with fiber breakage gave rise to the reduction of mechanical performance of recycled composites. The need for developing novel recyclable composites in the application of mechanical recycling becomes more urgent.

Thermotropic liquid crystalline polymers (TLCPs) represent a class of high-performance engineering thermoplastics, exhibiting high mechanical properties, light weight, excellent dimensional stability, and outstanding processability [25, 26]. The tensile modulus and strength of TLCPs (i.e., up to 100 GPa and 1.5 GPa, respectively, based on drawn filaments), are competitive with the mechanical properties of glass fibers (i.e., modulus ~72 GPa, strength ~3.5 GPa) [27, 28]. The density value of TLCP (~1.4 g/cm^3) is much lower compared to that of E-glass fiber (2.58 g/cm^3), indicating that the specific properties (tensile properties divided by the density) of TLCP are higher than the glass fiber [27, 29]. A material with high specific properties will be suitable for applications such as automotive and aerospace.

In order to enhance the mechanical properties of the pure matrix, TLCPs, acting as reinforcements, were directly blended with many commodity and engineering thermoplastics (e.g., polypropylene, poly(ethylene terephthalate), poly(ether ether ketone), etc.) [30-32]. These composites were known as *in situ* TLCP composites because TLCP was elongated into fibrils in processing operations such as injection molding. It was reported that TLCP fibrils were formed during the blending process of TLCPs with other thermoplastics [30, 33]. The dispersed TLCP in thermoplastics was deformed into fibrils by hydrodynamic forces (elongational and shear stresses). The deformation and breakup of the dispersed droplets in a polymer blend were mainly controlled by the viscosity ratio and capillary number [34]. Elongational flow was able to effectively deform the droplets over a greater range of viscosity ratios than the shear flow field.

The generated TLCP fibrils were considered to enhance the mechanical properties of thermoplastic materials. For instance, polyether sulfone (PES) was melt blended in an

extruder with TLCP, and the *in situ* 30 wt% TLCP/PES extruded strand showed a five-time increase in tensile modulus and a two-time improvement in tensile strength as compared to neat PES [33]. Additionally, highly oriented fibers were observed under a scanning electron microscope (SEM). De Souza and Baird [35] reported the generation of *in situ* TLCP composites based on the blends of partially miscible TLCP with poly(ether imide) (PEI) using the injection molding process. At 30 wt% TLCP reinforcement, the tensile modulus of TLCP/PEI was 8.7 GPa, where the tensile modulus of neat PEI was only 3 GPa. SEM demonstrated the skin-core morphological structure of TLCP/PEI composite. The elongational flow from the advancing front led to the formation of fibrils in the skin layer.

In addition to comparing TLCP composites to pure matrices, it is important to evaluate the properties of *in situ* TLCP composites as compared to conventional glass fiber reinforced materials. Bafna *et al.* [36] compared the mechanical properties of PEI reinforced with 30 wt% TLCP to short glass fiber reinforced PEI. The composites were prepared by the injection molding process. The tensile modulus of *in situ* TLCP composite (9.8 GPa) was found to be competitive with glass fiber reinforced PEI (9.2 GPa) at same fiber weight fraction. The tensile strength of TLCP composite (152 MPa) was not as high as that of the glass filled composite (170 MPa). Handlos *et al.* [30] performed injection modeling of 20 wt% TLCP reinforced poly(ethylene terephthalate) (PET) and compared its properties to those of a 20 wt% glass fiber/PET. The tensile modulus and tensile strength of TLCP/PET were 8.87 GPa and 96.6 MPa, respectively, and 20 wt% glass fiber/PET composite exhibited the tensile modulus and strength of 7.02 GPa and 107.8 MPa, respectively. Thus, the potential of *in situ* TLCP composites to compete with glass fiber reinforced thermoplastics has been demonstrated.

To further enhance the mechanical performance of TLCP reinforced composites, compatibilizing agents were used to promoting interfacial adhesion of incompatible blends such as polypropylene (PP) and TLCP [37, 38]. The poor adhesion between PP and TLCP was mitigated by the addition of maleic anhydride-grafted polypropylene (MAPP). MAPP enhanced the interfacial adhesion and reduced the interfacial tension, leading to a finer dispersion and uniform distribution of TLCP. O'Donnell and Baird [39] found that the addition of MAPP to TLCP/PP blends resulted in a significant improvement in both modulus and strength as compared to those of uncompatibilized blends. At 30 wt% TLCP with addition of MAPP, the tensile modulus of the composite increased from 3.0 GPa to 4.1 GPa, and the tensile strength improved from 19.7 to 37.6 MPa. Compatibilized TLCP/PP exhibited decreased interfacial tension and higher adhesion, which resulted in a fiber dispersion of TLCP within the matrix and higher mechanical performance.

Even though extensive investigations have been carried out on the processing of TLCP reinforced composites, only a few studies involved the recycling of TLCPs or their composites [40-42]. Bastida *et al*. [40] reported the effect of mechanical reprocessing on the structure and mechanical properties of pure TLCPs. Despite the overall tendency of decreasing the tensile properties with increasing number of reprocessing cycles, the tensile modulus and strength of TLCPs did not change significantly within the third recycling step. The influence of mechanical recycling had a stronger effect on the mechanical properties of copolyesteramide TLCP than copolyester TLCP due to structural changes coupled with the decrease in molecular weight and degree of crystallinity.

To investigate the influence of mechanical recycling on the properties of *in situ* TLCP reinforced composite, two recycling routes were utilized to prepare recycled *in situ*

TLCP/polycarbonate (PC) [41]. One was first recycling neat TLCP resin, and then recycled TLCP was blended into virgin PC. The other was the direct mechanical reprocessing of the TLCP reinforced PC composite up to four times. The recycled TLCP/virgin PC maintained the tensile modulus regardless of the number of recycling steps and only decreased in tensile strength at the first recycling step. In comparison, significant decreases in both the tensile modulus and strength of recycled TLCP/PC have been seen. The decrease in the performance of recycled TLCP/PC composite mainly ascribed to the degradation of polycarbonate rather than the TLCP.

To recover TLCP from a TLCP filled composite, Collier and Baird [42] developed a novel reclamation process to recycle TLCP. This process consisted of reactive extrusion and selective dissolution to separate TLCP and PP with the absence of organic solvent. More than 70 wt% TLCP could be reclaimed from the PP matrix with a purity of 97%. When the neat TLCP was partially replaced with recycled TLCP, no loss in mechanical properties of injection-molded *in situ* TLCP/PP composites was observed.

In view of the importance of developing recyclable composite and extremely scarce research work on recycling TLCP composites, it is of great interest to study the recyclability of TLCP/PP composites using mechanical recycling. It remains unknown whether TLCP/PP has greater recyclability than glass fiber reinforced polypropylene. In order to explore the potential of TLCP composite material in reducing composite waste and replacing glass fiber composite in a variety of applications, the recyclability and performance of TLCP composite must be compared against the benchmark glass fiber filled polypropylene. In this work, we report a systematic investigation of the influence of mechanical recycling on the mechanical, thermal, morphological, rheological, and thermo-

mechanical properties of *in situ* TLCP/PP and long glass fiber reinforced polypropylene. The number of recycles is selected to be three because the properties of TLCP do not change much within the third recycling step [40]. The processing temperature of recycling TLCP/PP was optimized to minimize the degradation of polypropylene using rheological and thermogravimetric analyses. It was also desired to determine whether MAPP could enhance the mechanical properties of TLCP/PP without influencing the recyclability

4.3 Experimental

4.3.1 Materials

The TLCP used for this study is a copolyesteramide consisting of 6-hydroxy-2-naphthoic acid (60 mol%), terephthalic acid (20 mol%) and aminophenol (20 mol%). The TLCP is provided by Celanese and is referred to as Vectra B950. The TLCP has a density of 1.4 g/cm^3 and a melting point around 280°C [43]. Long glass fiber (GF) reinforced polypropylene pellets were supplied by SABIC with 30 and 50 wt% of reinforcement. The pellets are 8 mm long and contain glass fibers of similar length. Injection molding grade polypropylene (PP) with a commercial name Pro-fax 6523 was supplied by LyondellBasell, which has a density of 0.9 g/cm^3. Maleic anhydride-grafted polypropylene (MAPP) was provided by Chemtura.

4.3.2 Mechanical Recycling of the Composites

The mechanical recycling of the composites was achieved by multiple injection molding and grinding processes. The content of the reinforcement was selected to be 30 or 50 wt%. Pellets of GF/PP were dried in a vacuum oven at 80°C for at least 24 hours. End-gate

plaques, approximately 80 mm long by 76mm wide by 1.5 mm thick, were injection molded using a BOY 35E machine. GF/PP pellets were injection molded with the manufacturer's recommended processing conditions, where the barrel temperature was set at 250°C and the mold temperature was 60°C [44]. A granulator (Cumberland/John Brown D-99050) was used to shred the injection-molded plaques into fine particulates. The particulates of GF/PP were dried again in a vacuum oven at 80°C for 24 hours before re-injection molding and re-grinding. This process was repeated three times and each reprocessing cycle was designated as re-0, re-1, re-2 and re-3, where re-0 was the first processing step involving the virgin material.

To recycle the TLCP reinforced composite, TLCP and PP (or PP/MAPP) were first blended in a single screw extruder at 290°C with a 1-inch diameter screw and L/D = 24. The blend material was extruded through a 3 mm capillary die (L/D=20), and then the composite strand was quenched in a water bath and pelletized into around 6 mm long pellets. The mechanical recycling of *in situ* TLCP filled composites was carried out in the same recycling scheme as glass fiber reinforced composite except for the processing temperature which was optimized to be 290°C. The blend containing MAPP was prepared by extruding PP with MAPP in the single screw extruder at 250°C; and then PP/MAPP was pelletized and mixed with TLCP in the same extruder at 290°C. The MAPP content in TLCP/PP/MAPP was kept as 10 wt%. Specimens were randomly selected from recycled composites for various characterization tests.

4.3.3 Thermal Stability Measurements of Polypropylene at Processing Temperature

A rheometer (TA Instruments ARES-G2) was used to analyze the thermal stability of PP at 250, 290 and 300°C using the small amplitude oscillatory time sweep mode. PP resin was dried in a vacuum oven at 80°C for 24 hours before running the rheological measurements. Pellets were loaded between parallel plate fixtures at the designated temperature under nitrogen. The complex viscosity was monitored over time with 1% strain and 10 rad/s angular frequency.

Isothermal thermogravimetric analysis (TA Instruments Q50) was performed on polypropylene resin at 290 and 300°C under the nitrogen atmosphere. The sample was heated up from room temperature to the testing temperature at 20°C/min. Then weight loss of the specimen was tracked as a function of time.

4.3.4 Mechanical Properties

Approximately 75 mm long by 8 mm wide strips were cut along the flow and transverse directions from the injection molded end-gate plaques. All tensile properties of the composites were measured by an Instron mechanical tester (Model 4204) with a 5 KN load cell. The cross-head speed was maintained at 1.27 mm/min, and the deformations of the specimens were measured with an extensometer (MTS 634.12). The tensile properties of each material were calculated by the average properties of at least five samples.

4.3.5 Fiber Length Measurement

To characterize the fiber attrition in recycling process, composite samples were burned in a muffle furnace at 500°C, and a mat of glass fibers remained. A small portion of fibers

was extracted from the mat of fibers with a needle coated by a thin layer of epoxy. The epoxy was burned off in the furnace at 500°C. Lengths of fiber were characterized by scanning fibers with a desktop scanner, and then were measured using image analysis software (ImageJ). More than 1000 of glass fibers were measured. Details of the fiber length measurement procedure were described in the reference [45].

4.3.6 Micro-mechanical Modeling

To investigate the structure-property relationship of glass fiber composite after recycling, micro-mechanical modeling was utilized to predicate the tensile modulus and strength of recycled GF/PP composites. The stiffness of recycled composites was predicated using the Cox-Krenchel model [46, 47]. The modified Kelly-Tyson model was used to estimate the tensile strength of recycled fiber reinforced composites [23, 48, 49].

4.3.7 Morphological Properties

The morphologies of recycled GF/PP, TLCP/PP/MAPP, and TLCP/PP were examined by scanning electron microscope (SEM). Specimens were fractured along the transverse direction in the liquid nitrogen, and then sputter coated with 10 nm thick gold. The fracture surface of each sample was characterized by a LEO (Zeiss) 1550 SEM with an accelerating voltage of 5 kV.

4.3.8 Thermal Properties (Differential Scanning Calorimetry (DSC) and Thermogravimetric Analysis (TGA))

A DSC (TA Instruments Discovery) was used to examine the thermal properties of recycled composites. Under nitrogen atmosphere, samples were subjected to a heat/cool/heat cycle. Samples were first equilibrated at 30°C for 5 min and then heated up to 250°C at 10°C/min.

The materials were cooled down to -50°C at -10°C/min, and then heated back to 250°C at 10°C/min. The glass transition temperature (T_g), melting temperature (T_m), and enthalpy of melting (ΔH_m) were determined by a TA Instruments TROIS software.

Thermal stabilities of recycled composites were analyzed by thermogravimetric analyzer (TA Instruments Q50) under nitrogen environment with a heating rate of 10°C/min and a temperature range of 50 to 700°C. The samples were equilibrated at 50°C for 5 min before starting the heating ramp.

4.3.9 Rheological Properties

Rheological tests were carried out at 290°C under nitrogen using a rheometer (TA Instruments ARES-G2) to investigate the influence of mechanical recycling on the viscosity of composite blends. The small amplitude oscillatory frequency sweep mode was used with an angular frequency range from 0.5 to 500 rad/s and 1% strain.

4.3.10 Thermo-mechanical Properties

To investigate how mechanical recycling affects the thermo-mechanical properties of the injection-molded plaques, dynamic mechanical thermal analysis (DMTA) was performed using a rheometer (ARES-G2). Rectangular strips were cut from injection-molded plaques along the flow direction, and samples were clamped between rectangular torsion fixtures. DMTA was carried out in a nitrogen atmosphere with a heating rate of 2°C/min, and a temperature range of -50 to 170 °C was selected.

4.4 Results and discussion

4.4.1 Optimization of the Processing Temperature of TLCP/PP Composites

The thermal stability of polypropylene at elevated temperature is examined, because, in order to generate *in situ* TLCP reinforced polypropylene, PP is directly melt blended with TLCP at the processing temperature which is above the melting point of the TLCP (T_m~280°C) [43, 50]. A parallel plate rheometer was operated in the small amplitude oscillatory time sweep mode under nitrogen. The evaluation of complex viscosity, $|\eta^*|$, of polypropylene as a function of time is shown in Fig. 4.1. $|\eta^*|$ of PP gradually decreases with time at 290 and 300°C. The residence time of overall recycling processes using the injection molding machine is around 12 minutes. $|\eta^*|$ of PP decreases by ~52% in 12 minutes at 300°C (Fig. 4.1). The thermal degradation of PP through chain scission leads to a decrease in viscosity. The rate of decrease of the $|\eta^*|$ at 300°C is much more rapid than at 290°C (Fig. 4.1). Blending PP with TLCP at 290°C can mitigate the severe thermal degradation of polypropylene. 250°C is the manufacturer's recommended injection molding processing temperature of GF/PP pellets. At this temperature, $|\eta^*|$ of PP stays constant, thereby suggesting that the thermal degradation of PP is negligible, as shown in Fig. 4.1 [44]. The processing temperature of recycling GF/PP is selected to be 250°C.

In addition to characterizing the thermal degradation of polypropylene by rheological analysis, isothermal TGA was used to investigate the thermal stability of PP at 290 and 300°C, as indicated in Fig. 4.2. Under a nitrogen atmosphere, the weight loss of polypropylene at 300°C is about 3%, and the weight change at 290°C is minimal, within 12 minutes. At 300°C, the weight loss of polypropylene resin indicates the formation of volatile degraded products, which may result in the poor mechanical properties of the final

products. Ballice and Reimer [51] investigated the thermal degradation of polypropylene, and the organic volatile products generated from thermal degradation were identified with gas chromatography/mass spectrometry. A noticeable degradation of PP began at 300°C. The major volatile organic compounds evolved from the thermal decomposition of polypropylene were 2-methyl-4-octene, 2-methyl-2-octene, 2-4 dimethyl-1-heptene, etc. The emission of volatile organic compounds may deteriorate the performance of materials. Based on the results of isothermal time sweep rheological test and TGA, the injection molding processing temperature of TLCP filled composites is selected to be 290°C.

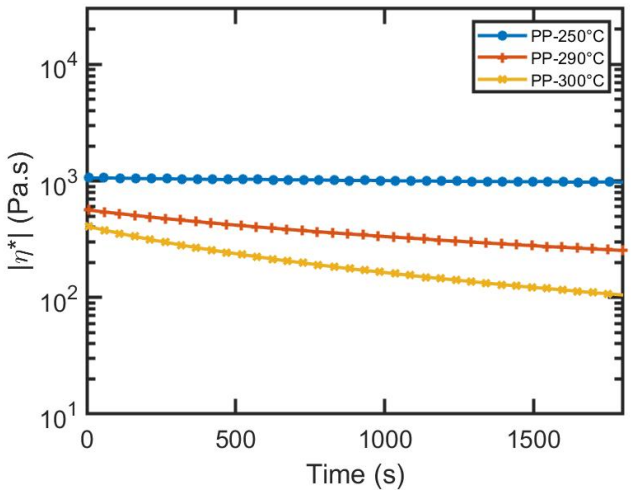

Figure 4. 1: The change of complex viscosity (|η*|) of polypropylene as a function of time under a nitrogen atmosphere

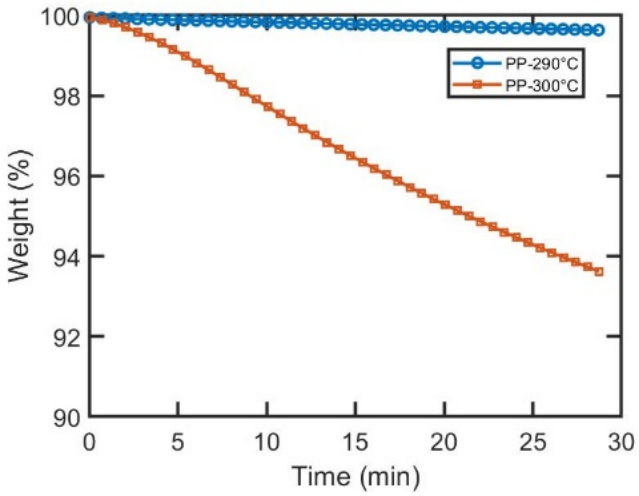

Figure 4. 2: Isothermal TGA of polypropylene at 290 and 300°C under a nitrogen atmosphere

4.4.2 Tensile Properties of Recycled Composites

Tensile tests of the first injection-molded (re-0) composite samples are carried out to assess the mechanical performances of these composites. The tensile properties of

TLCP/PP/MAPP, TLCP/PP, GF/PP, TLCP, and PP in the flow direction are presented in Table 4.1. By blending TLCP or GF with polypropylene, significant enhancements in the tensile properties of the composites are observed. The stiffness of composites is improved by six-fold with the addition of 50 wt% TLCP or glass fiber. The reinforcements also effectively enhance the tensile strengths of the composites. The tensile strength of the composite is improved 114% by blending 50 wt% TLCP. The incorporation of 50 wt% long glass fiber into polypropylene enables more than three times enhancement in the tensile strength of the composite. Glass fiber improves the tensile strength of the PP composite more than that of TLCP/PP composite. GF has a higher tensile strength (~3.5 GPa) than that of TLCP (~0.5 GPa) resulting in the difference in the level of reinforcement of injection molded composites [52, 53]. 30 wt% TLCP and glass fiber also enhance the mechanical properties of polypropylene as shown in Table 4.1.

Table 4.1 includes the specific tensile property of each material. The specific property was calculated through dividing the tensile property of each material by its density. By adding TLCP or glass fiber, the specific tensile properties of the polypropylene composites are increased appreciably. Materials with high strength-to-weight ratios have been widely employed for automotive and aerospace applications. The density of glass fiber is almost two times higher than those of the TLCP. The specific modulus of 50 wt% TLCP/PP/MAPP composites is 27% higher than that of glass fiber reinforced polypropylene, and the specific tensile strengths of 50 wt% TLCP/PP/MAPP are 17% lower than those of 50 wt% GF/PP.

To evaluate the performance of TLCP/PP composites in flow direction, the tensile modulus is predicted by the Halpin-Tsai equation [54]. The equation is simplified by assuming an

infinite fiber aspect ratio. The experimental tensile moduli of injection-molded pure TLCP and PP are used in the prediction. The tensile modulus of 30 wt% and 50 wt% TLCP/PP is lower than the predicted tensile modulus (~4.75 GPa and ~7.6 GPa, respectively). The Halpin-Tsai model assumes perfect adhesion between fiber and matrix, which is most likely not true for the TLCP and PP due to the incompatibility between the polymers.

To overcome the problem of incompatibility and poor adhesion and further improve the mechanical properties of TLCP reinforced polypropylene, maleic anhydride-grafted polypropylene (MAPP) is introduced. MAPP is able to enhance the interfacial adhesion of the blend and improve the compatibility between PP and TLCP [37]. From Table 4.1, the addition of MAPP increases the tensile modulus by 15% and the tensile strength by 21% as compared to the uncompatibilized 50 wt% TLCP/PP. In addition, the tensile modulus (~8.21 GPa) of TLCP/PP/MAPP is higher than that predicated by the Halpin-Tsai equation (~7.6 GPa). MAPP reduces the interfacial tension, leading to a finer dispersion, better adhesion and uniform distribution of TLCP, which improves the mechanical properties [39]. The comparison of morphological properties between TLCP/PP/MAPP and TLCP/PP will be discussed in the morphological subsection.

The mechanical properties of recycled TLCP/PP/ MAPP, TLCP/PP, and GF/PP (re1 to re3) in the flow direction are included in Fig. 4.3. After three reprocessing cycles, 50 wt% TLCP/PP/MAPP and TLCP/PP retain their tensile modulus and strength. Repeated mechanical recycling has no negative impact on the tensile properties of the TLCP filled composites. 30 wt% TLCP/PP also maintains tensile properties after recycling. The *in situ* TLCP/PP blend is capable of generating TLCP fibrils, where dispersed TLCP droplets are elongated into fibrils during polymer processing operations especially when the process

involves elongational flow [30]. During the injection molding process, TLCP fibrils are generated by elongational flow at the advancing front [55]. The generation of highly oriented TLCP fibrils at each recycling process enables the recycled composite with the level of reinforcement that is similar to virgin composite. Additionally, the regeneration of TLCP fibrils eliminates fiber breakage issue which has been commonly observed in the processing of glass or carbon fiber reinforced composites. The morphological characterization of TLCP/PP composites illustrates the regeneration of TLCP fibrils, which will be discussed in the morphological subsection.

On the other hand, mechanical recycling exerts a strong influence on the mechanical properties of glass fiber filled polypropylene, in which the tensile strength of 50 wt% GF/PP drops by 30% and the tensile modulus decreases from 7.8 to 7.4 GPa after the third reprocessing cycle. The tensile modulus and strength of 30 wt% GF/PP decrease from 5.2 to 4.5 GPa and 71.6 to 44.9 MPa, respectively. It is speculated that the decrease in the tensile properties of GF/PP with the increasing number of processing cycles is attributed to fiber attrition. In the composite theory, the aspect ratio (L/D) of fiber affects the mechanical properties of composites. Long fiber reinforced composites are able to achieve higher mechanical performance than short fiber reinforced composites [56]. Decreasing of fiber length in the final product usually decreases the stiffness, strength, and impact properties of composites [57]. Fiber length and micro-mechanical modeling are used to investigate the structure-property relationship of recycled GF/PP, which will be discussed in the next subsection.

Injection-molded end-gate plaques provide the information of properties of specimens in both flow and transverse directions. Fig. 4.4 demonstrates the mechanical performance of

recycled composites in the transverse direction. TLCP filled composites show little or no change in the tensile modulus and strength during three recycling steps. TLCP/PP/MAPP exhibits higher mechanical properties than TLCP/PP composites in the transverse direction. Thus, MAPP can enhance the mechanical properties of TLCP/PP in the flow and transverse directions. For the 50 wt% glass filled polypropylene, the tensile modulus decreases by 14% and the tensile strength drops from 41.4 to 24.5 MPa after three reprocessing cycles. Mechanical recycling also leads to a significant decrease in mechanical properties of 30 wt% GF/PP in transverse direction (Fig. 4.4).

Overall, the mechanical properties of TLCP reinforced composites are not influenced by recycling, but mechanical recycling has a strong negative effect on the mechanical properties of glass fiber filled polypropylene. The influence of mechanical recycling on the recycled 30 wt% GF/PP or 30 wt% TLCP/PP is very similar to those of 50 wt % GF/PP or 50 wt% TLCP/PP as shown in Figs. 4.3 and 4.4. The following discussions only compare the properties of 50 wt% TLCP/PP to GF/PP composite.

Table 4. 1: Tensile properties of the initial injection molded materials (re0) in the flow direction

Polymer	Modulus (GPa)	Specific Modulus ($Pa/(kg/m^3)$)*10^6	Strength (MPa)	Specific Strength ($Pa/(kg/m^3)$) *10^4
50 wt% TLCP/PP/MAPP	8.21 (±0.255)	7.46	53.09 (±1.91)	4.83
5350 wt% TLCP/PP	7.12 (±0.23)	6.47	43.96 (±1.64)	4.00

50 wt% GF/PP	7.84 (±0.37)	5.89	83.54 (±1.98)	6.29
30 wt% TLCP/PP	3.83 (±0.13)	3.80	30.64 (±0.66)	3.03
30 wt% GF/PP	5.21 (±0.34)	4.65	71.62 (±5.55)	6.39
TLCP	17.53 (±1.16)	12.52	130.5 (±8.05)	9.32
PP	1.23 (±0.06)	1.37	20.5 (±0.31)	2.28

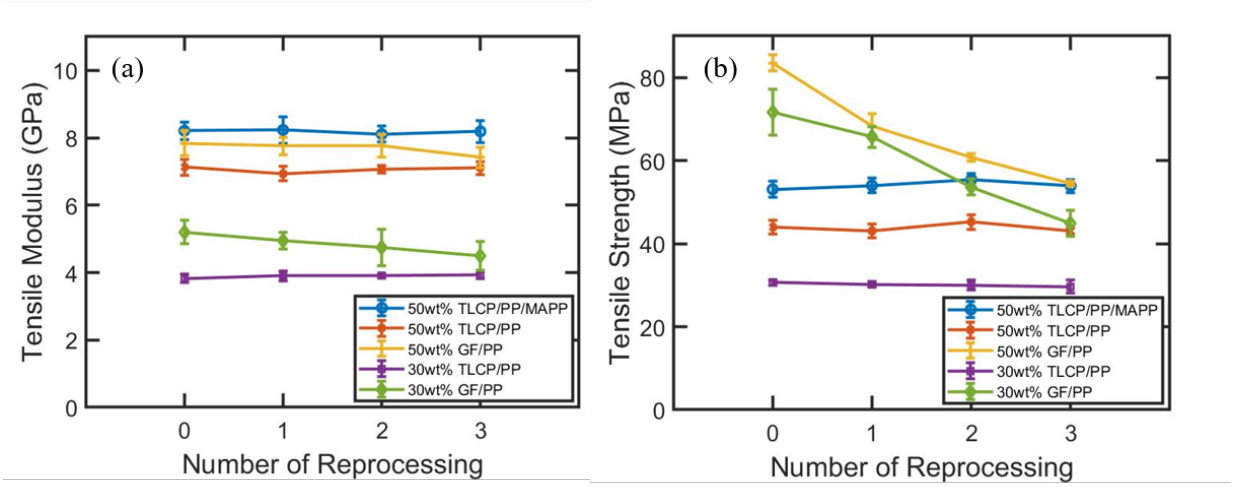

Figure 4. 3: Tensile properties of recycled TLCP/PP/MAPP, TLCP/PP, and GF/PP versus number of recycle steps in flow direction (a) tensile modulus; (b) tensile strength.

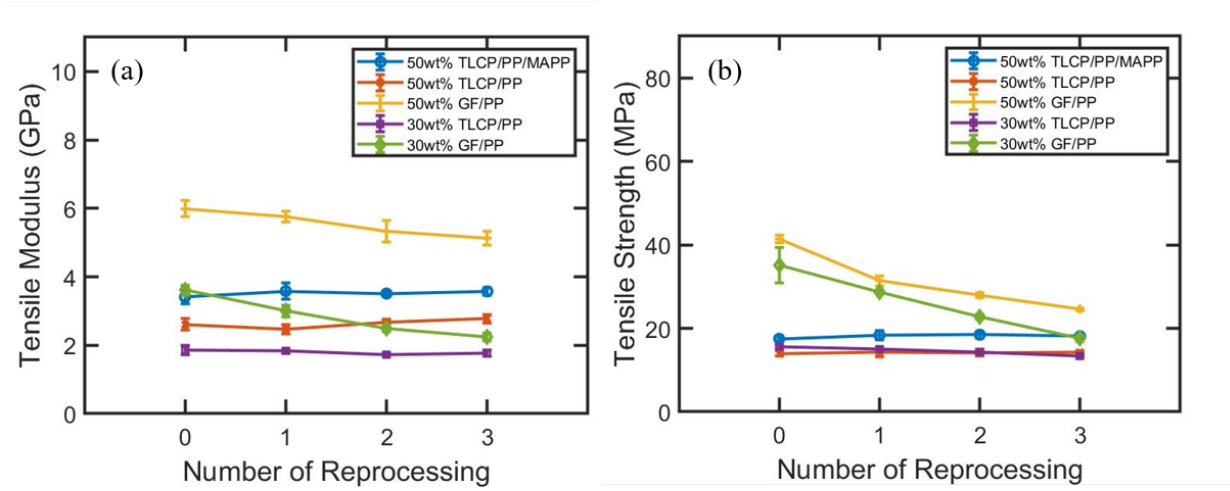

Figure 4. 4: Tensile properties of recycled TLCP/PP/MAPP, TLCP/PP, and GF/PP versus number of recycle steps in transverse direction (a) tensile modulus; (b) tensile strength.

4.4.3 Fiber Length and Micro-mechanical Modeling

After the injection molding process, fibers in the final part are not uniform in length. To investigate the influence of fiber attrition on the mechanical properties of glass filled composite, fiber length distributions of recycled GF/PP were quantified. The procedure of fiber length measurement is described in the experimental section. Fig. 4.5 shows the cumulative frequency of fibers as a function of fiber length of recycled 50 wt% glass fiber composites. The initial fiber length of glass fiber is around 8.0 mm. Severe fiber breakage occurs during the first injection molding cycle (re0), in which more than 90% of the fibers are shorter than 2 mm. Repeated injection molding and grinding lead to a much narrower distribution as compared to re0-GF/PP. For instance, 90% of the fibers of re3-GF/PP are shorter than 0.55 mm. Table 4.2 lists the number average (L_n) and weight average (L_w) of the fiber lengths of recycled GF/PP. Just one injection molding process results in the L_w of 1.83 mm. L_n and L_w keep decreasing with the increase of recycling number. In the 3rd reprocessing cycle, the reduction in the L_w is 74% as compared to re0-GF/PP. There is considerable fiber attrition during melt processing due to fiber-polymer interaction, fiber-fiber interaction, and fiber-processing equipment interaction. Researchers have observed the fiber shortening when recycling glass fiber/thermoplastic composites using mechanical reprocessing [19, 20, 22, 58].

By utilizing fiber length information of recycled GF/PP, tensile modulus and strength in flow direction are predicted by the Cox-Krenchel and the modified Kelly-Tyson model, respectively [23, 46, 56]. In Fig. 4.6, experimental tensile data are compared with computational modeling. Micro-mechanical models show good agreement with experimental results. Predicted tensile modulus and strength follow a similar trend that the properties increase with increasing fiber length. Mechanical properties increase slowly at the short fiber length region, followed by exponential growth at intermediate fiber length and eventually a plateau at the long fiber length region. The experimental value of both tensile modulus and strength decrease with the increasing number of reprocessing cycles. However, mechanical recycling has more impact on the tensile strength than the tensile modulus of recycled composites. 50 wt% GF/PP decreases 35% in tensile strength and 5% in tensile modulus after three recycling steps. This phenomenon may be explained by the different fiber lengths at rapid change on the Cox-Krenchel and Kelly-Tyson modeling curves. For tensile modulus, the maximum rate of decrease is around 0.2 mm. The weight average fiber lengths of recycled glass fiber composite are much higher than this value. Experimental tensile data fall into the upper region of the theoretical curve of tensile modulus, where tensile modulus is less sensitive to the change of fiber length. On the other hand, the steepest decrease of tensile strength on the modeling curve is about 1.4 mm. The weight average fiber lengths of recycled GF/PP are around this fiber length region. Therefore, tensile strength will be significantly impacted by decreasing fiber length. The good agreement between experimental data and micro-mechanical models suggests that fiber breakage is the major factor leading to deterioration in mechanical properties of glass fiber composite.

Deviations between predictions and experimental results of re0-GF/PP have been observed. Fiber bundles and fiber curvatures, which are not considered by the models, could reduce the effective fiber length, resulting in over-predication of mechanical properties for the first injection-molded composite [59, 60]. With the increasing number of recycling steps, the effect of fiber bundle and fiber curvature on the mechanical performance is mitigated through better dispersion of fibers and fiber shortening. Thus, theoretical predictions become more accurate for the properties of re1 to re3-GF/PP.

In conclusion, theoretical predictions are in agreement with the tensile properties of recycled glass fiber composites. Tensile modulus and strength decrease with the decreasing fiber length. Because the specific fiber length at the maximum rate of change of properties depends on the specific property, different extents of impact by recycling on the modulus and strength are observed in the experiment. The structure-property relationship of recycled GF/PP composites is successfully analyzed by micro-mechanical modeling.

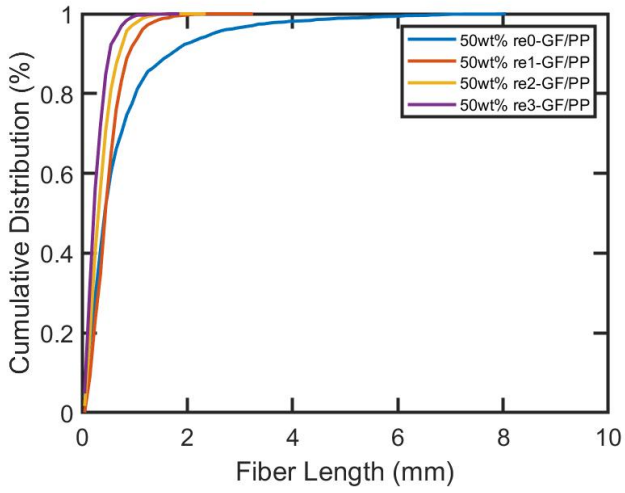

Figure 4. 5: Fiber length distributions of recycled 50 wt% glass fiber reinforced polypropylene

Table 4. 2: Number and weight average fiber lengths (mm) of recycled 50 wt% GF/PP

No. Recycle	0	1	2	3
L_n (mm)	0.792	0.487	0.412	0.346
L_w (mm)	1.829	0.644	0.548	0.465

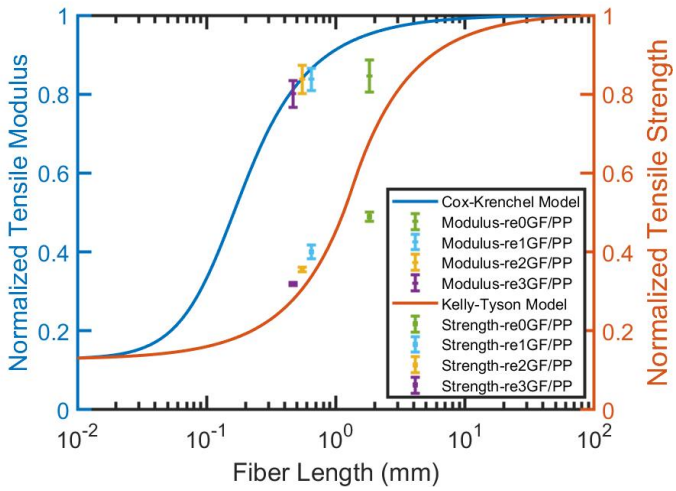

Figure 4. 6: Micro-mechanical predictions versus experimental mechanical properties of recycled 50 wt% GF/PP

4.4.4 Morphological Properties

To reveal the major factor which leads to the difference in mechanical performance of recycled composites, morphological properties of recycled TLCP and glass fiber reinforced polypropylene were analyzed by scanning electron microscopy (SEM). Fig. 4.7 shows the fracture surfaces of 50 wt% TLCP/PP and GF/PP. Samples were prepared by directly injecting the composite materials into the atmosphere. A large number of glass fibers are

present in the glass fiber reinforced composite sample, as shown in Fig. 4.7(a). Conversely, TLCP forms a spherical shape in the blend, as presented in Fig. 4.7(b). TLCP droplets cannot effectively reinforce the matrix compared to fibrils. The formation of TLCP fibrils usually occurs under strong elongational flow. Consequently, before the TLCP blend was injected under high pressure into the mold cavity, TLCP appears to be large and undeformed droplets in the matrix, while glass fiber composite exists as a fiber-matrix structure.

In the molding filling process, complex flow fields result in a skin-core morphology of injection molded parts [39, 55, 61]. For fiber filled systems, the skin layer contains highly oriented fibers, aligned parallel to the flow direction due to strong elongational flow developed at the melt front. The elongational flow moves fibers from the core region to walls where fibers quickly freeze along the cold mold wall and lock down their orientations. The core region consists of transversely oriented fibers. Because as fiber/polymer blend spreads to fill the mold cavity at the initial filling process, a strong expanding flow tends to orientate fibers in the transverse direction. The SEM images of re0 and re3 of each composite are shown in Fig. 4.8. All the samples were fractured along the transverse direction. The skin-core morphologies have been seen in all specimens. The skin-core structures of re0-GF/PP, re0-TLCP/PP/MAPP, and re0-TLCP/PP are shown in Figs. 4.8(a)-(b), (e)-(f), and (i)-(j), respectively. In the skin region, glass fibers align along the main direction of flow (Fig. 4.8(a)). The core region of re0-GF/PP with fibers oriented transversely to the flow direction is exhibited in Fig. 4.8(b). In Fig. 4.8(c) and (d), the re3-GF/PP composite shows a similar skin-core morphology.

TLCP filled composites also exhibit skin-core structures with or without MAPP. In the uncompatibilized TLCP/PP blend, the TLCP phase forms ribbons and fibers in the skin, as indicated in Fig. 4.8(i). In contrast, TLCP/PP/MAPP exhibits finer and uniform dispersion of TLCP, and individual fibrils can be identified, as shown in Fig. 4.8(e). The finer TLCP fibrils with more even distribution lead to higher level of reinforcement, thereby confirming that TLCP/PP/MAPP has better mechanical properties than the TLCP/PP composite. In Figs. 4.8(f) and 4.8(j), the core regions of TLCP filled composites exhibit large droplets and transversely oriented fibers.

To investigate how TLCP reinforced composites are able to maintain their tensile properties at each recycling step, morphologies of TLCP/PP before injection molding, re0-TLCP/PP, and re3-TLCP/PP are compared. As observed in Fig. 4.7, TLCP forms undeformed droplets before being injected into the mold. All the fibrils which appear in the injection-molded samples (Figs. 4.8(e) and (i)) are generated during the mold filling process. When TLCP is remelted and reprocessed using injection molding, it is able to regenerate highly oriented fibril structures, resulting in high stiffness and strength composite. Figs. 4.8(g) and (k) exhibit the appearance of fibrils in the skin regions of re3-TLCP/PP/MAPP and TLCP/PP. The appearance of TLCP fibrils in the SEM images confirms the regeneration of fibrils after recycling. In conclusion, the regeneration of fibrils enables the high level of reinforcement, and thereby recycled TLCP reinforced composites are as strong as virgin material. However, recycled glass fiber filled composite suffers fiber breakage and is not able to regenerate fibers during the injection molding process, leading to the loss of mechanical performance.

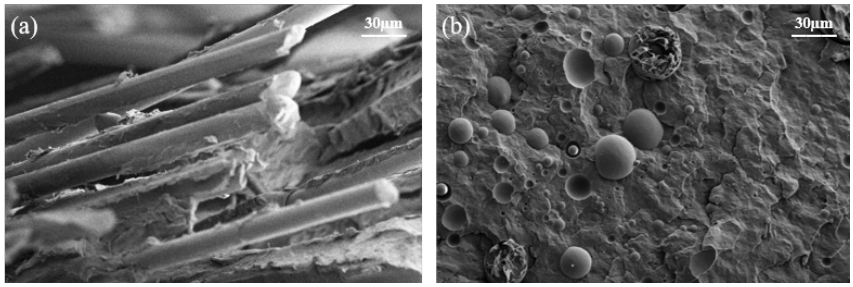

Figure 4. 7: SEM images of 50 wt% GF/PP and TLCP/PP. Samples were prepared by injection molding into air: (a) GF/PP (b) TLCP/PP.

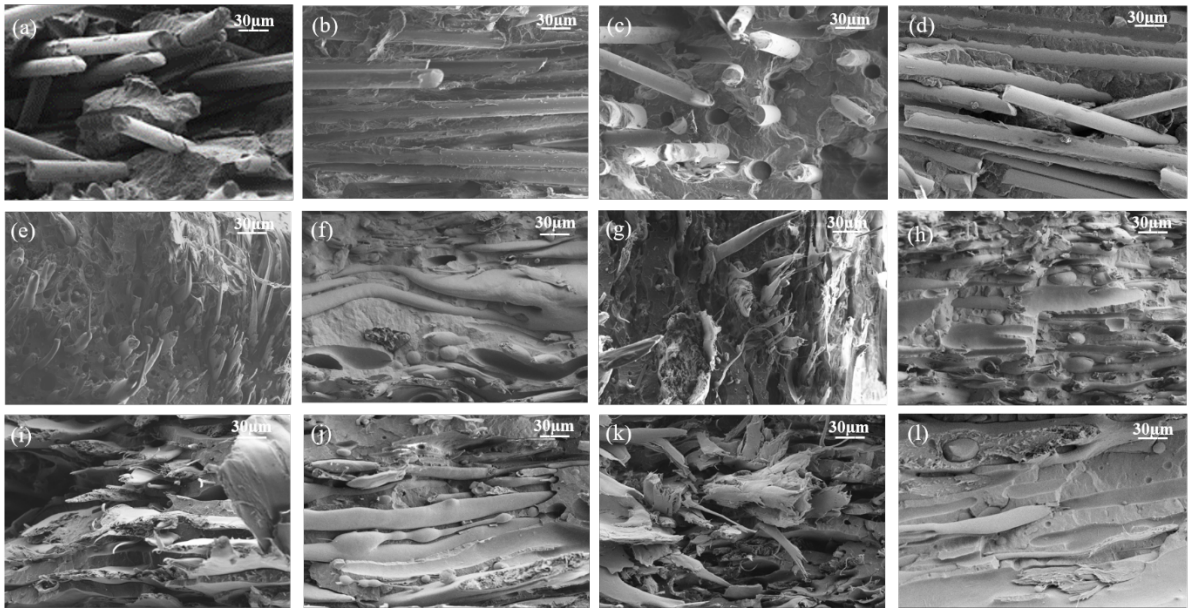

Figure 4. 8: SEM micrographs of skin and core of recycled 50 wt% GF/PP, TLCP/PP/MAPP and TLCP/PP. Samples were injected into mold (a) skin re0-GF/PP; (b) core re0-GF/PP; (c) skin re3-GF/PP; (d) core re3-GF/PP; (e) skin re0-TLCP/PP/MAPP; (f)

core re0-TLCP/PP/MAPP; (g) skin re3-TLCP/PP/MAPP; (h) core re3-TLCP/PP/MAPP; (i) skin re0-TLCP/PP; (j) core re0-TLCP/PP; (k) skin re3-TLCP/PP; (l) core re3-TLCP/PP.

4.4.5 Thermal Properties

DSC and TGA were used to examine the thermal properties of recycled materials. Because the thermal behavior of TLCP/PP/MAPP and TLCP/PP is very similar, the following discussion will focus on comparing the thermal properties of TLCP/PP/MAPP and GF/PP. Figs. 4.9 and 10 show the second heating and first cooling curves of recycled 50 wt% GF/PP and TLCP/PP/MAPP. Samples were first heated to 250°C at 10°C/min, cooled down to -50°C at -10°C/min, and reheated from 0 to 250°C at 10°C/min. The upper temperature limit of DSC was selected to be 250°C to avoid any thermal degradation of polypropylene during experiments and damaging the machine. In Fig. 4.9, the second heating curves of re0 and re3 GF/PP display similar glass transition temperatures (T_g) of PP at -12°C. The glass transition of polypropylene, in recycled TLCP filled composites, is also around -12°C shown in Fig. 4.9. The glass transition temperature of PP in both composites is unaffected by the recycling numbers. The endothermic peak, at 160°C, is corresponding to the melting point (T_m) of polypropylene (Fig. 4.9). There is no significant change of T_m as a function of the increasing number of reprocessing cycles for both composites. From the first cooling scans of recycled composites, the exothermic peaks of GF/PP and TLCP/PP/MAPP are 120°C and 117°C, respectively as shown in Fig. 4.10. No change in T_c was observed after three reprocessing cycles. The degrees of crystallinity (X_c) of GF/PP and TLCP/PP/MAP were calculated from the area under the melting endotherm with respect to the enthalpy of 100% crystalline polypropylene (ΔH_m^0 =207 J/g) [62]. The X_c values of re-0 GF/PP and re-3 GF/PP are 44% and 42%, respectively. The X_c of re-0

TLCP/PP/MAPP is 47% and re-3 TLCP/PP/MAPP is 46%. There is only a slight fluctuation in X_c with the increase of recycling numbers. The influence of the degree of crystallinity on the mechanical properties of recycled composites is negligible. Overall, the DSC results illustrate that mechanical recycling has no significant effect on the thermal properties of recycled glass fiber or TLCP reinforced composites.

TGA is utilized to characterize the thermal decompositions of recycled GF/PP and TLCP/PP. The weight loss (%) of each sample as a function of temperature is plotted in Fig. 4.11. Under a nitrogen environment, the single-step degradation is observed for re-0 GF/PP, where the 5% weight loss occurs at 438°C. This weight loss is due to the thermal degradation of polypropylene. TLCP reinforced composite decomposes in two steps. The first weight loss occurs around 459°C, attributed to the degradation of polypropylene. The decomposition of TLCP gives rise to the second weight loss. First maximum decomposition rates of GF/PP and TLCP/PP/MAPP occur at 489°C and 496°C, respectively. The thermal stability of TLCP filled composites is slightly higher than glass fiber reinforced polypropylene. The TGA curves of re3-TLCP or GF composites almost overlap with re0 composites, suggesting that recycling has no particular effect on the thermal degradation behaviors of TLCP or glass fiber reinforced composites. From DSC and TGA results, multiple mechanical recycling does not significantly change the thermal behavior of glass fiber and TLCP reinforced polypropylene.

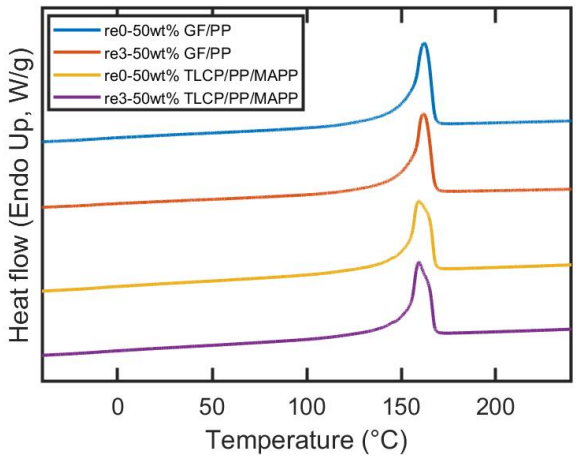

Figure 4. 9: DSC second heating curves of recycled 50 wt% GF/PP and TLCP/PP/MAPP.

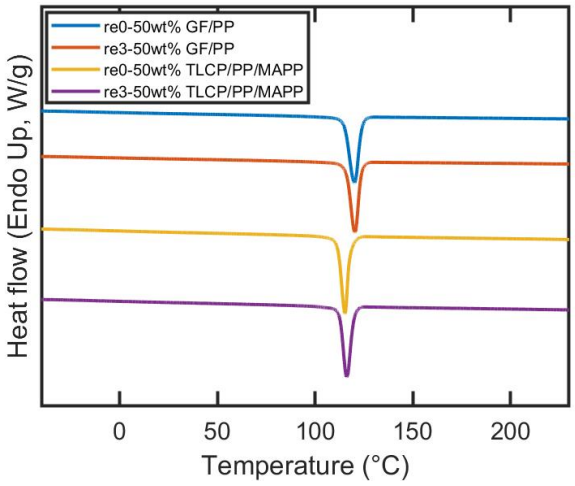

Figure 4. 10: DSC cooling scans of recycled 50 wt% GF/PP and TLCP/PP/MAPP.

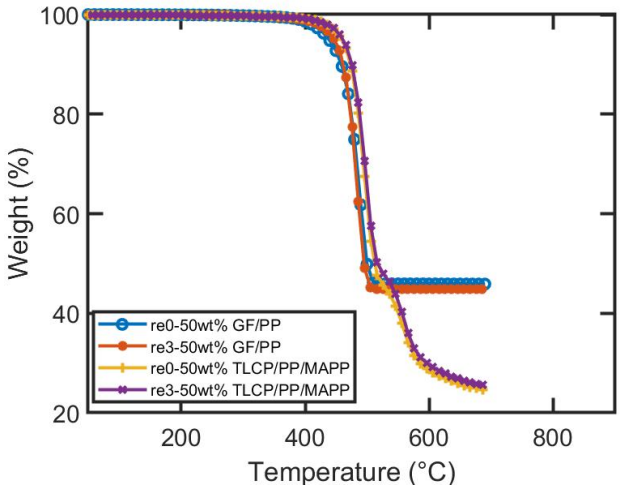

Figure 4. 11: TGA curves of recycled 50 wt% GF/PP and TLCP/PP/MAPP.

4.4.6 Rheological Properties

To characterize the rheological behavior of recycled glass fiber and TLCP reinforced composites, small amplitude oscillatory frequency sweep tests were carried out. The complex viscosity ($|\eta^*|$) is plotted as a function of angular frequency (ω) for 50 wt% GF and TLCP filled composites with different recycling numbers, as shown in Fig. 4.12. Because TLCP/PP/MAPP and TLCP/PP show similar rheological behavior, the figures include the comparison between TLCP/PP/MAPP and GF/PP. In Fig. 4.12(b), TLCP/PP/MAPP exhibited weak dependence of $|\eta^*|$ on ω at low frequency, and the correlation between complex viscosity and angular frequency becomes stronger with increasing frequency. For GF/PP, the complex viscosity plateau at low frequency is not observed, but rather the $|\eta^*|$ increases significantly with decreasing ω, as indicated in Fig. 4.12(a). This suggests the interactions of fiber-fiber and fiber-matrix increase the resistance to flow at low frequency. At high ω, these interactions are disrupted, and, thus, $|\eta^*|$ of

GF/PP melt decreases rapidly with increasing ω [63]. By comparing the $|\eta^*|$ of re0-GF/PP and re0-TLCP/PP/MAPP, the $|\eta^*|$ of glass fiber reinforced composite is found to be more than an order of magnitude higher than that of the TLCP composite in the low frequency region. It is well known that TLCPs exhibit low melt viscosity even comparing to many thermoplastics [64]. Glass fibers increase the viscosity of polymer blends, reducing the processability [65]. With the increase in the number of reprocessing cycles, $|\eta^*|$ of TLCP and glass fiber reinforced composites keep decreasing. Mechanical recycling has a stronger impact on the reduction of the complex viscosity of glass filled composite than that of the TLCP composite, especially in the low frequency region, because of the joint influence of fiber attrition and degradation of the matrix of the glass fiber composite. The decrease of $|\eta^*|$ of the recycled TLCP composite is due to the thermal and mechanical degradation of polypropylene and TLCP during the recycling process [40, 66].

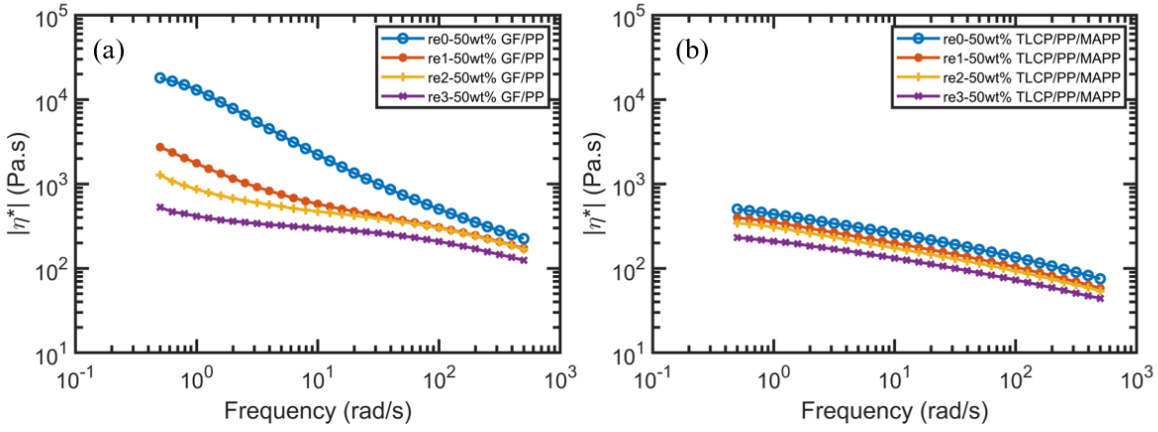

Figure 4. 12: Frequency sweep of recycled 50 wt% GF/PP and TLCP/PP/MAPP at 290 °C

4.4.7 Thermo-mechanical Properties

Dynamic mechanical thermal analysis (DMTA) was performed on injection-molded TLCP and glass fiber reinforced composites to determine the influence of recycling on the thermo-mechanical properties. There is no significant difference between the DMTA data of 50 wt% TLCP/PP/MAPP and TLCP/PP. DMTA curves of recycled TLCP/PP/MAPP are compared against recycled GF/PP composites. Fig. 4.13 illustrates the storage modulus spectra of re-0 to re-3 TLCP/PP/MAPP and GF/PP composites. The storage modulus indicates the rigidity of viscoelastic materials. The storage moduli of recycled TLCP/PP/MAPP composites decrease with increasing temperature, and several rapid declines in storage modulus are associated with thermal transitions of polypropylene and TLCP (Fig. 4.13(b)). The storage moduli of re-0 to re-3 TLCP/PP/MAPP overlap with each other, suggesting that TLCP reinforced composite retains its stiffness at various temperatures after several reprocessing cycles. Conversely, the storage moduli of recycled GF/PP only overlap when the ambient temperature is below the T_g of polypropylene, and a noticeable difference is observed between the storage moduli of recycled glass fiber composites at elevated temperature as shown in Fig. 4.13(a). In the glassy state, polymer chains of polypropylene are frozen, and the fiber length will not affect the stiffness of GF/PP. At elevated temperature, recycled GF/PP composites exhibit considerable reductions in stiffness. With the onset of segmental motion of the matrix polymer, the effect of fiber length on the stiffness of the composites is magnified. After three recycling steps, GF/PP decreases more than 37% of its stiffness at 100 °C. Due to the fiber breakage during recycling, shorter fibers may partially lose the ability to restrict the movement of polypropylene and decrease the overall stiffness of the composite [67, 68]. Mechanical

recycling imposes a significant impact on the thermal-mechanical properties of glass fiber filled composite and has no influence on the mechanical performance of TLCP reinforced composites even at elevated temperatures.

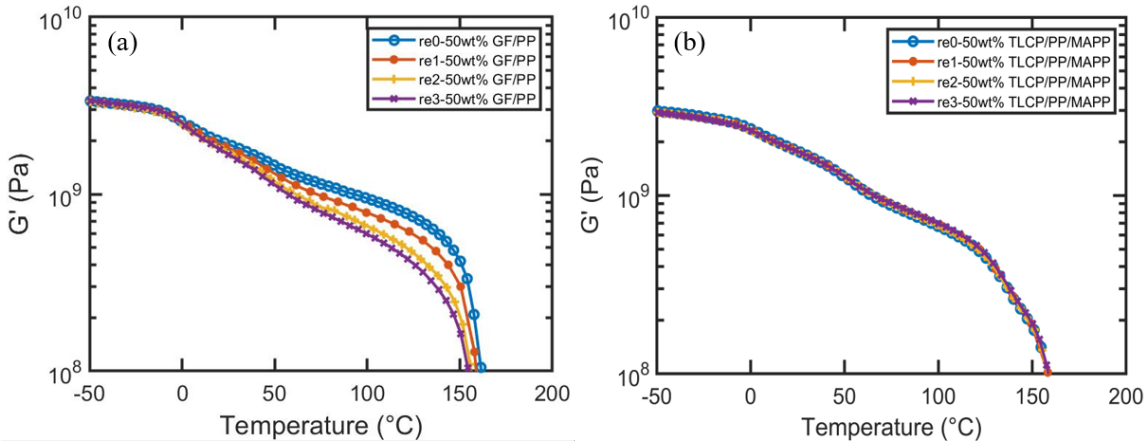

Figure 4. 13: Storage modulus versus temperature of recycled 50 wt% GF/PP and TLCP/PP/MAPP.

4.5 Conclusion

In situ TLCP reinforced polypropylene composites maintain high performance after mechanical recycling. The incorporation of maleic anhydride-grafted polypropylene into TLCP/PP composites has been found to significantly enhance the mechanical properties without influencing the performance after reprocessing, and the mechanical properties of TLCP/PP/MAPP are competitive with the mechanical properties of long glass fiber reinforced composite. Generation of TLCP fibrils during the mold filling process at every recycling step allows the same level of reinforcement, leading to no loss of mechanical performance. In contrast, recycled glass fiber reinforced composites show lower tensile properties, especially tensile strength (-30%), as compared to virgin glass fiber composite. Fiber breakage during recycling results in the decrease in mechanical properties of GF/PP.

Therefore, TLCP reinforced composites have greater recyclability than glass fiber filled composites.

To generate *in situ* TLCP composite, the processing temperature of injection molding TLCP/PP is selected to be higher than the melting point of TLCP. The processing temperature of blending them can be optimized through rheological analysis and TGA. The processing condition enables the generation of recyclable TLCP reinforced composites, which have comparable mechanical performance to long glass fiber filled propylene with the same fiber weight fraction.

Mechanical recycling has no significant influence on the thermal, rheological, and thermo-mechanical properties of TLCP/PP composites. On the other hand, for glass fiber filled systems, repetitive recycling has made large impacts on all the properties, except for thermal properties. The significant difference in the performance between recycled GF/PP and virgin GF/PP is mainly due to the fiber breakage. Micro-mechanical modeling illustrates the influence of fiber breakage on the mechanical properties of recycled GF/PP. The impact of recycling to different extents on modulus and strength is because the fiber length, in which the property has the maximum rate of change, is different for different properties. Given the greater recyclability relative to GF composite, light weight, and overall excellent performance, TLCP/PP is a promising candidate to replace glass fiber reinforced polypropylene in various applications. Being able to reuse TLCPs is not only an important cost factor but an environmental factor.

4.6 Acknowledgements

The authors would like to thank SABIC and Celanese for supplying the materials in this study.

4.7 Reference

1. Chen, T.; Mansfield, C. D.; Ju, L.; Baird, D. G., The influence of mechanical recycling on the properties of thermotropic liquid crystalline polymer and long glass fiber reinforced polypropylene. *Compos. Part B Eng.* **2020,** *200*, 108316.
2. Rajendran, S.; Scelsi, L.; Hodzic, A.; Soutis, C.; Al-Maadeed, M. A., Environmental impact assessment of composites containing recycled plastics. *Resources, Conservation and Recycling* **2012,** *60*, 131-139.
3. Pimenta, S.; Pinho, S. T., Recycling carbon fibre reinforced polymers for structural applications: Technology review and market outlook. *Waste Manage. (Oxford)* **2011,** *31*, 378-392.
4. Thomason, J.; Jenkins, P.; Yang, L., Glass fibre strength—a review with relation to composite recycling. *Fibers* **2016,** *4*, 18.
5. Jacob, A., Composites can be recycled. *Reinforced Plastics* **2011,** *55*, 45-46.
6. Oliveux, G.; Dandy, L. O.; Leeke, G. A., Current status of recycling of fibre reinforced polymers: Review of technologies, reuse and resulting properties. *Prog. Mater Sci.* **2015,** *72*, 61-99.
7. Tapper, R. J.; Longana, M. L.; Norton, A.; Potter, K. D.; Hamerton, I., An evaluation of life cycle assessment and its application to the closed-loop recycling of carbon fibre reinforced polymers. *Composites Part B: Engineering* **2019,** *184*, 107665.
8. Nakagawa, M.; Shibata, K.; Kuriya, H. In *Characterization of cfrp using recovered carbon fibers from waste cfrp*, Second International symposium on fiber recycling, Atlanta, Gergia, USA., Atlanta, Gergia, USA., 2009.
9. Liu, Y.; Meng, L.; Huang, Y.; Du, J., Recycling of carbon/epoxy composites. *J. Appl. Polym. Sci.* **2004,** *94*, 1912-1916.
10. Piñero-Hernanz, R.; Dodds, C.; Hyde, J.; García-Serna, J.; Poliakoff, M.; Lester, E.; Cocero, M. J.; Kingman, S.; Pickering, S.; Wong, K. H., Chemical recycling of carbon fibre reinforced composites in nearcritical and supercritical water. *Composites Part A: Applied Science and Manufacturing* **2008,** *39*, 454-461.
11. Cunliffe, A.; Jones, N.; Williams, P., Pyrolysis of composite plastic waste. *Environ. Technol.* **2003,** *24*, 653-663.
12. Pickering, S. J., Recycling technologies for thermoset composite materials—current status. *Composites Part A: applied science and manufacturing* **2006,** *37*, 1206-1215.
13. Liu, Y.; Farnsworth, M.; Tiwari, A., A review of optimisation techniques used in the composite recycling area: State-of-the-art and steps towards a research agenda. *Journal of cleaner production* **2017,** *140*, 1775-1781.
14. Zhang, J.; Chevali, V. S.; Wang, H.; Wang, C.-H., Current status of carbon fibre and carbon fibre composites recycling. *Composites Part B: Engineering* **2020,** *193*, 108053.
15. Shuaib, N. A.; Mativenga, P. T., Carbon footprint analysis of fibre reinforced composite recycling processes. *Procedia Manufacturing* **2017,** *7*, 183-190.
16. Colucci, G.; Ostrovskaya, O.; Frache, A.; Martorana, B.; Badini, C., The effect of mechanical recycling on the microstructure and properties of pa66 composites reinforced with carbon fibers. *J. Appl. Polym. Sci.* **2015,** *132*.
17. Tomioka, M.; Ishikawa, T.; Okuyama, K.; Tanaka, T., Recycling of carbon-fiber-reinforced polypropylene prepreg waste based on pelletization process. *J. Compos. Mater.* **2017,** *51*, 3847-3858.

18. Kuram, E.; Ozcelik, B.; Yilmaz, F., The influence of recycling number on the mechanical, chemical, thermal and rheological properties of poly (butylene terephthalate)/polycarbonate binary blend and glass-fibre-reinforced composite. *J. Thermoplast. Compos. Mater.* **2016,** *29*, 1443-1457.
19. Kuram, E.; Tasci, E.; Altan, A. I.; Medar, M. M.; Yilmaz, F.; Ozcelik, B., Investigating the effects of recycling number and injection parameters on the mechanical properties of glass-fibre reinforced nylon 6 using taguchi method. *Materials & Design* **2013,** *49*, 139-150.
20. Chrysostomou, A.; Hashemi, S., Influence of reprocessing on properties of short fibre-reinforced polycarbonate. *Journal of materials science* **1996,** *31*, 1183-1197.
21. Ayadi, A.; Kraiem, D.; Bradai, C.; Pimbert, S., Recycling effect on mechanical behavior of hdpe/glass fibers at low concentrations. *J. Thermoplast. Compos. Mater.* **2012,** *25*, 523-536.
22. Eriksson, P. A.; Albertsson, A. C.; Boydell, P.; Prautzsch, G.; Månson, J. A., Prediction of mechanical properties of recycled fiberglass reinforced polyamide 66. *Polym. Compos.* **1996,** *17*, 830-839.
23. Kelly, A.; Tyson, W. R., Tensile properties of fibre-reinforced metals: Copper/tungsten and copper/molybdenum. *J. Mech. Phys. Solids* **1965,** *13*, 329-350.
24. Colucci, G.; Simon, H.; Roncato, D.; Martorana, B.; Badini, C., Effect of recycling on polypropylene composites reinforced with glass fibres. *J. Thermoplast. Compos. Mater.* **2017,** *30*, 707-723.
25. Donald, A. M.; Windle, A. H.; Hanna, S., *Liquid crystalline polymers*. Cambridge University Press: 2006.
26. Chae, H. G.; Kumar, S., Rigid‐rod polymeric fibers. *J. Appl. Polym. Sci.* **2006,** *100*, 791-802.
27. Prashanth, S.; Subbaya, K.; Nithin, K.; Sachhidananda, S., Fiber reinforced composites-a review. *Journal of Material Sciences & Engineering* **2017,** *6*, 1-6.
28. Kalfon-Cohen, E.; Marom, G.; Wachtel, E.; Pegoretti, A., Characterization of drawn monofilaments of liquid crystalline polymer/carbon nanoparticle composites correlated to nematic order. *Polymer* **2009,** *50*, 1797-1804.
29. Williams, D. J., Applications for thermotropic liquid crystal polymer blends. *Advances in Polymer Technology: Journal of the Polymer Processing Institute* **1990,** *10*, 173-184.
30. Handlos, A.; Baird, D. G., Processing and associated properties of in situ composites based on thermotropic liquid crystalline polymers and thermoplastics. *Journal of Macromolecular Science, Part C: Polymer Reviews* **1995,** *35*, 183-238.
31. Crevecoeur, G.; Groeninckx, G., Morphology and mechanical properties of thermoplastic composites containing a thermotropic liquid crystalline polymer. *Polymer Engineering & Science* **1990,** *30*, 532-542.
32. Crevecoeur, G.; Groeninckx, G., Melt‐spinning of in‐situ composites of a thermotropic liquid crystalline polyester in a miscible matrix of poly (ether ether ketone) and poly (ether imide). *Polym. Compos.* **1992,** *13*, 244-250.
33. Kiss, G., In situ composites: Blends of isotropic polymers and thermotropic liquid crystalline polymers. *Polymer Engineering & Science* **1987,** *27*, 410-423.
34. Baird, D. G.; Collias, D. I., *Polymer processing: Principles and design*. John Wiley & Sons: 2014.
35. De Souza, J.; Baird, D. G., In situ composites based on blends of a poly (ether imide) and thermotropic liquid crystalline polymers under injection moulding conditions. *Polymer* **1996,** *37*, 1985-1997.

36. Bafna, S.; De Souza, J.; Sun, T.; Baird, D. G., Mechanical properties of in‐situ composites based on partially miscible blends of glass‐filled polyetherimide and liquid crystalline polymers. *Polymer Engineering & Science* **1993,** *33*, 808-818.
37. Datta, A.; Chen, H.; Baird, D. G., The effect of compatibilization on blends of polypropylene with a liquid-crystalline polymer. *Polymer* **1993,** *34*, 759-766.
38. Datta, A.; Baird, D. G., Compatibilization of thermoplastic composites based on blends of polypropylene with two liquid crystalline polymers. *Polymer* **1995,** *36*, 505-514.
39. O'Donnell, H. J.; Baird, D. G., In situ reinforcement of polypropylene with liquid-crystalline polymers: Effect of maleic anhydride-grafted polypropylene. *Polymer* **1995,** *36*, 3113-3126.
40. Bastida, S.; Eguiazabal, J.; Nazabal, J., Reprocessing of liquid‐crystal polymers: Effects on structure and mechanical properties. *J. Appl. Polym. Sci.* **1995,** *56*, 1487-1494.
41. Xu, Q.; Man, H., Recycling of the rodrun lc-5000 lcp/polycarbonate in situ composites. *Polymer* **2000,** *41*, 7391-7397.
42. Collier, M. C.; Baird, D. G., Separation of a thermotropic liquid crystalline polymer from polypropylene composites. *Polym. Compos.* **1999,** *20*, 423-435.
43. Postema, A.; Fennis, P., Preparation and properties of self-reinforced polypropylene/liquid crystalline polymer blends. *Polymer* **1997,** *38*, 5557-5564.
44. SABIC Verton technical data sheet. https://www.sabic.com/en/products/specialties/lnp-compounds/lnp-verton-compound?grade=mv008s (accessed 16 August).
45. Kunc, V.; Frame, B. J.; Nguyen, B. N.; Tucker III, C. L.; Velez-Garcia, G. In *Fiber length distribution measurement for long glass and carbon fiber reinforced injection molded thermoplastics*, In: Proceedings of the 7th Annual SPE Automotive Composites Conference and Exposition, Troy, Michigan, Society of Plastic Engineers: Troy, Michigan, 2007.
46. Cox, H., The elasticity and strength of paper and other fibrous materials. *Br. J. Appl. Phys.* **1952,** *3*, 72.
47. Krenchel, H., Fibre reinforcement. Akademisk forlag. *Copenhagen, Denmark* **1964**.
48. Bowyer, W.; Bader, M., On the re-inforcement of thermoplastics by imperfectly aligned discontinuous fibres. *Journal of materials Science* **1972,** *7*, 1315-1321.
49. Thomason, J., The influence of fibre length and concentration on the properties of glass fibre reinforced polypropylene: 7. Interface strength and fibre strain in injection moulded long fibre pp at high fibre content. *Composites Part A: applied science and manufacturing* **2007,** *38*, 210-216.
50. Qin, Y.; Brydon, D.; Mather, R.; Wardman, R., Fibres from polypropylene and liquid crystal polymer blends: 3. A comparison of polyblend fibres containing vectra a900, vectra b950 and rodrun lc3000. *Polymer* **1993,** *34*, 3597-3604.
51. Ballice, L.; Reimert, R., Classification of volatile products from the temperature-programmed pyrolysis of polypropylene (pp), atactic-polypropylene (app) and thermogravimetrically derived kinetics of pyrolysis. *Chemical Engineering and Processing: Process Intensification* **2002,** *41*, 289-296.
52. Baird, D. G.; Robertson, C. G.; De Souza, J. P. Liquid crystalline polymer-reinforced thermoplastic fibers. 5834560, Nov. 10, 1998, 1998.
53. Mallick, P. K., *Fiber-reinforced composites: Materials, manufacturing, and design*. CRC press: 2007.
54. Halpin, J.; Kardos, J., The halpin‐tsai equations: A review. *Polymer Engineering & Science* **1976,** *16*, 344-352.
55. Weng, T.; Hiltner, A.; Baer, E., Hierarchical structure in a thermotropic liquid-crystalline copolyester. *Journal of materials science* **1986,** *21*, 744-750.

56. Thomason, J., The influence of fibre length and concentration on the properties of glass fibre reinforced polypropylene: 5. Injection moulded long and short fibre pp. *Compos. Part A-Appl. S. Compos.* **2002,** *33*, 1641-1652.
57. Bijsterbosch, H.; Gaymans, R., Polyamide 6—long glass fiber injection moldings. *Polym. Compos.* **1995,** *16*, 363-369.
58. Bernasconi, A.; Rossin, D.; Armanni, C., Analysis of the effect of mechanical recycling upon tensile strength of a short glass fibre reinforced polyamide 6, 6. *Engineering fracture mechanics* **2007,** *74*, 627-641.
59. Nguyen, B. N.; Bapanapalli, S. K.; Holbery, J. D.; Smith, M. T.; Kunc, V.; Frame, B. J.; Phelps, J. H.; Tucker III, C. L., Fiber length and orientation in long-fiber injection-molded thermoplastics—part i: Modeling of microstructure and elastic properties. *J. Compos. Mater.* **2008,** *42*, 1003-1029.
60. Chen, H.; Baird, D. G., Prediction of young's modulus for injection molded long fiber reinforced thermoplastics. *Journal of Composites Science* **2018,** *2*, 47.
61. Kenig, S., Fiber orientation development in molding of polymer composites. *Polym. Compos.* **1986,** *7*, 50-55.
62. Bu, H. S.; Cheng, S. Z.; Wunderlich, B., Addendum to the thermal properties of polypropylene. *Die Makromolekulare Chemie, Rapid Communications* **1988,** *9*, 75-77.
63. Shenoy, A. V., *Rheology of filled polymer systems*. Springer Science & Business Media: 2013.
64. Gotsis, A. D.; Baird, D. G., Rheological properties of liquid crystalline copolyester melts. Ii. Comparison of capillary and rotary rheometer results. *J. Rheol.* **1985,** *29*, 539-556.
65. Garcia, M.; Eguiazabal, J.; Nazábal, J., Processability, morphology and mechanical properties of glass fiber reinforced poly (ether sulfone) modified by a liquid crystalline copolyester. *Polym. Compos.* **2003,** *24*, 686-696.
66. Gonzalez-Gonzalez, V. A.; Neira-Velazquez, G.; Angulo-Sanchez, J. L., Polypropylene chain scissions and molecular weight changes in multiple extrusion. *Polym. Degrad. Stab.* **1998,** *60*, 33-42.
67. Capela, C.; Oliveira, S.; Pestana, J.; Ferreira, J., Effect of fiber length on the mechanical properties of high dosage carbon reinforced. *Procedia Structural Integrity* **2017,** *5*, 539-546.
68. Zhang, D.; He, M.; Qin, S.; Yu, J., Effect of fiber length and dispersion on properties of long glass fiber reinforced thermoplastic composites based on poly (butylene terephthalate). *RSC advances* **2017,** *7*, 15439-15454.

5 Development of Recyclable and High-performance *In-situ* Hybrid TLCP Composites

The third research objective is addressed in this chapter and the manuscript was published in: **T. Chen**, D. Kazerooni, L. Ju, D. A. Okonski, D. G. Baird "Development of Recyclable and High-performance *in situ* Hybrid TLCP/glass fiber composites", *Journal of Composites Science* **2020**, *4*, 125 [1]

Chapter 5 Development of Recyclable and High-performance *In-situ* Hybrid TLCP Composites

Tianran Chen[1], Dana Kazerooni[1], Lin Ju[1], David A. Okonski[2], and Donald G. Baird[1]

[1]*Macromolecules Innovation Institute and Department of Chemical Engineering, Virginia Tech, Blacksburg, VA 24061*

[2]*GM Global Research & Development Center, Warren, MI, 48092*

5.1 Abstract

By combing the concepts of *in situ* thermotropic liquid crystalline polymer (TLCP) composite and conventional fiber composite, a recyclable and high-performance *in situ* hybrid polypropylene-based composite was successfully developed. The recycled hybrid composite was prepared by injection molding and grinding processes. Rheological and thermal analyses were utilized to optimize the processing temperature of the injection molding process to reduce the melt viscosity and minimize the degradation of polypropylene. The ideal temperature for blending the hybrid composite was found to be 305°C. The influences of mechanical recycling on the different combinations of TLCP and glass fiber composites were analyzed. When the weight fraction ratio of TLCP to glass fiber was 2 to 1, the hybrid composite exhibited better processability, improved tensile performance, lower mechanical anisotropy, and greater recyclability as compared to the polypropylene reinforced by either glass fiber or TLCP alone.

5.2 Introduction

Early constructs of machines – like automobiles, locomotives, and aircraft – were designed using dense metals with high strength capabilities, but recent advancements in material science have enabled fiber-reinforced composites to replace traditional metals because of higher strength-to-weight ratios [2-4]. For instance, aluminum has traditionally been one of the most common metals used in the aerospace industry but its usage dropped from 50% in the Boeing 777 aircraft to only 20% in the Boeing 787 [2]. The advantages that fiber reinforced composite materials have over traditional metal materials include: 1) light weight, 2) high stiffness & strength, 3) corrosion resistance, and 4) design flexibility; these attributes have been embraced by the automotive industry which has increased its use of fiber-reinforced composite materials to improve fuel efficiency and reduce greenhouse gas emissions.

Among all of the different types of reinforcements utilized on a commercial scale, 65% of the revenue generated by the sale of fiber reinforced materials comes from glass fiber [5]. In 2020, the global glass fiber reinforced composites market is expected to grow to about 60 billion dollars [6]. Glass fiber is especially attractive as the reinforcement for composites because of low cost, superior mechanical, and physical properties (e.g., stiffness & strength, impact resistance, stability, and durability). The tensile modulus and strength of E-glass fiber are around 72 GPa and 3.5 GPa respectively; this outperforms aluminum with a tensile modulus of 68.9 GPa and tensile strength of 310 MPa [7, 8].

Thermotropic liquid crystalline polymers (TLCPs) is another type of reinforcement that is being extensively studied and used in both academia and industry [9, 10]. Tremendous efforts have been made toward the development of TLCPs that exhibit high modulus and

strength coupled with outstanding melt processability [9, 11, 12]. The drawn TLCP filaments display a modulus of up to 100 GPa and tensile strength of about 1.5 GPa, which is comparable to the performance of E-glass fiber [13].

Both glass fiber and TLCP have excellent mechanical performance, high strength-to-weight ratio, and chemical resistance, but glass fiber is still the more attractive reinforcement choice over TLCP for three major reasons. First, TLCPs are more expensive than glass fiber; depending on the grade of TLCP, the cost may range from 8 to 12 dollars per pound [14]. Second, glass fiber has a higher tensile strength than TLCPs, especially when the TLCP is not generated using the fiber spinning or strand extrusion process. The full reinforcing potential of TLCP fiber cannot be achieved under other processing techniques. Finally, glass fiber reinforced composites have lower mechanical anisotropy than their TLCP-filled counterparts; this is primarily due to the TLCP fibrils being created *in situ* under strong unidirectional elongation and shear flow [15].

One of the advantages of using TLCPs in reinforcing thermoplastic materials is the processability. It is well known that the incorporation of glass fibers into thermoplastics results in a substantial increase in viscosity which gives rise to the difficulty in processing and high energy consumption [9]. During the processing of a TLCP composite melt, TLCP molecules adopt extended chain conformation rather than a random coil displayed by conventional thermoplastics [16]; therefore, the melt viscosities of TLCP reinforced composites become much lower than that of glass filled composites, leading to more facile processing. In addition, the surface smoothness of TLCP reinforced composites is greater than that of composites reinforced by glass fiber only [17]. The higher surface smoothness is related to the diameter of TLCP fibrils, which is

one order of magnitude less than glass fiber. Also, the density of TLCP is around 1.4 g/cm^3 which is about half the density of E-glass fiber (2.58 g/cm^3) [8, 18]. The composite parts which utilize TLCP exhibit lower weight than those of glass fiber, making the TLCP composite an attractive material specifically for transportation applications. Finally, the recyclability of TLCP composite has been found to be superior to glass-filled systems [19]. TLCP is able to regenerate the highly oriented molecular structure during the reprocessing while glass fiber would suffer severe fiber breakage during the recycling process.

To capitalize on the advantages of using TLCPs and glass fibers, composites consisting of both TLCPs and glass fiber as reinforcements in thermoplastics have been studied [20-25]. The *in situ* hybrid composite consists of three components: microscopic TLCP fibrils, macroscopic conventional fibers (i.e.; glass and carbon fiber), and the matrix polymer [25]. Bafna *et al.* [23] reported the use of glass fiber and TLCP reinforcements to enhance the mechanical properties and reduce the mechanical anisotropy of *in situ* TLCP composites with polyetherimide (PEI) as the matrix material. Tensile and flexural moduli increased and the anisotropy reduced with increasing glass fiber content. Furthermore, the creep performance of PEI composites improved when TLCP and glass fiber were blended together. Another study looked to combine the advantages of short fiber composites and TLCP composite; He *et al.* [25] investigated the mechanical, rheological, and morphological properties of hybrid *in situ* carbon fiber or glass fiber/TLCP composite systems. The improvement in tensile and flexural properties, lower melt viscosity, and more oriented fibers in the flow direction have been observed.

Although composite materials have a variety of advantages, one of the major challenges for fiber reinforced composites is their recyclability. The disposal of composite waste in an environmentally friendly manner is a crucial task to our society. Typically, fiber-reinforced composite materials are very difficult and energy intensive to recycle due to the nature of heterogeneity, technology limitations, high recycling cost, and low quality of recycled products. More restrictive environmental legislation drives the market toward recycling and reusing fiber reinforced composites. There are three major recycling methods to reclaim fiber reinforced composites: 1) thermal process, 2) solvolysis, and 3) mechanical recycling [26-28]. Mechanical recycling has less environmental impact, can recover both fiber and matrix polymer, and requires no use of solvents as compared to thermal and solvent methods [29]. Mechanical recycling uses the principles of shredding or crushing the composite part into small particulates and then feeding these into a manufacturing machine to produce recycled parts. The recycled composites have very limited applications. Usually, the recycled composites, acting as "filler", are blended with virgin materials to make a product with similar performance as new "virgin" parts. The incorporation level of the recycled composites is usually no more than 10 wt% to minimize the negative impact from the recycled materials [29].

Mechanical recycling is considered environmentally friendly and cost-effective; however, the application of this method is hindered because the recycling process reduces the performance of subsequent composite parts. Extensive investigations have been carried out on the influence of mechanical recycling on the properties of glass or carbon fiber reinforced composites [30-33]. The mechanical properties of fiber reinforced composites decrease significantly after mechanical recycling. This is mainly due to fiber

attrition during the recycling process. The need for developing a recyclable and high-performance composite is becoming extremely urgent.

Previous work explored the effect of mechanical recycling on the properties of TLCP and glass fiber reinforced polypropylene [19]. The results illustrated that the TLCP composite had superior recyclability relative to that of its glass fiber reinforced counterpart. It is of great interest to determine whether there exists a formulation of TLCP, glass fiber, and matrix polymer which may be mechanically recycled without compromising the mechanical performance of the subsequent composite part. The objective of this work is to utilize glass fiber and TLCP to develop a recyclable and high-performance *in situ* polypropylene-based hybrid composite. The *in situ* hybrid composites were mechanically recycled once by injection molding and grinding processes. The processing temperature was optimized through rheological analyses to improve the processability and reduce the thermal degradation of polypropylene. The optimal formulation of glass fiber and TLCP enables the best combination of high recyclability, high mechanical properties, and low mechanical anisotropy of the hybrid composite.

5.3 Experimental

5.3.1 Materials

The thermotropic liquid crystalline polymer (TLCP) for this study, trade name Vectra B950 and made by Celanese, is an aromatic poly(ester-co-amide), composed of 6-hydroxy-2-naphthoic acid (60 mol%), terephthalic acid (20 mol%), and aminophenol (20

mol%). The melting point of Vectra B950 is around 280°C [34]. The long glass fiber (GF) reinforced polypropylene was provided by SABIC as 8.0 mm long pellets with a reinforcement loading of 50 wt%. The unfilled matrix polypropylene (PP), catalog name Pro-fax 6523, was purchased from LyondellBasell and has a melt flow rate of 4.0 g/10 min at 230°C [35].

5.3.2 Melt compounding and recycling of hybrid composites

There were four combinations of glass fiber and TLCP composite used in this study. These composites were designated as 30GF/PP, 20GF10TLCP/PP, 10GF20TLCP/PP, and 30TLCP/PP. The number before the component represents the weight percent of that particular reinforcement in the composite. For instance, the 20GF10TLCP/PP means that the composite consists of 20 wt% glass fiber, 10 wt% TLCP, and 70 wt% polypropylene. The weight fraction of reinforcement in each composite was kept at 30 wt%. To prepare the hybrid composites, the materials (e.g., TLCP, 50 wt% GF/PP, and PP) were dried in a vacuum oven at 80°C for 24 hours. A single screw extruder with a 1-inch diameter screw and L/D ratio of 24 was used for compounding the TLCP and PP at 290°C. The extrudate was cooled down in a water bath and pelletized. The TLCP/PP and GF/PP pellets were injection molded (BOY 35E) into end-gate plaques to form the pristine hybrid composite. The pristine hybrid composites were shredded by a granulator (Cumberland/John Brown D-99050). The recycled hybrid composites were prepared by injection molding the shredded materials. The injection molding temperature was optimized at 305°C based on rheological analyses.

5.3.3 Rheological measurements of polypropylene, TLCP, and hybrid composite

An ARES-G2 rheometer with 25 mm parallel plates was used to investigate the viscoelastic properties of TLCP at four different experimental temperatures: 290, 300, 305, and 310ºC; all work was completed under a nitrogen atmosphere unless expressly stated otherwise. Each sample was equilibrated to the experimental temperature for 5 minutes. First, pure TLCP pellets were loaded directly into the rheometer and then tested using a shear step strain at a strain of 0.5% [36]. Relaxation modulus (G) at each temperature was plotted against time. Further experimentation on the pure TLCP pellets included running a small amplitude oscillatory shear (SAOS) frequency sweep per temperature to obtain the complex viscosity, storage modulus, and loss modulus. Next, virgin PP material was first tested using SAOS rheology under time sweep mode at each temperature. The complex viscosity of PP was tracked as a function of time per temperature. Finally, all the compositions of recycled GF/TLCP/PP hybrid materials were used to measure the complex viscosity for each composition using the SAOS frequency sweep at 305ºC.

5.3.4 Mechanical Properties

Rectangular bars having dimensions of 75.0 x 8.0 x 1.5 mm were cut from the injection molded end-gated plaques of the different reinforcement ratios of pristine and recycled hybrid composites. At least ten replicates for each composition were tested (five bars were cut in the flow direction and five bars were cut in the perpendicular to flow or transverse direction). The tensile properties of each hybrid composite were the average properties of at least five plaques. All tensile properties of each material were measured using an Instron uniaxial tensile tester (Model 4204) with a 5 kN load cell. The tensile

strains of the specimen were measured with an extensometer (MTS 634.12). The cross-head speed was set at 1.27 mm/min.

5.3.5 Differential Scanning Calorimetry (DSC) Characterization

A DSC (TA Instruments Discovery) was used to examine the thermal properties of TLCP. Under a nitrogen atmosphere, a sample was subjected to a heat/cool/heat cycle. Material was first equilibrated at 50°C for 5 minutes and then heated up to 320°C at 10°C/min. The materials were cooled down to 50°C at -10°C/min and then heated back to 320°C at 10°C/min. The melting temperature (T_m) was determined by the TA Instruments TROIS software.

5.4 Results and discussion

5.4.1 Optimization of the injection molding temperature

To generate the *in situ* TLCP/glass fiber/polypropylene composites, the processing temperature has to be optimized with a series of rheological analyses. One advantage of blending TLCPs with other thermoplastics is the reduction in melt viscosity which results in an improvement of the polymer blend's processability. TLCPs have lower melt viscosity when compared to many thermoplastics; so, to take advantage of this, thermal and rheological properties of TLCPs need to be examined. The TLCP used in this study has a melting point around 280°C [34]. The rheological properties of TLCP above its melting point are critical in the processing this material. Transient behaviors of TLCPs are related to the rigid TLCP molecules and domain structure [36, 37]. The transient responses of pure TLCP at various test temperatures, following step strain were measured, as shown in Fig.

5.1. The relaxation modulus (G) is plotted against time on the log-log scale. At the testing temperatures below 305℃, the relaxation modulus decreases gradually over time, producing a long relaxation tail. This is graphically demonstrated by the relaxing curves at 290 and 300℃. On the other hand, the relaxation modulus (G) sharply drops when the temperature is equal and above 305℃. It is speculated that the slow decay of the relaxation modulus at low temperature is due to the presence of unmelted crystals in the TLCP [36]. As the temperature further increases, TLCP crystals change to a liquid phase causing the long relaxation tail to disappear as seen by a dramatic drop in the relaxation modulus at the temperatures of 305 and 310℃.

The complex viscosity ($|\eta^*|$) of pure TLCP was measured using a rheometer in the frequency sweep mode. Fig. 5.2 illustrates the complex viscosity of TLCP as a function of frequency for each experimental temperature. At 290 and 300℃, the $|\eta^*|$ is more than an order of magnitude higher than the complex viscosity of TLCP at 305 and 310℃, suggesting the TLCP has greater resistance to flow at lower temperatures. This further reinforces the idea that at low temperatures there may be unmelted TLCP crystals. The TLCP melt exhibits a weak dependence between the complex viscosity and frequency at a temperature of 305℃ and above. On the other hand, the relationship between complex viscosity and frequency at 290 and 300℃ unveils a stronger correlation with the change of angular frequency. TLCPs usually exhibit three distinct regions of shear viscosity in which the first reflects a shear thinning behavior at low shear rates, followed by a Newtonian plateau, and eventually finishes with another shear thinning region at high shear rates [38]. In between the frequency range of 1 to 500 rad/s, the Newtonian region is not seen for the temperature at 290 and 300℃, instead the TLCP shows the shear thinning behavior over

the entire frequency sweep range. Only the Newtonian plateau and first shear thinning region are observed at 305℃ and 310℃, which is probably due to the angular frequency not being low enough. Since the complex viscosities of TLCP at 305 and 310℃ almost overlap with each other, the viscosity of TLCP is not very sensitive to the changes in temperature in this temperature region. Because the lowest complex viscosity of TLCP at all frequency is exhibited at the temperature of 305 and 310℃, the ideal processing temperature of TLCP blends would have to be equal to or higher than 305℃ so as to reduce the viscosity during processing.

The viscoelastic properties of pure TLCP at different temperatures were studied using oscillatory shear rheology. Fig. 5.3 illustrates the change of storage (*G'*) and loss (*G"*) modulus of TLCP as the function of angular frequency at varying operational temperatures. Storage modulus and loss modulus measure the stored energy and energy dissipated as heat, respectively. At 290℃, the storage modulus is higher than the loss modulus over the entire frequency range, suggesting that the TLCP exhibits a solid-like character. After a 10℃ increase, the curves for *G'* and *G"* crossover at 200 rad/s. The crossover frequency characterizes the transition of a polymer melt from the elastic (solid-like) to the viscous (liquid-like) state. At 305℃ and above, the *G"* is higher than *G'* at all angular frequencies, indicating that the TLCP behaves like a viscous liquid. The $G'' > G'$ over the entire frequency range is probably due to the complete melt of TLCP crystals. The transitioning effect observed from the dramatic change of viscoelastic properties of TLCP with increase on the testing temperature reinforces the notion that the existence of TLCP crystals significantly impacts the rheological behavior of TLCP.

A differential scanning calorimeter (DSC) was utilized to study the melting behavior of pure TLCP and to confirm any residual crystals of TLCP at temperatures above 280°C. Two distinct transition phases are observed during the melting of TLCP as shown by the two peaks in the DSC heating scan in Fig. 5.4. The first peak is observed at around 280°C, and the second peak is observed around 297°C. The different crystal structures develop during the process leading to the mesophase transition of TLCP [39]. Literature reports state that the melting point of TLCP is around 280°C [34]. Several studies have successfully melt processed the PP with TLCP between 285 to 300°C, resulting in improved mechanical performance [34, 40, 41]. Nevertheless, to utilize the low viscosity effect of TLCP, the processing temperature must be high enough to melt all the TLCP crystals. Thus, the melting endotherm ends around 305°C, which confirms the TLCP crystals have completely melted and shows consistency with the results obtained from the rheological analyses.

Before processing the *in situ* hybrid GF/TLCP/PP composite, the PP used as the matrix of the composite needs to be tested to make sure it can withstand the high temperatures for processing. The high processing temperature improves the processability of the polymer blend but also raises the concern for the thermal degradation of the polypropylene. The thermal stability of polypropylene is measured using the isothermal time sweep rheological test. Fig. 5.5 shows the complex viscosity ($|\eta^*|$) of polypropylene as a function of time at different experimental temperatures. The isothermal rheological tests were carried out under a nitrogen atmosphere to simulate the nitrogen purge hopper used during the injection molding process. The overall residence time exposed to high temperature for processing is around 240 seconds.

During this time the viscosities of polypropylene decrease by about 14.6% at 290℃ and 42.9% at 310℃. Polypropylene undergoes severe thermal degradation at 310℃. The degradation rate of polypropylene at 300℃ and 305℃ in the nitrogen environment is much lower than at 310℃, where the complex viscosity drops around 26.7% at 305℃. similar, which is much lower than the degradation rate at 310℃ (Fig. 5.5). Therefore, to achieve better processability and reduce the thermal degradation of the polypropylene, 305℃ was selected as the processing temperature for injection molding the hybrid composite materials.

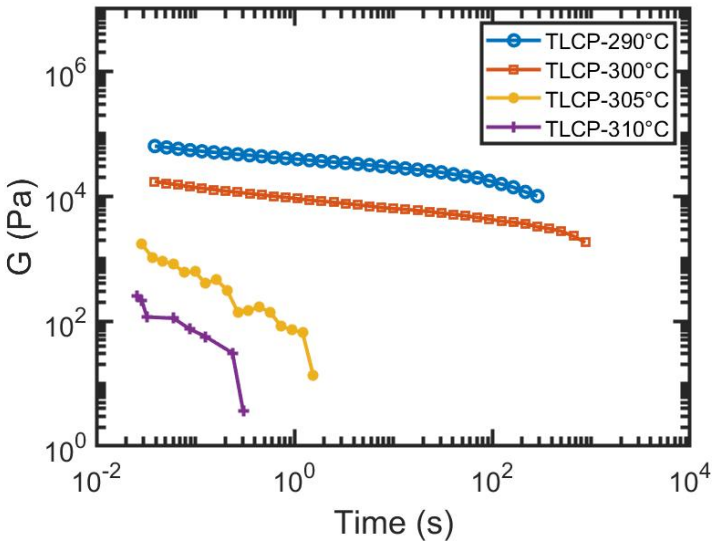

Figure 5. 1: Stress relaxation of pure TLCP following a step shear strain transient step strain at different test temperatures.

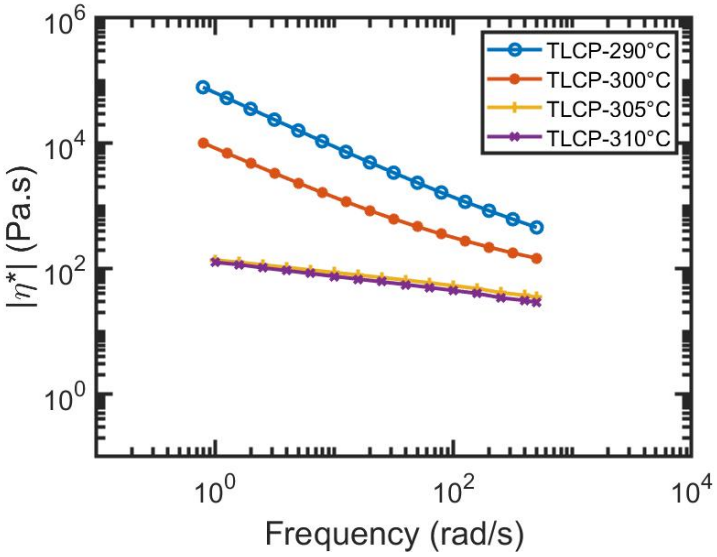

Figure 5. 2: Complex viscosity of TLCP at temperature from 290 to 310℃.

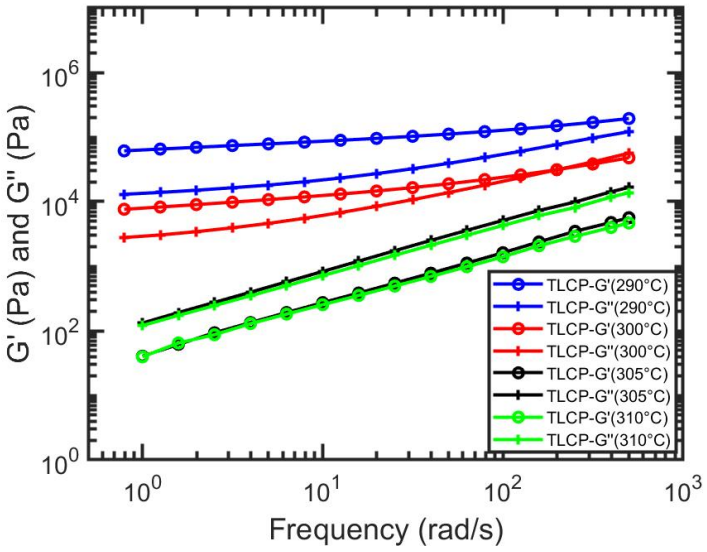

Figure 5. 3: Storage modulus and loss modulus of TLCP at different temperatures above its melting point.

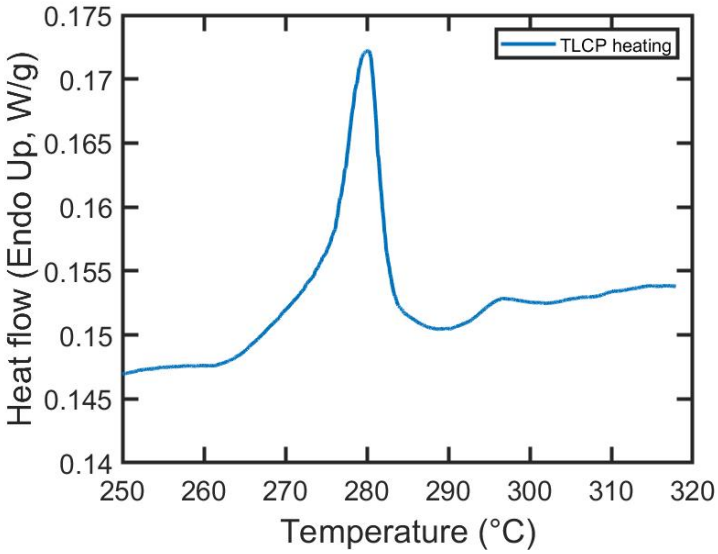

Figure 5. 4: DSC heating scan of TLCP material with the heating rate of 10℃/min.

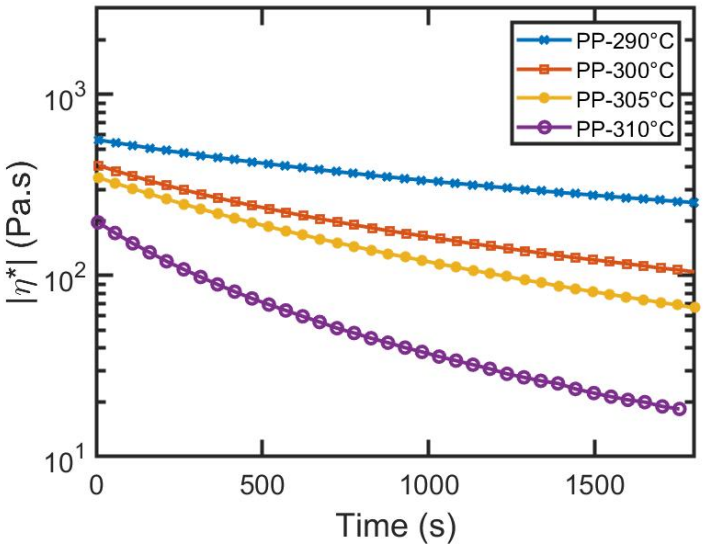

Figure 5. 5: Thermal stability of polypropylene at various temperatures (isothermal time sweep mode).

5.4.2 Rheology of *in situ* TLCP/GF hybrid composites

To characterize the rheological properties of the recycled hybrid composite, small amplitude oscillatory shear (SAOS) frequency sweep tests were carried out at 305℃. The complex viscosity is plotted against the angular frequency for each formation of recycled hybrid composite, as indicated in Fig. 5.6. Hybrid composites with varying TLCP and glass fiber compositions display dramatic differences in rheological behaviors. At low frequencies, the viscosity increases with increasing glass fiber concentration. When glass fiber is used as the sole reinforcement in the composite, the viscosity jumps two-fold compared to its TLCP counterpart at 305℃. At low frequencies, the complex viscosity plateau is not observed for glass filled hybrid composite, but rather the complex viscosity appreciably increases with the decrease in angular frequency. This response of the composite to low frequency is due to the fiber-fiber and glass fiber-matrix interactions in glass filled systems [42]. As frequency increases, these interactions are interrupted, and the complex viscosity of glass filled composite decreases dramatically. On the other hand, TLCP/PP shows overall weak dependence between complex viscosity and angular frequency. The incorporation of glass fibers into TLCP/PP composite significantly increases the complex viscosity of the hybrid composite. Especially, in the low angular frequency, the complex viscosity of hybrid composite increases exponentially with the addition of glass fiber. The hybrid composite with a higher concentration of TLCP shows significant reduction in viscosity, thereby confirming that TLCP reduces the viscosity of

polymer blends [9]. Not only does the TLCP increase the processability of GF/PP composite by lowering the melt viscosity but also mitigates the fiber breakage issue by reducing stresses acting on the fibers by the matrix polymer. In turn, diminishing fiber breakage leads to higher mechanical performance of the composites [43-45].

One concern regarding this rheological test is the thermal degradation of polypropylene at 305°C, which decreases the complex viscosity over time. This may cause the ill-defined viscosity data at high frequency (rheological test sweeps the frequency from low to high), but this frequency sweep test provides a method to qualify the benefit of higher TLCP concentration resulting in the lower viscosity of a hybrid composite.

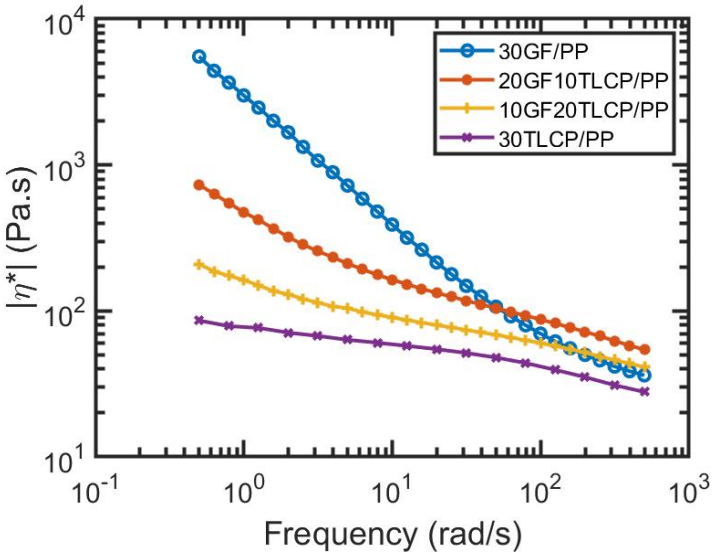

Figure 5. 6: SAOS frequency sweep of hybrid composites at 305°C in nitrogen atmosphere.

3.3 Mechanical properties of recycled TLCP/GF hybrid composite

The first injection molded samples are defined as pristine materials (blue). The recycled composites (red) are obtained through grinding the pristine materials and re-injection molding into end-gate plaques. The tensile properties of each hybrid composite are depicted in Fig. 5.7 to Fig. 5.9. The modulus of pristine 30 wt% GF/PP is 5.07 GPa, and the modulus of pristine TLCP/PP is about 3.83 GPa. The low modulus of the TLCP blend is speculated to have originated from the injection molding process which is unable to achieve high elongational deformation. The tensile modulus of 26 wt% TLCP/PP is reported to be 13.5 GPa when the sample is prepared by strand extrusion [46]. By replacing 10 wt% of the TLCP with glass fiber, the tensile modulus improves by 7.4%. The tensile modulus of hybrid composite falls in between the 30 wt% GF/PP and TLCP/PP. To determine the effect of mechanical recycling on the hybrid composite materials, the pristine composites were ground and injection molded into end-gate plaques. After recycling, the tensile modulus of GF/PP composite dropped to 4.87 GPa while the tensile modulus of TLCP/PP remains the same. The major factor for the decrease in the GF/PP composite modulus is fiber attrition during the recycling process [33]. The TLCP is able to regenerate the TLCP fibrils during the mold filling process; so, TLCP filled composites maintain their mechanical performance after mechanical recycling. In addition, the recyclability of a glass filled composite is improved with the presence of TLCP as seen with the 20GF10TLCP/PP hybrid composite only losing 4.1% of its modulus after recycling.

The tensile strengths of pristine and recycled hybrid composites are shown in Fig. 5.8. The tensile strength of pristine GF/PP is much higher than that of TLCP/PP because the tensile strength of the TLCP (~0.5 GPa) is lower than the tensile strength of GF (~3.5

GPa); the same difference in the properties of composites is also expected to be seen [46, 47]. By adding glass fiber into the TLCP blend, the tensile strength is enhanced significantly. Replacing 10 wt% TLCP with glass fiber enables the improvement of the tensile strength from 36.8 to 50.0 MPa. Mechanical recycling imposes different degrees of impact on the tensile strength of hybrid composites. The tensile strength of 30 wt% GF/PP drops from 71.5 to 61.7 MPa after recycling; however, there is only a 9.6% decrease in the tensile strength of 20GF10TLCP/PP. Just as for tensile modulus, this is due to the severe fiber length attrition during the blending and grinding processes. The higher content of glass fiber and higher melt viscosity accelerate the fiber breakage during processing. The short glass fiber composite shows lower mechanical properties than the long glass fiber composite [45]. The higher content of TLCP in the hybrid composite lessens the decrease in the mechanical properties of the composites after recycling.

The mechanical properties of hybrid composites in the transverse-to-flow direction were measured and are shown in Fig. 5.9. The rectangular bar is cut from injection-molded, end-gate plaques in the direction perpendicular-to-flow in order to obtain the performance of hybrid composites in the transverse-to-flow direction. Similar to the mechanical behaviors in the flow direction, the tensile properties of TCLP/PP are lower than the GF/PP due to the combining effect of different mechanical properties of pure materials used and processing methods. The addition of 10 wt% glass fiber improves the tensile modulus of TLCP/PP from 1.8 to 2.5 GPa. In terms of recyclability, the large decrease in the mechanical properties of GF/PP after recycling is seen in Fig. 5.9. The extent of the decrease in the mechanical properties of the composites after recycling in the transverse-to-flow direction is mitigated by replacing glass fiber with TLCP. The tensile strength of

10GF20TLCP/PP only decreases from 21.4 to 20.2 MPa after mechanical recycling while the 30 wt% TLCP/PP composite exhibits little or no change in the tensile modulus and strength in the transverse-to-flow direction. Hybrid composite formulations provide the balance between recyclability and mechanical performance.

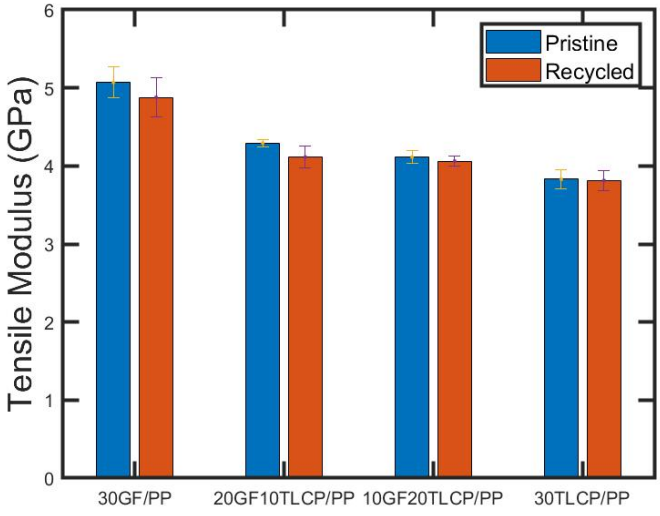

Figure 5. 7: Tensile modulus of pristine and recycled hybrid composites in the flow direction

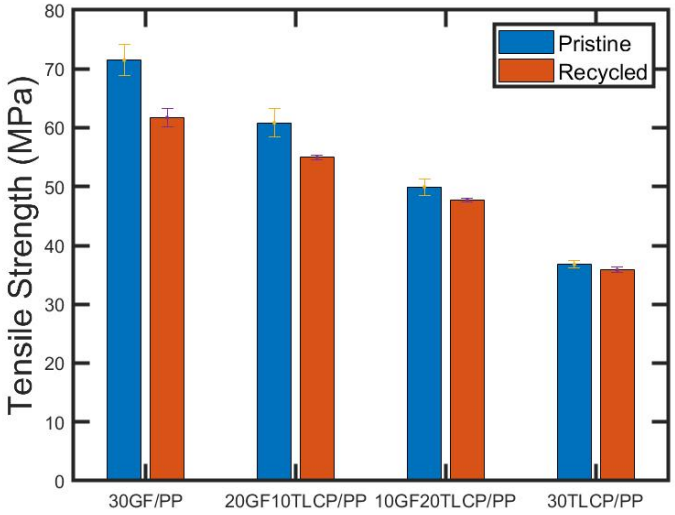

Figure 5. 8: Tensile strength of pristine and recycled hybrid composites in the flow direction

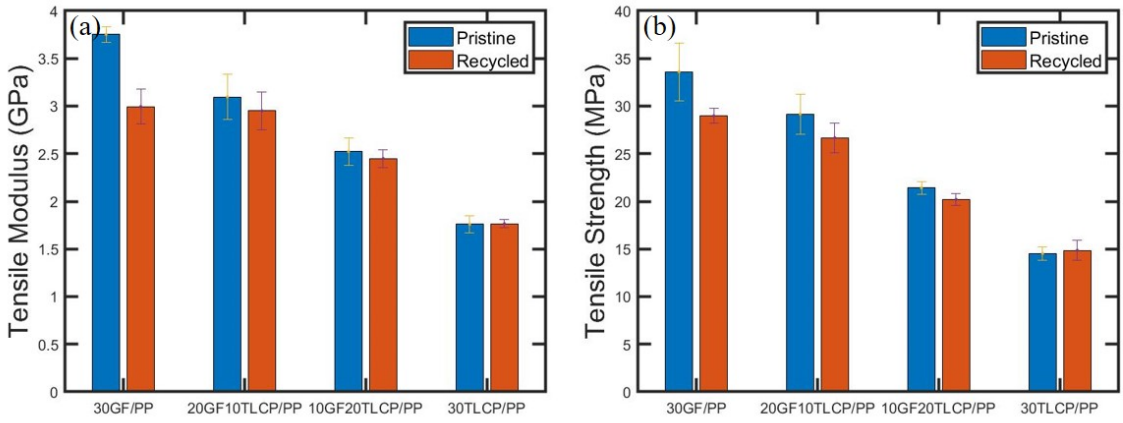

Figure 5. 9: Tensile properties of hybrid composites in the transverse-to-flow direction

5.4.3 Mechanical anisotropy of the hybrid TLCP/GF composite

Mechanical anisotropy is an important parameter to evaluate the performance of the composite material. Table 5.1 illustrates the tensile modulus of the composites in the flow and transverse-to-flow directions as well as the mechanical anisotropy. Mechanical anisotropy is the ratio of the property in the flow direction over the property in the transverse-to-flow direction. Several studies have been published about the mechanical anisotropy of injection-molded composites [23, 48, 49].

TLCP composites have significantly higher mechanical anisotropy than their glass filled counterparts, which is caused by TLCP fibrils being generated in the direction of elongational flow developed at the melt front. The transverse-to-flow direction has much less TLCP fibrils than the flow direction. With a higher content of TLCP in the blend, the degrees of mechanical anisotropy increase rapidly [49]. This is one of the major limitations when using *in situ* TLCP composites. For glass filled composites, the glass fibers can be aligned in both flow and transverse-to-flow directions through flow kinematics during the mold filling process leading to less mechanical anisotropy. As indicated by Table 5.1, the modulus of 30 wt% TLCP/PP is 3.83 and 1.76 in the flow and transverse-to-flow directions, respectively. The anisotropy for the TLCP/PP composite is calculated to be 2.2; however, the mechanical anisotropy of glass fiber reinforced polypropylene is only 1.35. Therefore, the anisotropy of TLCP-filled composite can be lessened with the addition of glass fiber which is demonstrated in Table 5.1 where we see the 10GF20TLCP/PP hybrid composite having its mechanical anisotropy reduced by 26%. The hybrid composites effectively reduce mechanical anisotropy of *in situ* TLCP composite.

Table 5. 1: Mechanical anisotropy of hybrid composites

Material	Modulus (GPa) Flow	Modulus (GPa) Transverse	Mechanical Anisotropy
30GF/PP	5.07	3.75	1.35
20GF10TLCP/PP	4.25	3.10	1.37
10GF20TLCP/PP	4.11	2.52	1.63
30TLCP/PP	3.83	1.76	2.2

5.4.4 Recyclability of the hybrid TLCP/GF composite material

To evaluate the recyclability of each composite material, the mechanical properties of the recycled composite were compared against its pristine counterpart. The normalized values of the tensile properties of hybrid composites are presented in Fig. 5.10. The normalized values are obtained by dividing the tensile properties of the recycled composites by their pristine material properties. For tensile properties of hybrid composites in the flow direction, the normalized values increase with increasing weight fraction of TLCP, suggesting the improvement in the recyclability with the presence of TLCP (Fig. 5.10(a)). 30 wt% GF/PP only retains 86% of its tensile strength after recycling, and 10GF20TLCP/PP retains 96% of its tensile strength as compared to the pristine composite. The tensile modulus in the flow direction is not significantly impacted by mechanical recycling. The different impact of recycling on tensile modulus and strength is because of the different sensitivity of each property on the change in fiber length [45].

Fig. 5.10(b) exhibits the normalized tensile properties of hybrid composite in the transverse-to-flow direction. The properties follow a similar trend as before where properties increase with increasing TLCP concentration. The tensile modulus of GF/PP drops significantly after recycling which may due to the joint influence of fiber breakage and decrease of fiber orientation in the transverse-to-flow direction. In the injection molding process, long fiber polymer blends have a larger core region where fibers are randomly oriented [50, 51]. These effects may lead to large drops in the tensile modulus of GF/PP in the transverse-to-flow direction. The normalized values of tensile properties are significantly influenced by the content of glass fiber and TLCP in both the flow and transverse-to-flow directions. The recycling process has a greater impact on the tensile strength of composite materials than their tensile modulus in both the flow and transverse-to-flow directions.

Knock-down (KD) factor is used to quantify the degree of recyclability of a hybrid composite where a low KD factor means better recyclability. The knock-down factor for a composite is determined by comparing the property of recycled material relative to its pristine material [52]. The KD factor is defined by the following equation:

$$KD = \left(1 - \frac{P_r}{P_v}\right) \times 100\ (\%)$$

Where P_r/P_v is the ratio of recycled material to the pristine material property. Table 5.2 shows the KD factor of each composite in the flow direction. The KD factor of tensile modulus and strength for glass fiber reinforced polypropylene is 3.8 and 13.7, respectively. The KD factor decreases in value with increasing TLCP concentration thereby confirming that the higher TLCP weight fraction in a TLCP/GF hybrid composite gives rise to greater

recyclability. Composites with a KD factor less than 5 are typically considered to be within design limits for various applications where the recycled part can be used to replace that made of pristine material [52]. The formulation of 10 wt% glass fiber and 20 wt% TLCP results in the creation of a recyclable and high-performance hybrid material. Based on Fig. 5.10, the formulation that contains a ratio of 2 to 1 or higher TLCP to glass fiber will yield a recyclable hybrid composite.

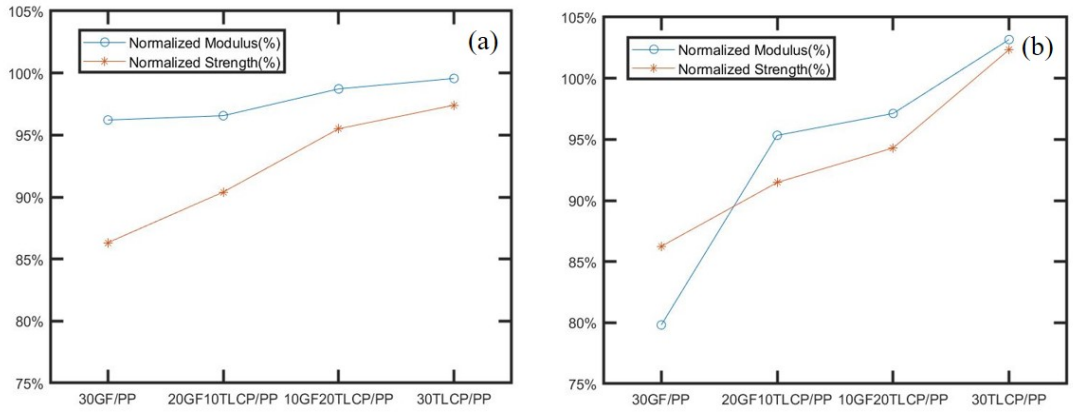

Figure 5. 10: Percentage of mechanical properties of recycled composite to pristine composite in (a) flow direction; (b) transverse-to-flow directions.

Table 5. 2: The Knock Down (KD) factor of the *in situ* hybrid composite

Material	KD (Modulus)	KD (Strength)
30GF/PP	3.8	13.7
20GF10TLCP/PP	2.4	9.6

10GF20TLCP/PP	1.3	4.5
30TLCP/PP	0.4	2.6

5.5 Conclusion

It has been found that the combination of TLCP fibrils and glass fiber can result in a high-performance and recyclable hybrid composite. The processing temperature of the injection-molding process was determined by rheological analyses and DSC. To provide a low viscosity blend to ensure that all the TLCP crystals are melted and to reduce excessive thermal degradation of polypropylene, the composites were processed at 305°C. *In situ* hybrid composites were successfully generated at the optimized processing temperature. Due to the hybrid nature of the glass fiber and TLCP, the *in situ* hybrid composite exhibited balanced performance with respect to processability, mechanical properties, and recyclability. The 10 wt% glass fiber and 20 wt% TLCP hybrid composite material was the best formulation of hybrid composite because it lowered the melt viscosity thereby increasing its processability while maintaining high tensile properties, lowered mechanical anisotropy, and increased recyclability of the TLCP/GF hybrid composite.

5.6 Acknowledgment

Support from General Motor (GM) is gratefully acknowledged. The authors would like to thank Celanese and SABIC for providing materials.

5.7 Reference

1. Chen, T.; Kazerooni, D.; Ju, L.; Okonski, D. A.; Baird, D. G., Development of recyclable and high-performance in situ hybrid tlcp/glass fiber composites. *J. Compos. Sci.* **2020,** *4*, 125.
2. Lu, K., The future of metals. *Science* **2010,** *328*, 319-320.
3. Rajak, D. K.; Pagar, D. D.; Menezes, P. L.; Linul, E., Fiber-reinforced polymer composites: Manufacturing, properties, and applications. *Polymers* **2019,** *11*, 37.
4. Clyne, T.; Hull, D., *An introduction to composite materials*. Cambridge university press: 2019.
5. Report, M. A. Fiber reinforced polymer (frp) composites market analysis by fiber type. https://www.grandviewresearch.com/industry-analysis/fiber-reinforced-polymer-frp-composites-market (accessed 29-6-2020).
6. Report, M. R. Gfrp composites market by end-use industry. https://www.marketsandmarkets.com/Market-Reports/glass-fiber-reinforced-plastic-composites-market-142751329.html (accessed 30-6-2020).
7. Asm aerospace specification metals inc. Aluminum 6061-t6. http://asm.matweb.com/search/SpecificMaterial.asp?bassnum=MA6061T6 (accessed 5-6-2020).
8. Prashanth, S.; Subbaya, K.; Nithin, K.; Sachhidananda, S., Fiber reinforced composites-a review. *J. Mater. Sci. Eng* **2017,** *6*, 1-6.
9. Weiss, R. A.; Wansoo, H.; Nicolais, L., Novel reinforced polymers based on blends of polystyrene and a thermotropic liquid-crystalline polymer. *Polym. Eng. Sci.* **1987,** *27*, 684-691.
10. Chae, H. G.; Kumar, S., Rigid-rod polymeric fibers. *J. Appl. Polym. Sci.* **2006,** *100*, 791-802.
11. Wang, X.-J.; Zhou, Q.-F., *Liquid crystalline polymers*. World Scientific Publishing Company: 2004.
12. Donald, A. M.; Windle, A. H.; Hanna, S., *Liquid crystalline polymers*. Cambridge University Press: 2006.
13. Kalfon-Cohen, E.; Marom, G.; Wachtel, E.; Pegoretti, A., Characterization of drawn monofilaments of liquid crystalline polymer/carbon nanoparticle composites correlated to nematic order. *Polymer* **2009,** *50*, 1797-1804.
14. Collier, M. C. Reclamation and reprocessing of thermotropic liquid crystalline polymer from composites of polypropylene reinforced with liquid crystalline polymer. Virginia Tech, 1998.
15. Handlos, A. A.; Baird, D. G., Processing and associated properties of in-situ composites based on thermotropic liquid-crystalline polymers and thermoplastics. *J. Macromol. Sci.-Rev. Macromol. Chem. Phys.* **1995,** *C35*, 183-238.
16. Collyer, A. A., *Liquid crystal polymers: From structures to applications*. Springer Science & Business Media: 2012; Vol. 1.
17. Baird, D. G.; Huang, J., Injection molding of polypropylene reinforced with thermotropic liquid crystalline polymer microfibrils. Part ii: Effect of impact toughening. *J. Inj. Mold. Tech.* **2002,** *6*, 107.
18. Williams, D., Applications for thermotropic liquid crystal polymer blends. *Adv. Polym. Tech.* **1990,** *10*, 173-184.
19. Chen, T.; Mansfield, C. D.; Ju, L.; Baird, D. G., The influence of mechanical recycling on the properties of thermotropic liquid crystalline polymer and long glass fiber reinforced polypropylene. *Compos. Part B Eng.* **2020,** *200*, 108316.

20. Yu, X. B.; Wei, C.; Xu, D.; Lu, C. H.; Yu, J. H.; Lu, S. R., Wear and mechanical properties of reactive thermotropic liquid crystalline polymer/unsaturated polyester/glass fiber hybrid composites. *J. Appl. Polym. Sci.* **2007,** *103*, 3899-3906.
21. YU, X.; Chun, W.; LU, S.; YU, J.; Deng, X.; LU, C., Preparation and mechanical properties of tlcp/up/gf in-situ hybrid composites. *T. Nonferr. Metal. Soc.* **2006,** *16*, s529-s533.
22. Huang, J.; Baird, D. G., Injection molding of polypropylene reinforced with thermotropic liquid crystalline polymer microfibrils. Part iii: Combination of glass and tlcp. *J. Inj. Mold. Tech.* **2002,** *6*, 187.
23. Bafna, S. S.; Desouza, J. P.; Sun, T.; Baird, D. G., Mechanical-properties of in-situ composites based on partially miscible blends of glass-filled polyetherimide and liquid-crystalline polymers. *Polym. Eng. Sci.* **1993,** *33*, 808-818.
24. He, J. S.; Zhang, H. Z.; Wang, Y. L., In-situ hybrid composites containing reinforcements at two orders of magnitude. *Polymer* **1997,** *38*, 4279-4283.
25. He, J. S.; Wang, Y. L.; Zhang, H. Z., In situ hybrid composites of thermoplastic poly(ether ether ketone), poly(ether sulfone) and polycarbonate. *Compos. Sci. Technol.* **2000,** *60*, 1919-1930.
26. Pickering, S. J., Recycling technologies for thermoset composite materials - current status. *Compos. Pt. A-Appl. Sci. Manuf.* **2006,** *37*, 1206-1215.
27. Piñero-Hernanz, R.; Dodds, C.; Hyde, J.; García-Serna, J.; Poliakoff, M.; Lester, E.; Cocero, M. J.; Kingman, S.; Pickering, S.; Wong, K. H., Chemical recycling of carbon fibre reinforced composites in nearcritical and supercritical water. *Compos. Part A-Appl. S. Compos.* **2008,** *39*, 454-461.
28. Cunliffe, A. M.; Jones, N.; Williams, P. T., Pyrolysis of composite plastic waste. *Environ. Technol.* **2003,** *24*, 653-663.
29. Oliveux, G.; Dandy, L. O.; Leeke, G. A., Current status of recycling of fibre reinforced polymers: Review of technologies, reuse and resulting properties. *Prog. Mater. Sci.* **2015,** *72*, 61-99.
30. Chrysostomou, A.; Hashemi, S., Influence of reprocessing on properties of short fibre-reinforced polycarbonate. *J. Mater. Sci.* **1996,** *31*, 1183-1197.
31. Kuram, E.; Ozcelik, B.; Yilmaz, F., The influence of recycling number on the mechanical, chemical, thermal and rheological properties of poly(butylene terephthalate)/polycarbonate binary blend and glass-fibre-reinforced composite. *J. Thermoplast. Compos. Mater.* **2016,** *29*, 1443-1457.
32. Colucci, G.; Ostrovskaya, O.; Frache, A.; Martorana, B.; Badini, C., The effect of mechanical recycling on the microstructure and properties of pa66 composites reinforced with carbon fibers. *J. Appl. Polym. Sci.* **2015,** *132*, 9.
33. Eriksson, P. A.; Albertsson, A. C.; Boydell, P.; Prautzsch, G.; Manson, J. A. E., Prediction of mechanical properties of recycled fiberglass reinforced polyamide 66. *Polym. Compos.* **1996,** *17*, 830-839.
34. Postema, A. R.; Fennis, P. J., Preparation and properties of self-reinforced polypropylene liquid crystalline polymer blends. *Polymer* **1997,** *38*, 5557-5564.
35. Lyondellbasell Pro-fax 6523 technical data sheet. https://www.lyondellbasell.com/en/polymers/p/Pro-fax-6523/cca46629-99c9-4596-8390-83b67fd362ff (accessed 6-6-2020).
36. Done, D.; Baird, D. G., Transient flow of thermotropic liquid-crystalline polymers in step strain experiments. *J. Rheol.* **1990,** *34*, 749-762.
37. Viola, G. G.; Baird, D. G., Studies on the transient shear-flow behavior of liquid-crystalline polymers. *J. Rheol.* **1986,** *30*, 601-628.

38. Cocchini, F.; Nobile, M. R.; Acierno, D., Transient and steady rheological behavior of the thermotropic liquid-crystal copolymer 73/27 hba hna. *J. Rheol.* **1991,** *35*, 1171-1189.
39. Chung, T. S.; Cheng, M.; Pallathadka, P. K.; Goh, S. H., Thermal analysis of vectra b950 liquid crystal polymer. *Polym. Eng. Sci.* **1999,** *39*, 953-962.
40. Datta, A.; Baird, D. G., Compatibilization of thermoplastic composites based on blends of polypropylene with 2 liquid-crystalline polymers. *Polymer* **1995,** *36*, 505-514.
41. Qin, Y.; Brydon, D. L.; Mather, R. R.; Wardman, R. H., Fibers from polypropylene and liquid-crystal polymer blends .3. A comparison of polyblend fibers containing vectra-a900, vectra-b950 and rodrun-lc3000. *Polymer* **1993,** *34*, 3597-3604.
42. Shenoy, A. V., *Rheology of filled polymer systems*. Springer Science & Business Media: 2013.
43. Vonturkovich, R.; Erwin, L., Fiber fracture in reinforced thermoplastic processing. *Polym. Eng. Sci.* **1983,** *23*, 743-749.
44. Zhang, G.; Thompson, M. R., Reduced fibre breakage in a glass-fibre reinforced thermoplastic through foaming. *Compos. Sci. Technol.* **2005,** *65*, 2240-2249.
45. Thomason, J. L., The influence of fibre length and concentration on the properties of glass fibre reinforced polypropylene: 5. Injection moulded long and short fibre pp. *Compos. Pt. A-Appl. Sci. Manuf.* **2002,** *33*, 1641-1652.
46. Baird, D. G.; Robertson, C. G.; De Souza, J. P. Liquid crystalline polymer-reinforced thermoplastic fibers. US5834560, 1998.
47. Mallick, P. K., *Fiber-reinforced composites: Materials, manufacturing, and design*. CRC press: 2007.
48. Mortazavian, S.; Fatemi, A., Effects of fiber orientation and anisotropy on tensile strength and elastic modulus of short fiber reinforced polymer composites. *Compos. Pt. B-Eng.* **2015,** *72*, 116-129.
49. Mehta, A.; Isayev, A. I., Rheology, morphology, and mechanical characteristics of poly(etherether ketone)-liquid crystal polymer blends. *Polym. Eng. Sci.* **1991,** *31*, 971-980.
50. Toll, S.; Andersson, P. O., Microstructure of long-fiber and short-fiber reinforced injection molded polyamide. *Polym. Compos.* **1993,** *14*, 116-125.
51. Thomason, J. L., Micromechanical parameters from macromechanical measurements on glass reinforced polyamide 6,6. *Compos. Sci. Technol.* **2001,** *61*, 2007-2016.
52. Eriksson, P. A.; Albertsson, A. C.; Boydell, P.; Manson, J. A. E., Durability of in-plant recycled glass fiber reinforced polyamide 66. *Polym. Eng. Sci.* **1998,** *38*, 348-356.

6 Conclusions and Recommendations

Chapter 6: Conclusions and Recommendations

6.1 Conclusions

1. The influence of mechanical recycling on the mechanical, thermal, rheological, and thermo-mechanical properties of TLCP reinforced polypropylene (PP) and glass fiber (GF)/polypropylene was investigated. TLCP/PP retained mechanical properties after mechanical recycling because of the regeneration of TLCP fibrils during the mold filling step. In contrast, mechanical recycling has a significant impact on the mechanical performance of glass fiber/polypropylene. The tensile strength of 30 wt% GF/PP decreased from 72 to 45 MPa and the tensile modulus dropped after three reprocessing cycles. Fiber length attrition during the injection molding grinding process resulted in a significant reduction in the mechanical properties of recycled glass fiber reinforced polypropylene.

2. The recyclable and high performance hybrid fiber reinforced composite was prepared by combining the TLCP and glass fiber together as the reinforcing material. The rheological analyses of TLCP and polypropylene were performed to lower the melt viscosity and reduce the thermal degradation of the matrix. The ideal processing temperature of blending TLCP, glass fiber, and polypropylene was at 305℃. The formulation with a weight fraction ratio of 2 to 1 for TLCP to glass fiber led a recyclable TLCP/glass fiber reinforced hybrid composites which exhibited balanced performance in terms of mechanical properties, mechanical anisotropy, and processability.

3. Outstanding mechanical properties and lightweight TLCP reinforced composite filaments were fabricated using the dual extrusion technique. The method of selecting the

processing temperatures to blend TLCP and polyamide (PA) was rigorously determined using rheological analyses to minimize the thermal degradation of the matrix polymer and utilize the super-cooled TLCP melt. The optimal printing temperature which led to the highest mechanical properties of the lay-down TLCP/PA was determined to be 280°C. The 3D printed TLCP/PA composite parts exhibited excellent mechanical performances which were competitive with the traditional fiber reinforced counterparts

6.2 Recommendations for Future Work

1. The TLCP reinforced polypropylene was mechanically recycled by repeated injection molding and grinding. Due to the large difference between the processing temperatures of TLCP and polypropylene, the optimized processing temperature still resulted in the thermal degradation of the matrix. Other matrix polymers (such as polyphenylene sulfide and polyether ether ketone) which have overlapping processing temperatures with the TLCP may be chosen to prevent the thermal degradation issue during the recycling and achieve a higher number of reprocessing cycles.

2. The TLCP/polyamide composite filament generated using the dual extrusion process exhibited a nonuniform distribution of TLCP fibrils in the polyamide matrix. This may be due to large differences in viscosity between TLCP and polyamide. One suggestion is to use another type of polyamide which has similar melt viscosity as TLCP in the same processing temperature. The large difference in viscosity lowers the rate of striation thinning. The other approach is to increase the number of mixing elements in the static

mixer system which could increase the degree of striation and improve the mixing efficiency.

3. The delamination between the 3D printed layers of TLCP/polyamide composite was observed when the concentration of TLCP was above 40 wt%. The delamination issue was mainly attributed to the poor interlayer adhesion. When the concentration of TLCP is high at the surface of the filament, less matrix material is able to diffuse through the printed layers and a weak interlayer bond is formed. To overcome the poor interlayer adhesion between printed layers, the sheath-core composite filament could be developed where the TLCP core is surrounded by the matrix polymer sheath to overcome the poor interlayer adhesion issue.

4. The TLCP/polyamide composite strand prepared by dual extrusion process exhibited an oval-shaped cross section. The nip-roller was used to draw the extrudate into composite filament which may cause this oval-shaped cross section. In the future, the vertical dual extrusion process could be utilized to generate the composite filament with a circular shape cross section.

5. The draw ratio of the TLCP/polyamide composite filament generated by the dual extrusion process was low because of the equipment limitation. The low draw ratio limited the composite filament to achieve better mechanical properties. The higher draw ratio led to higher tensile properties. A nip-roller that is capable of imparting higher draw ratios is recommended to be used in order to generate composite filament with higher mechanical properties.